Dynamics of Ribosome Association
with the Endoplasmic Reticulum Membrane

Dissertation

zur Erlangung des Doktorgrades der Fakultaet fuer Biologie

der Ludwig-Maximilians-Universitaet Muenchen

vorgelegt von

Dipl.-Biochem.

Julia Schaletzky

Mai 2006

Die vorliegende Arbeit wurde an der Harvard Medical School in Boston, MA (USA) unter der Anleitung von Prof. Tom Rapoport durchgefuehrt. Die dreidimensionale Struktur der von mir isolierten Komplexe wurde in Kollaboration mit Prof. Chris Akey (Boston University, USA) unter Anleitung von Dr. Jean-François Ménétret durch Cryo-Elektronenmikroskopie ermittelt.

Die vorliegende Arbeit wurde zur Beurteilung eingereicht am 01.06.2006.

Gutachter:
Prof. Dr. J. Soll
PD Dr. E. Schleiff
Prof. Dr. M. Hayashi
Prof. Dr. K. Jung

Rigorosum: 20.09.2006

Ehrenwoertliche Versicherung

Hiermit versichere ich, dass ich die vorliegende Arbeit selbstaendig verfasst und keine anderen als die von mir angegebenen Quellen und Hilfsmittel verwendet habe. Ferner erklaere ich, dass ich anderweitig nicht versucht habe, eine Dissertation einzureichen oder mich einer Doktorpruefung zu unterziehen. Die vorliegende Arbeit ist nicht als Ganzes oder in Teilen einer weiteren Pruefungskommission vorgelegt worden.

Boston, 12.05.06   ....

                                                              (Julia Schaletzky)

ACKNOWLEDGEMENTS

TABLE OF CONTENTS

1 ABSTRACT

Protein translocation across the endoplasmic reticulum (ER) membrane is fundamental for protein sorting and secretion in all kingdoms. Translocation occurs through a protein-conducting channel in the ER membrane, which is formed by Sec61. Targeting of ribosome-nascent chain complexes (RNCs) to Sec61 is mediated by the signal recognition particle (SRP) and its cognate receptor (SR). However, Sec61 has a high affinity for nontranslating ribosomes and it is largely occupied in vivo.

We addressed how RNC-SRP complexes can efficiently associate with the rER membrane, although most Sec61 seems to be occupied. We found that the spontaneous dissociation of ribosomes from the ER membrane is extremely slow. Surprisingly, membrane binding of RNC-SRP complexes does not require or cause the dissociation of prebound ribosomes. Instead, RNC-SRP complexes use a Sec61 population for translocation that cannot be bound by nontranslating ribosomes or RNCs alone. Complex formation between RNC-SRP and SR at the ER membrane facilitates the interaction between the RNC and the free Sec61.

We have used biochemical and structural approaches to investigate why the free Sec61 fails to be bound by nontranslating ribosomes. Our data suggests that Sec61 is present in two interconvertible forms in the membrane, that are in an equilibrium with each other and provide high-affinity and low-affinity binding sites for ribosomes. The former are quickly occupied, while the latter remain free. The high-affinity binding sites are formed by tetrameric rings of Sec61, which provide several connections that each can break and reform, but together prevent the ribosome from detachment. In contrast, the low-affinity binding sites may correspond to lower oligomeric states of Sec61. Consistent with that, we could capture monomers or dimers of Sec61 bound to eukaryotic ribosomes by electron cryo-microscopy. A ribosome-bound Sec61 dimer was only observed in presence of a nascent chain, which could indicate that Sec61 oligomerization is induced by translocation of a nascent chain. We obtained similar results for bacterial ribosome-channel complexes. However, the low-affinity binding site seems to be more abundant in bacterial membranes, which indicates that the prokaryotic equilibrium between low- and high-affinity binding sites is adjusted differently from eukaryotes.

We propose a model, in which Sec61 exists in different oligomeric states in the ER membrane. Tetrameric Sec61 provides a high-affinity binding site for ribosomes and is readily occupied in vivo. Monomeric or dimeric Sec61 is accessible for targeting by the SRP pathway, which facilitates the interaction between RNC and free Sec61. After transfer of the nascent chain into the channel and dissociation of SR and SRP, more Sec61 molecules could be recruited to stabilize the interaction with the translating ribosome. A dynamic oligomerization equilibrium of Sec61 is thus the core of a mechanism that would guarantee efficient protein translocation in vivo.

ZUSAMMENFASSUNG

Die Translokation sekretorischer Proteine in das Lumen des endoplasmatischen Retikulums (ER) ist evolutionaer konserviert und ueberlebenswichtig in Eukaryoten und Prokaryoten. Der Proteinkomplex Sec61 bildet einen Kanal, durch den Substratproteine transloziert werden koennen. Die Zielsteuerung translatierender Ribosomen (RNCs) an das ER wird vom Signal-Erkennungs-Partikel (SRP) zusammen mit seinem Rezeptor (SR) erreicht. Das Translokon Sec61 hat eine hohe Affinitaet auch fuer nicht-translatierende Ribosomen und ist deshalb in vivo groesstenteils besetzt.

Die vorliegende Arbeit untersucht, warum RNC-SRP Komplexe effizient an die ER-Membran binden koennen, obwohl Sec61 bereits von Ribosomen besetzt ist. Unsere Ergebnisse zeigen, dass die extrem langsame Dissoziation vorgebundener Ribosomen nicht fuer die Bindung von RNCs an die Membran notwendig ist. Auch fuehrt die Zielsteuerung von RNC-SRP Komplexen an das ER nicht zur Verdraengung vorgebundener Ribosomen. Wir konnten zeigen, dass RNC-SRP Komplexe auf eine Population von Sec61 zugreifen, die von Ribosomen oder RNCs nicht direkt gebunden werden kann. Dabei kann der RNC-SRP Komplex mit dem membranstaendigen SR interagieren, worauf die Bindung des RNCs an das freie Sec61 vermittelt wird.

Die freie Sec61-Subpopulation wurde sowohl biochemisch als auch strukturbiologisch untersucht. Unsere Ergebnisse zeigen, dass Sec61 in zwei ineinander umwandelbaren Formen in der Membran vorliegt. Diese stehen im Gleichgewicht und generieren hochaffine und niedrigaffine Bindungsstellen fuer Ribosomen am ER. Waehrend erstere sofort von Ribosomen besetzt werden, bleiben letztere zunaechst frei. Die hochaffinen Bindungsstellen bestehen aus einem ringfoermigen Sec61-Tetramer, das mehrere Kontakte zum Ribosom ausbilden kann. Einzelne Kontakte koennen brechen und sich wieder neu bilden, waehrend das Ribosom von den noch bestehenden Kontakten gehalten wird und somit stabil gebunden bleibt. Die niedrigaffinen Bindungsstellen werden dagegen vermutlich von kleineren Sec61-Einheiten gebildet. Cryo-Elektronenmikroskopische Studien zeigen, dass Sec61-Monomere und Dimere an eukaryotische Ribosomen binden koennen. Ein Sec61-Dimer wurde nur in Gegenwart einer naszierenden Kette beobachtet, was darauf hinweisen koennte, dass die Oligomerisierung von Sec61 durch den Beginn der Translokation induziert wird.

Aehnliche Ergebnisse konnten fuer prokaryotische Ribosomen-Kanal-Komplexe erhalten werden. In bakteriellen Membranen scheint sich bevorzugt die niedrigaffine Bindungsstelle zu bilden, was darauf hindeutet, dass das Gleichgewicht zwischen niedrig- und hochaffinen Bindungsstellen in Prokaryoten anders eingestellt ist als in Eukaryoten.

Wir schlagen ein Modell vor, in dem der Proteinkanal Sec61 in unterschiedlichen oligomeren Zustaenden in der ER-Membran vorliegt. Sec61-Tetramere bilden hochaffine Bindungsstellen fuer Ribosomen und sind deshalb in vivo besetzt. Sec61-Monomere oder Dimere koennten mit Hilfe von SRP von sekretorischen RNCs gebunden werden. Nachdem die Signalsequenz von Sec61 erkannt worden ist und den RNC-Sec61-Komplex stabilisiert hat, koennten sich zusaetzliche Sec61-Komplexe anlagern und die Interaktion mit dem translatierenden Ribosom stabilisieren. Ein dynamisches Oligomerisierungsgleichgewicht von Sec61 wuerde damit die Grundlage fuer einen Mechanismus bilden, der effiziente Proteintranslokation auch in der Gegenwart eines Ueberschusses an nicht-translatierenden Ribosomen sicherstellt.

2 INTRODUCTION

The compartimentalization of protein synthesis in the cytosol requires the sorting of proteins to defined destinations within or outside of the cell. In prokaryotes, proteins that have to be secreted cross the bacterial inner membrane. Eukaryotic secretory proteins do not directly traverse the plasma membrane. Instead, they are first imported into the endoplasmic reticulum (ER), and then packed into vesicles. These vesicles fuse with the Golgi apparatus, where posttranslational modifications occur. Vesicles coming from the Golgi apparatus fuse with the plasma membrane, releasing their soluble content into the extracellular space, while the transmembrane proteins remain in the plasma membrane.

In both prokaryotes and eukaryotes, secretory proteins can cross the membrane by translocation through a protein-conducting channel, the translocon. It is formed by the Sec61 complex in the eukaryotic ER membrane, or the homologous SecY complex in the inner membrane of prokaryotes (for review, see Wickner and Schekman, 2005; Osborne et al., 2005). Both consist of three subunits, Sec61α(52 kD), β(14 kD), and γ(8 kD), and SecY(49kD), E(14kD), and G(11kD), respectively. Sec61α and SecY span the membrane ten times and form an aqueous channel, which is able to translocate substrate domains into the lumen while releasing transmembrane-domains laterally into the lipid bilayer. Sec61α and SecY are essential for viability in yeast and bacteria, as is the single spanning Sec61γ and the homologous SecE (Deshaies and Schekman, 1987; Riggs et al,. 1988; Stirling et al., 1992). Sec61β is not essential, but improves the efficiency of translocation (Kalies et al., 1998). In S.cerevisiae, there is a second Sec61 complex termed Ssh1 that is not essential for viability and seems to have a specialized function (Finke et al., 1996). Mammalian substrate proteins can be translocated through the bacterial channel and vice versa, underscoring the high degree of evolutionary conservation.

2.1 Different ways of protein translocation

Unlike cytosolic proteins, secretory proteins carry an up to 20 amino acids long hydrophobic signal sequence that directs them to the ER. The hydrophobicity of the signal sequence determines if the protein is translocated co- or posttranslationally (Ng et al., 1996; Driessen et al., 2001) and flanking charges can influence its orientation in the membrane (Higy et al., 2004). The signal sequence is recognized by Sec61,

opening the channel (Jungnickel et al., 1995). After translocation of the remainder of the protein has occured, the signal sequence of secretory proteins is eventually cleaved off by signal peptidase, releasing the mature protein into the ER lumen. Membrane proteins retain their signal anchor, which facilitates the partitioning of subsequent transmembrane helices into the lipid bilayer (Heinrich and Rapoport, 2003).

Protein translocation can occur post- or cotranslationally, i.e. both nascent chains released from and associated with the ribosome can be substrates. In eukaryotes, translocation occurs mainly cotranslationally at the rough ER, a part of the ER that is studded with membrane-bound ribosomes (Figure 1). The mRNA for a secretory protein is translated in the cytosol until the signal sequence has emerged from the ribosomal exit tunnel and is recognized by the signal recognition particle (SRP). SRP stalls translation and targets the bound ribosome-nascent chain complex (RNC) to the ER by the GTP-dependent interaction with its membrane-bound receptor (SRP-receptor, SR). The RNC is transferred to Sec61 and the nascent chain is released by SRP, so that translation can resume. The signal sequence is recognized by Sec61 (Jungnickel et al., 1995) and the emerging nascent chain is translocated while being elongated by the Sec61-bound ribosome. SRP and its receptor reciprocally stimulate its binding partner's GTPase activity and dissociate from each other. Cotranslational translocation is driven by the GTP-dependent ribosomal elongation cycle of the bound ribosome, as Sec61 is a passive channel. As translocation proceeds, lumenal chaperones bind the nascent chain and glycosylation takes place, capturing the translocation substrate in the ER lumen (Walter and Blobel, 1983; Kleizen and Braakman, 2004). After termination of translation, the large ribosomal subunit appears to remain bound to Sec61 with high affinity, while the small subunit can dissociate (Borgese et al., 1973; Borgese et al., 1974; Seiser and Nicchitta, 2000).

During posttranslational translocation, the energy needed for achieving unidirectionality in translocation is provided by ATPases. In eubacteria, posttranslational translocation substrates are pushed through the channel by the cytosolic ATPase SecA (for review, see Mori and Ito, 2001), which undergoes conformational changes during its ATPase cycle (Economou and Wickner, 1994).
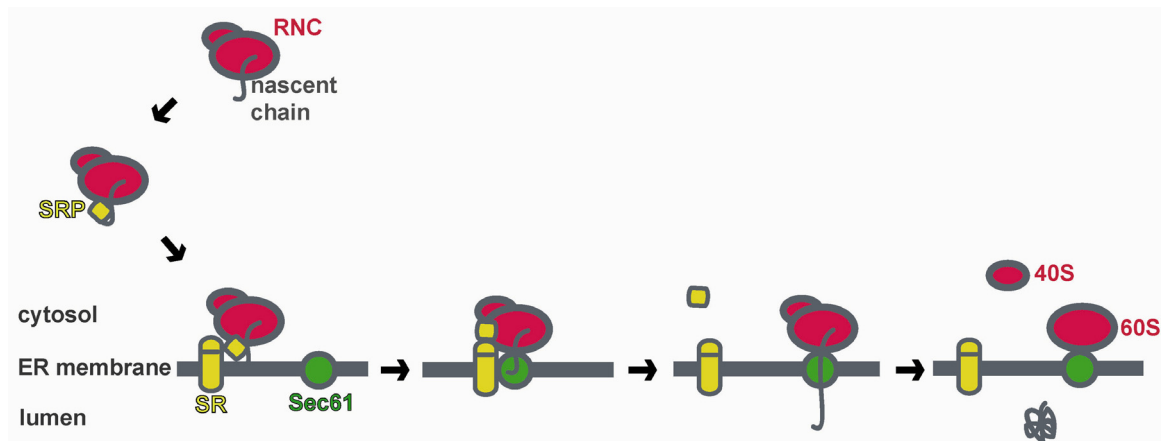
Figure 1: Cotranslational translocation in eukaryotes. The translocation substrate is translated in the cytosol until the signal sequence is recognized by SRP (yellow). The RNC is targeted to the ER membrane (grey) by the GTP-dependent interaction of SRP with the SRP receptor (SR, yellow; upper part: SRα; lower part: SRβ). The nascent chain is transferred to the Sec61 complex (green), SR and SRP reciprocally activate each other's GTPase activity and dissociate. After signal sequence cleavage (not depicted) and termination of translation, the secretory protein is set free in the ER lumen. The large ribosomal subunit likely remains bound.

Eukaryotes use a ratcheting mechanism to achieve posttranslational translocation (Matlack et al., 1999; Plath et al., 1998). In this mode of translocation, Sec61 forms a complex with a heterotetramer of Sec62 and Sec63 in the membrane (Deshaies et al., 1991, Panzner et al., 1995). Sec63 recruits the lumenal chaperone BiP, a member of the Hsp70 family, and activates it by stimulating its ATPase activity. Active BiP functions as a "Brownian ratchet", binding the translocation substrate once it has appeared in the ER lumen and preventing the nascent chain from backsliding into the cytosol. The random motion of the substrate through the channel allows more BiP molecules to bind, until translocation is complete and the substrate is released into the ER lumen.

2.2 Protein translocation by Sec61

Different lines of evidence show that Sec61 forms a protein-conducting channel in the ER membrane: Sec61 was first isolated in a screen for secretion defects in S.cerevisiae (Deshaies and Schekman, 1987). Systematic studies with photoreactive probes within the translocation substrate revealed that it only contacts Sec61α and lipid during translocation (Mothes et al., 1994). When reconstituted into proteoliposomes, the Sec61 complex was sufficient to achieve transport of translocation substrates across the membrane (Goerlich and Rapoport, 1993; Neuhof et al., 1998). Fluorescence quenching experiments showed that Sec61 forms an

aqueous pore in the membrane (Crowley et al., 1994), and electrophysiological measurements showed that the opened channel can conduct ions (Simon and Blobel, 1991). The recent 3.2Å crystal structure of an archaebacterial Sec61 homolog (SecYEβ) from Methanococcus jannaschii solubilized in detergent shows an hourglass-shaped channel in its closed state (van den Berg et al., 2004). Viewed from the cytosol, the complex has an approximately square shape and contains one copy of each of the three subunits, with the small SecE and Secβ located at the periphery (Figure 2A). The arrangement of transmembrane segments corresponds to the low-resolution structure of E.coli SecY complex in a lipid bilayer, as determined by electron microscopy of two-dimensional crystals (Breyton et al., 2002).
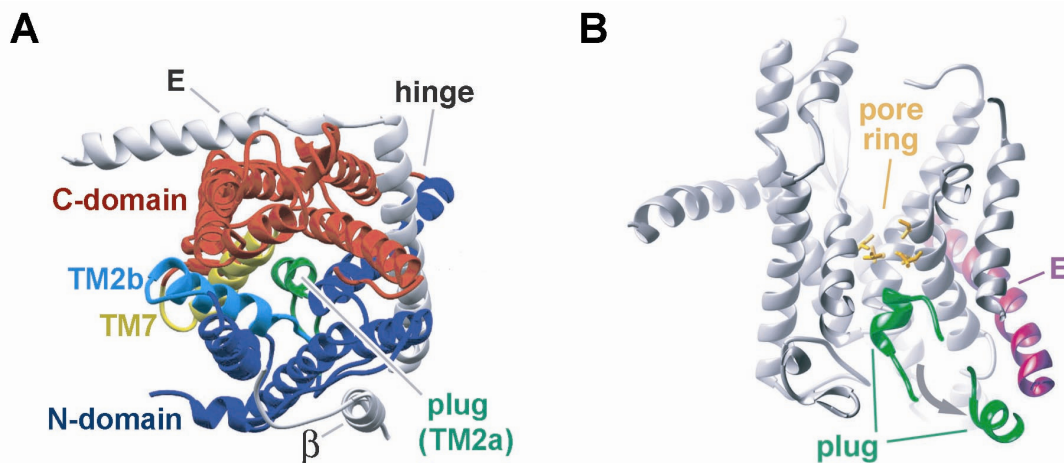
Figure 2: X-ray structure of SecYEβ from M. jannaschii (from van den Berg et al., 2004). **A)** Viewed from the cytosolic side. The N- and C-terminal domains of SecY are depicted in blue and red, respectively. The central plug (TM2a, green) and the helices between which transmembrane-segments intercalate (TM2b, cyan; TM7, yellow) are shown. SecE and Secβ are marked in grey. **B)** Side view of SecYEβ (cytosolic side on top). Sec E is labeled purple, the central constriction of the pore is yellow (pore ring), the plug domain (green) is closing the channel. Possible plug movement during channel opening is depicted, locating the plug close to SecE in the open conformation (Harris and Silhavy, 1999).

The ten transmembrane segments of SecY are organized in an N- and a C-terminal domain (TM1-5 and 6-10, respectively). The domains are pseudosymmetrical and form a bilobed structure that is connected by the loop between TM5 and 6 on the extracellular side. The subunit SecE seems to form a clamp that holds the two domains together (Figure 2A). Crosslinking experiments show that the signal sequence of a secretory protein is intercalated between TM2b and TM7 while contacting lipids, defining the location of the lateral gate (Plath et al., 1998). The SecYEβ complex can therefore be envisioned as a "clamshell", that can open on one side to release transmembrane helices into the lipid bilayer, and is held together on the

other side by a SecE-stabilized hinge region between TM5 and 6. The pore of the channel seems to be located in the center of a single copy of the SecY complex, which is also the most conserved region. When crossing the membrane, the nascent chain contacts the predicted pore-lining residues (Cannon et al., 2005). In its closed state, SecYEβ resembles a funnel, that tapers to a close in the middle of the membrane and is blocked on the lumenal side by a small helical segment (TM2a; Figure 2B). This segment is conformationally dynamic and leaves the pore during translocation, as suggested by crosslinking experiments between TM2a and SecE (Harris and Silhavy, 1999; Tam et al., 2005; Figure 2B). It therefore seems to be a plug domain, that is removed during translocation and opens the channel towards the lumen. In addition, widening of the pore is likely required for translocation, as the diameter of the central constriction observed in the crystal structure is too small to accomodate a polypeptide, even if it is in an extended conformation. Biochemical experiments suggest that the channel can transport fairly large structures, such as a 13 residue disulfide-bonded loop (Tani et al., 1990) or translocation substrates modified with a bulky group (Kurzchalia et al., 1988, De Keyzer et al., 2002). Molecular dynamics simulations suggest that the pore region is flexible enough to allow an object of 10-12Å diameter to be moved through (Tian and Andriocioaei, 2006; Gumbart and Schulten, 2006). The glycine-rich loops between TM4 and TM5 and between TM9 and TM10 could contribute to the flexibility of the SecY complex, which would be able to give rise to an estimated opening with maximally 15-20Å diameter (van den Berg et al., 2004).

2.3 The oligomeric state of Sec61

While M. jannaschii SecYEβ crystallizes as a monomer in detergent solution (van den Berg et al., 2004), E.coli SecYEG forms a dimer when crystallized in a membrane (Breyton et al., 2002) or when bound to RNCs in detergent solution (Mitra et al., 2005). Fluorescence resonance energy transfer (FRET) measurements in membranes provide evidence that two or more SecY-complexes associate to form an oligomer (Mori et al., 2003; Scheuring et al., 2005). Similar measurements, together with freeze-fracture experiments and native gel electrophoresis, indicate that the E.coli SecY-complex exists in a concentration-dependent equilibrium between monomers, dimers and tetramers, and that subunit exchange between oligomers can occur (Collinson et al., 2001; Bessonneau et al., 2002; Scheuring et al., 2005).

In the mammalian system, Sec61 complex solubilized in detergent gives rise to particles of different sizes, probably due to different oligomeric states (Jean-François Ménétret, personal communication). In cells, FRET can be observed between Sec61 complexes, indicating oligomerization (Snapp et al., 2004). Freeze-fracture experiments suggest that ribosomes can induce Sec61-oligomerization (Hanein et al., 1996). When bound to ribosomes, Sec61 is present in a large oligomeric ring, most likely a tetramer (Menetret et al., 2005).

Taken together, the Sec61/SecY-complex seems to have the ability to form oligomers of different stoichiometry. It is unclear, how many Sec61/SecY complexes are necessary to form a protein-conducting channel. Crosslinks between the translocating nascent chain and the E.c. SecYEG channel form within the central pore observed in the X-Ray structure (Cannon et al., 2005; van den Berg et al., 2004), suggesting that a single SecYEG complex may suffice for channel formation.

2.4 Ribosome binding to the rough endoplasmic reticulum

Purified rough endoplasmic reticululm (rER) from secretory tissues is densely populated by membrane-bound ribosomes when analyzed by electron microscopy and by biochemical methods (Adelman et al., 1973). The major ribosomal binding site in the ER membrane is provided by Sec61 (Goerlich et al., 1992; Kalies et al., 1994). In vitro binding of nontranslating ribosomes to Sec61 occurs rapidly and with nanomolar affinity both with ribosome-stripped rER microsomes (PKRMs) and reconstituted vesicles containing purified Sec61 (Borgese et al., 1974; Kalies et al., 2000; Prinz et al., 2000). The interaction between ribosomes and Sec61 is evolutionarily conserved, as channels and ribosomes from different species can form stable complexes (Prinz et al., 2000). Binding is mediated by the 28S RNA of the large ribosomal subunit and the cytosolic domains of Sec61, including loop 8 (between TM8 and 9) of Sec61α (Sabatini et al., 1966, Borgese et al., 1974; Prinz et al., 2000; Raden and Gilmore, 2000; Cheng et al., 2005). Structures for ribosomes bound to detergent-solubilized Sec61/SecY-complex have been determined in E.coli, S.cerevisae and C.familiaris by electron cryo-microscopy (Mitra et al., 2005; Beckmann et al., 2001; Menetret et al., 2000 and 2005, respectively; Figure 3). In E.coli, purified RNCs were bound to SecYEG in detergent. One SecYEG-dimer is bound to the ribosomal exit site, another one is unpysiologically bound to the L1 domain of the large ribosomal subunit (Figure

3C; Mitra et al., 2005). Also in S.cerevisiae, purified RNCs were bound to Sec61p in detergent. Sec61p is bound close to the exit site of the ribosome, likely as a trimer (Figure 3B). When nontranslating ribosomes are bound to Sec61p instead, the channel density appears smaller (Beckmann et al., 2001). In the mammalian system, several structures of the ribosome-channel complex solubilized from native membranes and proteoliposomes have been determined by electron cryo-microscopy.
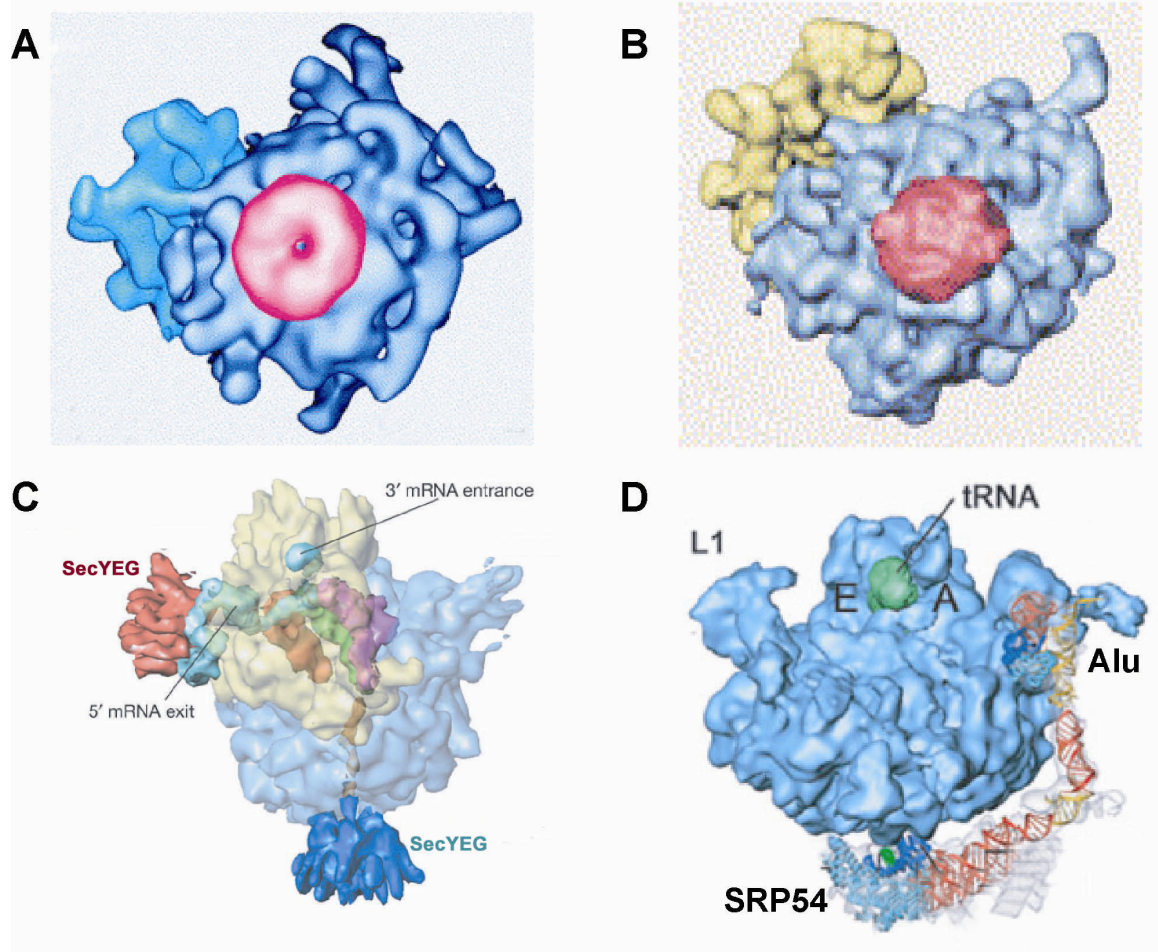
Figure 3: Electron cryo-microscopy structures of Sec61/SecY-complexes bound to ribosomes. **A)** Purified C.familiaris Sec61 (pink) bound to a rabbit ribosome (blue: 60S, cyan: 40S; from Menetret et al., 2000). **B)** Purified S.cerevisiae Sec61p (red) bound to a S. cerevisiae ribosome (blue: 60S; yellow: 40S; from Beckmann et al., 2001). **C)** Purified E.coli SecYEG (blue; red: nonphysiologically bound SecYEG) bound to an E.coli RNC translating a short fragment of the bacterial inner membrane protein FtsQ fused to the SecM stalling sequence (light blue: 50S; yellow: 30S; from Mitra et al., 2005; Nakatogawa et al., 2004). **D)** Molecular model of mammalian SRP bound to the ribosome. Only the large ribosomal subunit (blue) is shown. X-ray structures of parts of the SRP (helices) have been modeled into the Cryo-EM structure. The location of the S-domain (SRP54) and the Alu-domain is indicated. tRNA denotes the nascent-chain-associated tRNA that was observed. E: Exit site; A: Acceptor site; L1: L1 stalk of the large subunit (from Halic et al., 2004)

They display an approximately 100Å wide ring of Sec61, most likely a tetramer, bound to the ribosomal exit site of the large subunit (Figure 3A; Menetret et al., 2000, Morgan et al., 2002, Menetret et al., 2005). The ribosome forms several contacts with Sec61, that are mostly located on one side of the tetramer (Menetret et al., 2005).

Why the Sec61/SecY-complex is bound to ribosomes in different oligomeric states, is unclear. At the low resolution of the structures (15-30Å), neither can individual Sec61/SecY complexes be identified within the oligomer, nor can the nascent chain be seen. The presence of the nascent chain is only indicated by the peptidyl-tRNA in the peptidyltransferase-center (PTC) of the RNC (Beckmann et al., 2001). To further elucidate the mechanism of translocation, higher resolution structures of the Sec61/SecY complex bound to the ribosome are necessary. Because the channel is small compared to the ribosome, the computational alignment of the particles in cyro-electron microscopy is dominated by the latter, leading to improvement of ribosome resolution without concomitant improvement of Sec61-complex resolution (Menetret et al., 2005). In addition, the Sec61/SecY-complex might also be bound in different conformations or in different oligomeric states, instead of displaying one defined conformational state necessary for a high-resolution structure (Frank, 2002).

2.5 SRP-dependent targeting

In all three kingdoms of life, co-translational targeting to the eukaryotic endoplasmic reticulum or the bacterial inner membrane is mediated by the signal-recognition-particle (SRP) and its membrane-associated receptor (SRP-receptor, SR), which function as molecular matchmakers and deliver secretory RNCs to the translocon (for review, see Keenan et al., 2001; Egea et al., 2005).

SRP is a ribonucleoprotein containing six proteins (SRP54, SRP19, SRP68, SRP72, SRP9, SRP14) and a 600-nucleotide RNA in eukaryotes (Nagai et al., 2003; Sauer-Eriksson and Hainzl, 2003). The essential eubacterial SRP is more compact, consisting only of one protein (SRP54) and a 110-nucleotide RNA (Brown and Fournier, 1984; Phillips and Silhavy, 1992). Eukaryotic SRP forms an L-shaped complex, that can be divided into two functional units, the Alu- and the S-domain (Andrews et al., 1985; Andrews et al., 1987). The Alu-domain causes a pause in translation when bound to a RNC (Walter et al., 1981, Mason et al., 2000), as its binding site overlaps with the elongation factor binding site on the ribosome (Terzi et al., 2004). The S-domain contains the GTPase SRP54, which recognizes the emerging

signal sequence in a methionine-rich hydrophobic groove and mediates binding to the SRP-receptor (Clemons et al., 1999; Batey et al., 2000; Wild et al., 2001; Kuglstatter et al., 2002). SRP can bind to nontranslating ribosomes, but the affinity is strongly increased once a signal sequence is present (Walter et al., 1981; Flanagan et al., 2003). An electron cryo-microscopy structure of mammalian SRP bound to a secretory RNC confirms that the Alu-domain binds the ribosome at the interface between the small and the large subunit and that SRP54 binds close to the ribosomal exit site, interfering with Sec61 binding (Figure 3D, Halic et al., 2004). The eukaryotic SRP-receptor contains two GTPase subunits, SRα and its membrane-anchor SRβ. SRP54 and SRα can bind tightly to each other in the presence of GTP (Rapiejko and Gilmore, 1997), forming a head-to-head symmetrical heterodimer and burying both GTPs at the interface (Egea et al., 2004). This involves conformational changes in both subunits (Jagath et al., 2000; Shepotinovskaya and Freymann, 2002), and exposes the ribosomal exit site, so that Sec61 can be bound (Pool et al., 2002; Halic et al., 2006). After the RNC has been transferred to the translocon, SRP and SRα reciprocally stimulate each other's GTPase activity, hydrolyse GTP and dissociate (Connolly et al., 1991). GTPase activation is achieved by substrate twinning, i.e. the 3'-OH of the SRP-bound GTP is hydrogen-bonded to the γ-phosphate of the SRα-bound GTP, and vice versa (Egea et al., 2004; Focia et al., 2004). SRP-type GTPases have a low affinity for nucleotides on their own and exchange GDP and GTP rapidly without a guanine nucleotide exchange factor (GEF) (Jagath et al., 1998; Miller et al., 1993). The SRβ-GTPase is also necessary for SRP-dependent targeting (Ogg et al., 1998), but its function is unclear. As there is evidence for SRβ interacting with both Sec61 and the RNC during targeting, it may coordinate signal sequence release from SRP with ribosome binding to the translocon (Bacher et al., 1999; Fulga et al., 2001).

SRP-dependent targeting is thought to function mainly by localizing secretory RNCs at the ER membrane. In vitro, however, efficient membrane targeting of RNCs can be achieved in the absence of SRP (Neuhof et al., 1998; Raden and Gilmore, 1998). In the absence of SRP-receptor, SRP even hinders translocation (Goerlich and Rapoport, 1993), as its binding site overlaps with the Sec61 binding site of the large ribosomal subunit (Halic et al., 2004; Menetret et al., 2005). So why is SRP needed if both RNC binding and translocation of the substrate can take place without it? Most binding and

translocation experiments have been performed using rough ER (rER) membranes that had been stripped of bound ribosomes (PKRMs), therefore containing freely accessible Sec61. In vivo, however, different lines of evidence point to the Sec61 complex being constitutively occupied by ribosomes: Sec61 has a high affinity for nontranslating ribosomes (Borgese et al., 1974; Prinz et al., 2000), that are abundant in the cytosol. Isolated rER membranes have a high content of both nontranslating and translating ribosomes, consistent with electron micrographs showing the rER densely populated with ribosomes (Palade, 1955; Adelman et al., 1973). In hepatocytes, 75% of the total ribosomes are bound to the rER (Blobel and Potter, 1967). After termination of translocation, the large subunit stays bound to Sec61p, while small subunits can exchange with the cytosolic pool (Borgese et al., 1973; Seiser and Nicchitta, 2000).

Hence, secretory RNCs face competition from both prebound ribosomes and cytosolic ribosomes when targeting to the ER membrane. RNC binding to microsomes can be prevented by membrane-bound or free ribosomes in vitro. In the presence of SRP, however, RNCs can efficiently bind to Sec61, regardless of the amount of nontranslating ribosomes present (Neuhof et al., 1998, Raden and Gilmore, 1998). Therefore, SRP appears to give RNCs a competitive advantage over nontranslating ribosomes during targeting to the Sec61 complex. This might explain why SRP is necessary for translocation in vivo, but not in a situation where competing ribosomes are absent. How SRP mechanistically achieves targeting of RNCs to a membrane saturated with ribosomes, has so far remained elusive.

3 AIM

Secretory RNCs are generated in the cytosol and targeted to the ER membrane by the SRP-pathway. To translocate their nascent chain across the ER membrane, the RNCs have to bind the translocon Sec61. However, Sec61 has a high affinity for nontranslating ribosomes, and seems to be occupied in vivo. It is therefore unclear how an RNC-SRP complex can obtain a Sec61 binding site and ensure efficient translocation. The aim of this work was to elucidate the mechanism of SRP-dependent targeting when Sec61 is occupied by nontranslating ribosomes. Specifically, we wanted to address how Sec61 is made accessible during SRP-dependent targeting, using both biochemical and structural approaches.

4 RESULTS

4. 1 Characterization of Ribosome binding to the rough ER membrane

Secretory tissues like pancreas contain large amounts of rough ER membrane that can be purified by sucrose gradient centrifugation (Walter and Blobel, 1983). The ER membrane is disrupted during purification and forms vesicles (microsomes). Rough microsomes (RMs) are studded with endogenous ribosomes that are bound to the protein-conducting channel Sec61 and can be visualized by electron microscopy (Kalies et al., 1994, Adelman et al., 1973). The ribosomes can be removed by a combination of Puromycin and high salt treatment. The antibiotic Puromycin releases the nascent chain, whereupon the ribosomes can be dissociated by high salt concentrations (Adelman et al., 1973). These membranes (Puromycin/KOAc treated rough microsomes, PKRMs) are devoid of endogenous ribosomes and can be used for ribosome binding and dissociation experiments (Blobel and Dobberstein, 1975b; Goerlich et al., 1992, Kalies et al., 1994). They can also recapitulate protein translocation, signal sequence cleavage and protein glycosylation (Walter and Blobel, 1983).

To investigate how fast nontranslating ribosomes dissociate from the ER membrane, we prepared RMs and PKRMs. 80S ribosomes were purified and covalently radiolabeled. When separated on a sucrose gradient, they migrated as intact 80S particles with the radiolabel attached (Figure 4A). To investigate binding of radiolabeled ribosomes, we devised a sedimentation assay. In this assay, PKRMs were almost quantitatively sedimented while most of the unbound ribosomes remained in the supernatant (data not shown). To control for the sedimentation of ribosomal aggregates, experiments were conducted with or without membranes in parallel. As membrane sedimentation is a quick assay, we were able to measure kinetics of dissociation.

To validate the assay, we determined the apparent binding constant for binding of radiolabeled ribosomes to Sec61 in PKRMs (Figure 4B). Ribosome binding to Sec61 was saturable and described by a hyperbolic curve. The apparent K_D was determined by nonlinear regression to be 50nM, the apparent number of binding sites 3.6pmol/eq (Figure 4B). This is similar to published values on both affinity and number of binding sites (Prinz et al., 2000).
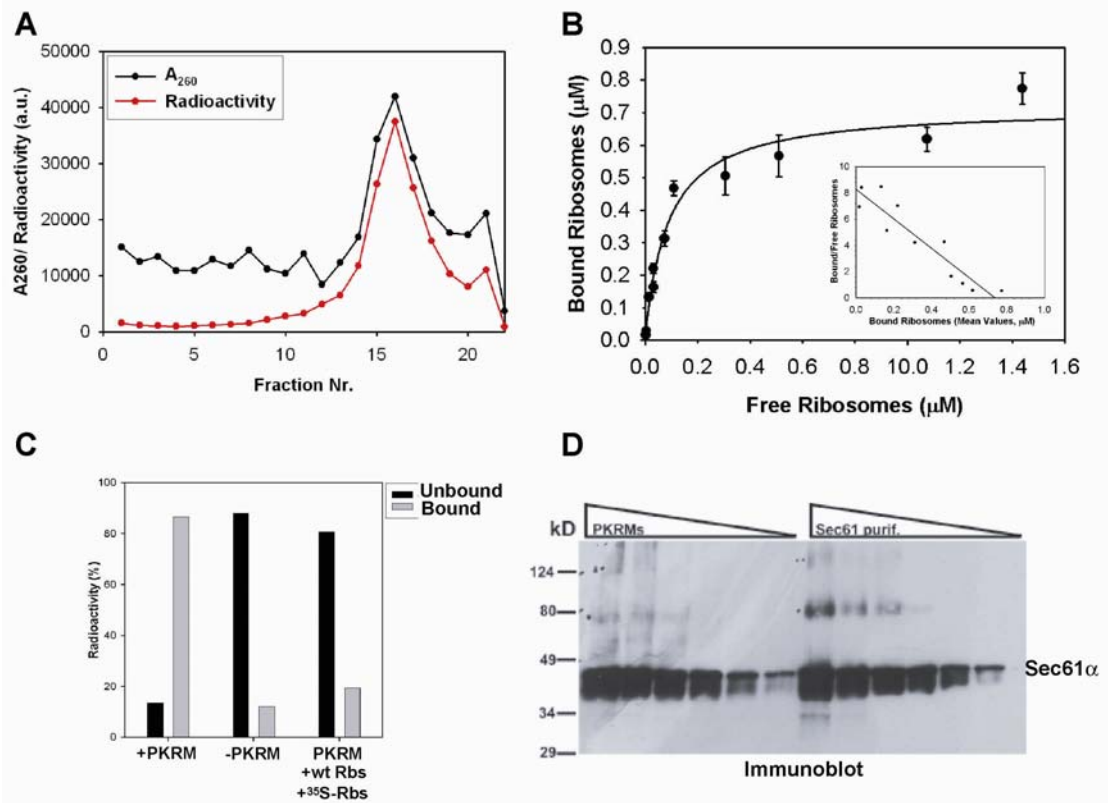
Figure 4: Validation of the binding assay. **A)** Radiolabeled ribosomes are intact and pure. 80S Ribosomes were covalently labeled with a ^{35}S-linked and purified. Radiolabeled ribosomes migrate as intact 80S particles in a sucrose gradient as judged by absorbance of the RNA at 260nm (black line) and the radiolabel is attached to the ribosomes (red line). Fractions were taken from top to bottom. **B)** The sedimentation assay is suitable for determining ribosome binding. PKRMs were incubated with increasing concentrations of radiolabeled ribosomes, sedimented and analyzed by scintillation counting. Inset: Scatchard Plot of the data depicted. The ratio of bound to free ribosomes is plotted over the concentration of bound ribosomes (μM). The apparent Binding constant K_D^{app} was determined to be 50 nM, the number of binding sites B_{max} 3.6 pmol/eq. **C)** Ribosome binding is specific. PKRMs were used to bind radiolabeled ribosomes and sedimented (first panel). Without PKRMs, only little sedimentation of ribosomes was observed (second panel). Preincubation of PKRMs with unlabeled ribosomes prevented binding of radiolabeled ribosomes (third panel). **D)** Quantitative Immunoblotting for Sec61α to determine the Sec61 content of PKRMs. Corresponding amounts of purified Sec61 and PKRMs were loaded (8.5 ng to 0.3 μg of Sec61 and 0.01-0.2 eq PKRM). Sec61α has a MW of 52kD, but is running anomalously fast at 35kD (Deshaies et al., 1991). 1.7 μg Sec61 (24 pmol) was found to be present in 1 eq PKRMs, yielding around 7 Sec61 molecules per binding site.

To estimate how many Sec61 molecules constitute a binding site, quantitative immunoblotting was performed to determine the concentration of Sec61 in the PKRM preparation (Figure 4D). A ribosome to Sec61-ratio of 1:7 was estimated, again being consistent with published data (Prinz et al, 2000). Aggregation of ribosomes was negligible (Figure 4C, middle panel). Presaturating the PKRMs with unlabeled ribosomes abolished binding of radiolabeled ribosomes (Figure 4C, left vs right panel). This shows that the ribosome binding is specific and that the labeling reaction

has not interfered with ribosome binding. In summary, the binding of radiolabeled ribosomes to PKRMs as investigated by a new sedimentation assay is saturable, specific and consistent with published results.

Next, we investigated how fast ribosomes dissociated from the membrane. The ratio between ribosomes and PKRMs was chosen so that more than 90% of the ribosomes bound to the membrane. Dissociation was measured by rapid 100x dilution, which effectively inhibits rebinding of ribosomes (data not shown). Samples taken at different time points were cooled on ice, effectively stopping dissociation (data not shown). Free and bound ribosomes were separated using the sedimentation assay. Ribosome binding was found to be extremely stable (Figure 5A). Even incubation at 28°C for two hours did not lead to significant dissociation of bound ribosomes (Figure 5A). Consistent with previous findings, bound ribosomes could be quantitatively removed by high salt concentrations (Figure 5B; Adelman et al., 1973; Goerlich et al., 1992). The low dissociation rate lead us to the prediction that rough microsomes retained their bound ribosomes completely during purification. We used radiolabeled ribosomes to probe the channel occupancy in rough microsomes (Figure 5C). Binding of radiolabeled ribosomes to RMs was effectively prevented by bound endogenous ribosomes (Figure 5C, white bars). When endogenous ribosomes were stripped off (PKRMs), radiolabeled ribosomes bound efficiently to the membranes (Figure 5C, black bars; the same amount of Sec61 was used in all experiments). These data agree well with observations on liver RMs, which can only bind ribosomes when endogenous ribosomes are removed, even after prolonged storage (Shires et al., 1971, Shires et al., 1974). Endogenous canine ribosomes remain stably bound after isolation of membranes from dog pancreas, despite strong mechanical stress during tissue homogenization, several sucrose gradient centrifugations and subsequent long-term storage at -80°C (Adelman et al., 1973).

In conclusion, the binding of ribosomes to the ER membrane is very stable and dissociation is very slow.
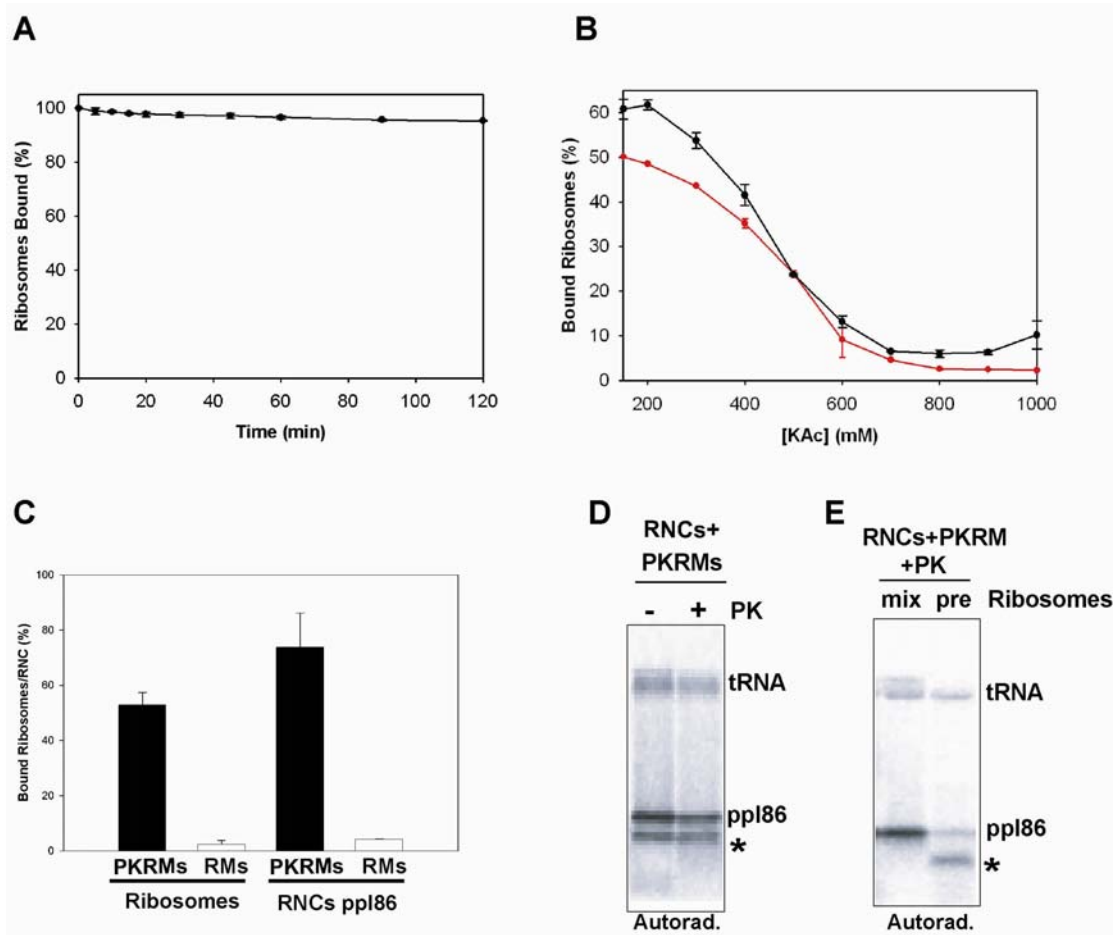
Figure 5: Sec61-bound ribosomes do not significantly dissociate. **A)** Dissociation curve of radiolabeled ribosomes bound to PKRMs. Dissociation was induced by 100x dilution with RBB buffer at 28°C. Membranes were sedimented and analyzed by scintillation counting **B)** Ribosome binding can be influenced by the salt concentration. Radiolabeled ribosomes were bound in the presence of RBB buffer with different salt concentrations for 30min on ice (black line) or bound at 150mM KAc and dissociated with increasing amounts of salt for 2h at 28°C (red line), sedimented and analyzed by scintillation counting. **C)** Rough microsomes (RMs) from dog pancreas are saturated with ribosomes. Radiolabeled Ribosomes and purified ppl86-RNCs could not bind to RMs (white bars; no SRP present). When endogenous ribosomes are stripped off the RMs by Puromycin/high salt treatment (PKRMs), both nontranslating ribosomes and RNCs can bind to the membranes. Binding was assessed by sedimentation and scintillation counting. **D)** Ppl86 interacts with Sec61 and is therefore protected from proteinase K (PK). The asterisk indicates a 40 amino acid degradation fragment protected in the ribosomal exit tunnel (Malkin and Rich, 1967). tRNA denotes a fraction of the nascent chain associated with peptidyl-tRNA after gelelectrophoresis. **E)** Prebound ribosomes block interaction of the nascent chain with Sec61. Purified ppl86 RNCs were either mixed with nontranslating ribosomes during binding to PRKMs ("mix") or nontranslating ribosomes were bound first ("pre"). Both samples were treated with proteinase K (PK).

4. 2 Characterization of SRP-dependent targeting under competition conditions

These results raise an important question: If nontranslating ribosomes are blocking the binding site and fail to dissociate, how can RNCs find an available channel for translocation of their emerging nascent chain? It is known that a translocating nascent

chain contributes significantly to the interaction between the RNC and Sec61 (Adelman et al., 1973; Jungnickel and Rapoport, 1995). We therefore investigated if purified RNCs could access Sec61 in rough microsomes. We used the N-terminal 86 amino acids of the secretory model substrate preprolactin (ppl86) as a nascent chain. The stop codon was omitted, and the mRNA was translated to its 3' end, yielding a stable complex of ribosome, mRNA and nascent chain (Gilmore et al., 1991, Jungnickel and Rapoport, 1995). Binding of ppl86-RNCs to rough microsomes was efficiently prevented by endogenous ribosomes (Figure 5C, white bars). Once they were removed, ppl86-RNCs could bind to the membranes (Figure 5C, black bar). The nascent chain was protected from protease digestion, indicating it had inserted into the channel (Figure 5D).

Thus, binding of purified RNCs and nontranslating ribosomes to the ER membrane is efficiently prevented by endogenous ribosomes. This is consistent with the slow dissociation of prebound ribosomes (Figure 5A). Although the nascent chain represents a significant advantage in affinity for RNCs, it cannot be employed, as the binding site is inaccessible. This is illustrated by RNCs productively interacting with Sec61 when they are mixed with nontranslating ribosomes before binding (Figure 5E, "mix"), but not when nontranslating ribosomes are allowed to bind first (Figure2E, "pre"). Affinity differences can only have an effect if the two ligands can compete for the binding site. Although it may be thermodynamically favourable, binding of the higher affinity ligand will be kinetically hindered if the lower affinity ligand does not dissociate. This is most likely to be the situation in the cell, where nontranslating ribosomes are constantly present and occupy the protein-conducting channel while the synthesis of secretory nascent chains begins. RNCs can overcome this targeting problem with the help of the SRP pathway (Neuhof et al., 1998; Raden and Gilmore, 1998). Although not necessary when the channel is freely accessible, the SRP pathway ensures efficient targeting in the presence of occupied Sec61.

To recapitulate the effect of SRP, translation intermediates were generated by in vitro translation of a truncated ppl86 mRNA in a wheat germ extract in the absence or presence of purified canine SRP. Wheat germ SRP present in the extract has no effect, as it fails to interact with the canine SRP-receptor (Prehn et al., 1987). PKRMs were presaturated with nontranslating ribosomes or incubated with buffer and reisolated by sedimentation. When RNCs were added, the nascent chain efficiently inserted in the absence of prebound ribosomes, as judged by protease protection (Figure 6A, lanes

3,5,7,9). In the presence of prebound ribosomes, however, SRP was required for insertion of ppl86 (Figure 6A, lanes 4 vs 10). The protease-resistant band does not appear upon addition of SRP buffer (data not shown).

This SRP-dependent targeting can occur on membranes containing only Sec61 and the SRP-receptor (Neuhof et al., 1998). Purified Sec61 and SRP-receptor were reconstituted into proteoliposomes (Figure 6B, Immunoblot), and used for a targeting assay as before. Again, in the absence of prebound ribosomes, targeting was possible without SRP (Figure 4B, lanes 4,6). Prebound ribosomes prevented ppl86 interaction with Sec61, unless SRP was present (Figure 6B, lanes 5 vs 7).

As previous experiments had been conducted in an in vitro translation extract, the requirement for cytosolic factors other than SRP had not been ruled out. In order to investigate if the reaction could also take place in the absence of cytosol, we purified ppl86-RNC-SRP complexes from an in vitro translation reaction by sedimentation and subsequent sucrose gradient centrifugation (Figure 6C, inset). Rabbit reticulocyte lysate was used instead of wheat germ extract for translation, as rabbit SRP interacts well with the canine SRP-receptor (Meyer et al., 1982). The addition or omission of GTP to the purified RNC-SRP-complexes was used to assay for SRP activity, as SRP can only form a stable complex with its receptor in the presence of GTP (Rapiejko and Gilmore, 1997). When membranes were stripped of ribosomes, efficient binding was observed for both nontranslating ribosomes and RNC-SRP complexes, in the presence and absence of GTP (Figure 6C, bar graph). When rough microsomes (RMs) carrying bound ribosomes were used in the absence of GTP, binding of both nontranslating ribosomes and RNC-SRP-complexes was prevented. In the presence of GTP, however, RNC-SRP-complexes could bind to the membranes, while nontranslating ribosomes could not (Figure 6C, bar graph). Protease protection experiments conducted with the same membranes confirmed that the nascent chain insertion into Sec61 was dependent on GTP in RMs (Figure 6C, autoradiography, lane 8 vs 11) and GTP-independent in PKRMs (Figure 6C, autoradiography, lane 2 vs 5). Taken together, these data confirm that SRP can mediate targeting of RNCs to Sec61 in the presence of prebound ribosomes and show that SRP and SR are necessary and sufficient for this reaction.
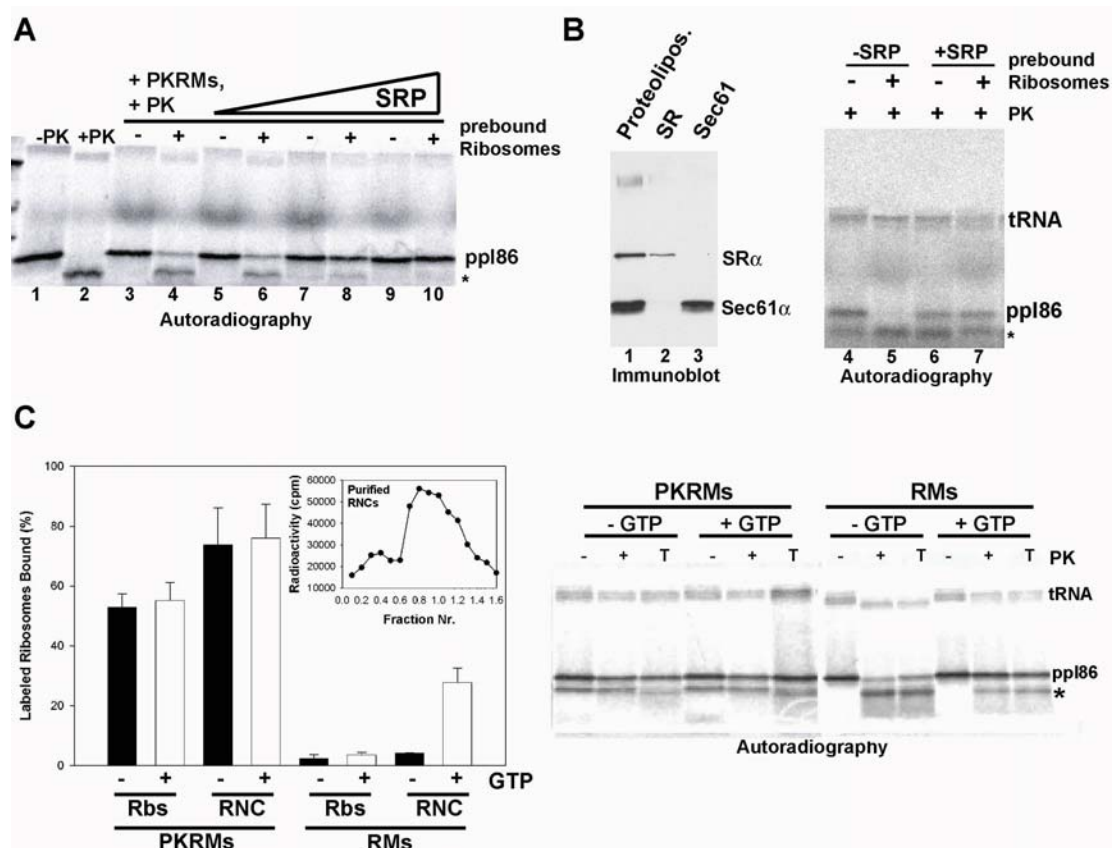
Figure 6: SRP is necessary and sufficient for targeting under competition conditions **A)** RNCs carrying ppl86 were synthesized in vitro in a wheat germ system, and incubated in the absence or presence of PKRMs, that were either untreated or preincubated with non-translating ribosomes and reisolated. Different amounts of purified canine SRP (0, 5, 15, 30 fmol) were added during the incubation, as indicated. Nascent chain insertion into the translocation channel was assessed by treatment with proteinase K (PK). The samples were analyzed by SDS-PAGE and autoradiography. The asterisk indicates the nascent chain fragment protected by the ribosome alone. **B)** Left panel: Proteoliposomes generated from purified Sec61p complex (lane 3) and SR (lane 2) were separated by SDS-PAGE and analyzed by immunoblotting with antibodies to Sec61α and SRα (lane 1). Right panel: The proteoliposomes were pre-incubated with non-translating ribosomes as indicated and tested for SRP-dependent membrane targeting of RNCs carrying ppl86 as in A). **C)** Targeting of purified retic ppl86-RNC/SRP complexes (RNCs) is GTP-dependent. Sucrose-gradient purified RNCs (left panel, inset) and radiolabeled ribosomes (Rbs) were used to assess binding to ribosome-free PKRMs and ribosome-bearing RMs in the presence and absence of 180μM GTP. Binding was performed for 30min at 28°C in RBB buffer (+/-GTP) and membranes were sedimented and analyzed by scintillation counting (left panel). Right panel: Protease (PK) protection experiment using the RNC-samples from the left panel. Labeling as in A; T: Preincubation with 1% Triton before PK addition.

How does SRP achieve this? As the membrane is saturated with prebound ribosomes that do not spontaneously dissociate (Figure 5A), SRP cannot use their dissociation-reassociation equilibrium to achieve binding. Protease protection experiments revealed that the nascent chain is accomodated in Sec61, the same protein nontranslating ribosomes are bound to (Kalies et al., 1994). In order to resolve this conundrum, we investigated if SRP-dependent targeting displaces prebound

ribosomes. We optimized the amount of membranes present in the reaction and the amount of ribosomes used for presaturation for SRP-dependent targeting (data not shown). We bound radiolabeled ribosomes to PKRMs, reisolated the membranes and performed targeting of unlabeled ppl86 to under these optimized conditions (Figure 7A). Membranes were sedimented and analyzed by scintillation counting to determine if radiolabeled ribosomes had dissociated during targeting.

Prebound ribosomes did not dissociate during incubation, consistent with the stable binding that has been observed before (Figure 7A, compare "t=0" (before incubation) with "Bf" (after incubation)). The addition of ppl86-RNCs did not lead to significant dissociation of prebound ribosomes (Figure 7A, "-SRP"). Interestingly, performing the same experiment in the presence of SRP did not enhance the dissociation of prebound ribosomes (Figure 7A, "+SRP"). The very same experiment with the labels switched, i.e. using unlabeled prebound ribosomes but labeled ppl86, showed that SRP-dependent targeting took place (Figure 7B, lane 4 vs 6). Adding more radiolabeled ribosomes to the membrane did not increase binding, indicating that the membrane was saturated with nontranslating ribosomes (Figure 7A, "presat"). Thus, although SRP can target ppl86-RNCs to a membrane saturated with ribosomes, no dissociation of the prebound ribosomes is observed.

To extend these surprising findings, we devised a new assay that allowed us to simultaneously look at both prebound and targeted ribosomes in one experiment. Instead of using nontranslating ribosomes to occupy Sec61, we used purified RNCs carrying a short fragment of the cytosolic protein firefly luciferase. Because of the molecular weight difference, the 120 amino acid long luciferase fragment (luc120) could be detected in the same gel as the ppl86. The luc120-RNCs displayed a saturable binding curve and did not significantly dissociate over time, mimicking the behaviour of nontranslating ribosomes (data not shown). As luc120 is a cytosolic protein, it is not recognized by Sec61 and digested in the presence of protease. For this reason, cosedimentation of luc120- or ppl86-RNCs with membranes was used to detect Sec61 binding. Luc120 does only sediment when membranes are present (Figure 7C, lane 2 vs 4). After incubating with an excess of luc120, membranes were isolated and used in targeting assays (Figure 7C,D; lanes 9-12, 15, 16, 20-24). Controls for aggregation were performed by omitting membranes (Figure 7C,D lanes 5-8, 13, 14, 17-20).
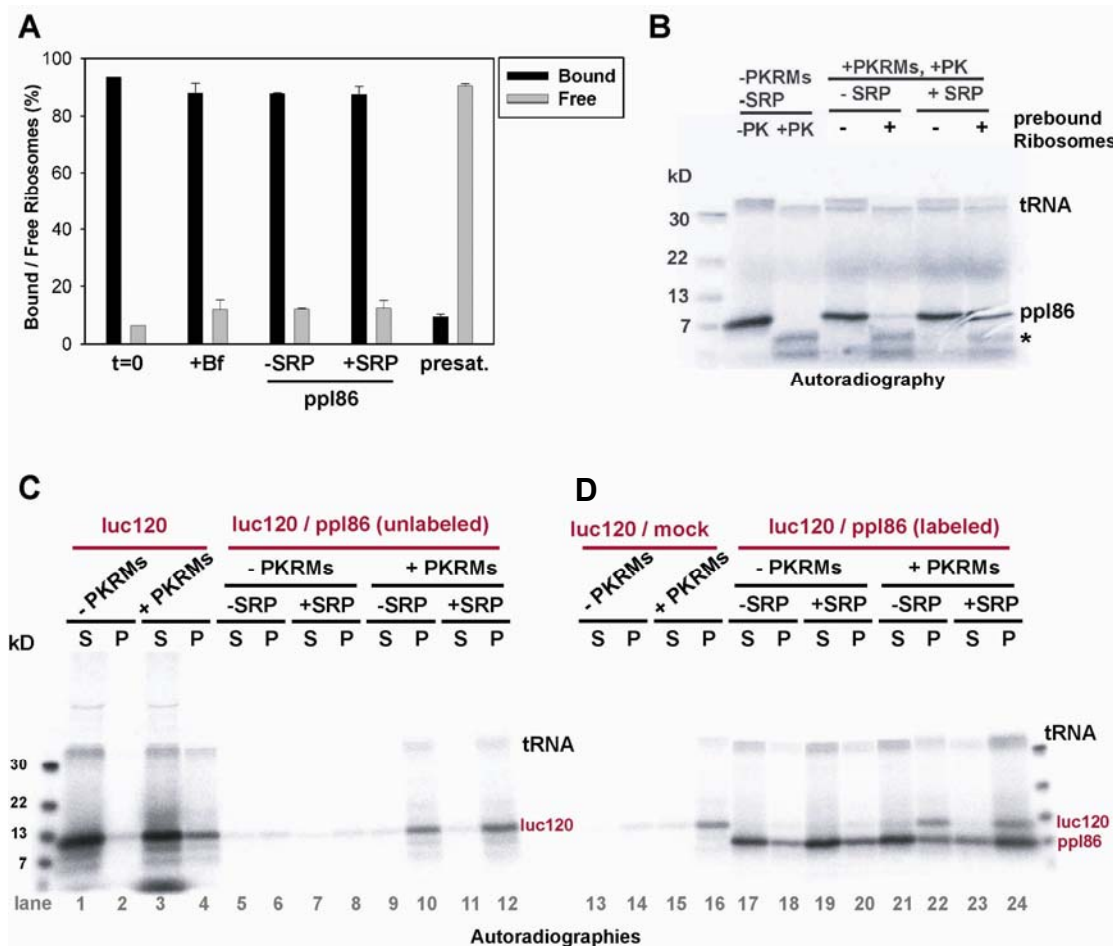
Figure 7: SRP-dependent targeting does not lead to displacement of prebound ribosomes. **A)** PK-RMs were pre-incubated with saturating amounts of purified, radiolabeled ribosomes, and re-isolated. Ribosome dissociation from these membranes was analyzed by a second sedimentation, either immediately (t=0), or after incubation with a translation mix containing RNCs carrying ppl86, in the absence or presence of SRP, or after incubation with buffer (+Bf). In one sample (presat.), the pre-incubation was done with unlabeled, instead of labeled, ribosomes. The membranes were re-isolated, and tested for ribosome binding by incubation with radiolabeled ribosomes and sedimentation. **B)** As in A), but the PK-RMs were pre-incubated with saturating concentrations of unlabeled non-translating ribosomes. The membranes were then incubated with RNCs carrying radiolabeled ppl86, in the absence or presence of SRP. Insertion of the nascent chain into the channel was tested by treatment with proteinase K (PK). The asterisk indicates the nascent chain fragment protected by the ribosome alone. tRNA shows the position of non-hydrolyzed peptidyl-tRNA. **C,D)** PKRM were preincubated with an excess of translation mix containing RNCs carrying radiolabeled luc120 and re-isolated (lane 4). A control was performed without membranes (lane 2). The membranes were then incubated with a translation mix containing RNCs carrying either unlabeled (lanes 5-12) or labeled ppl86 (lanes 17-24), or with a translation mix lacking mRNA (mock; lanes 13-16). Following sedimentation of the membranes, the samples were analyzed by SDS-PAGE and autoradiography. Controls were performed in the absence of membranes (lanes 5-8 and 13, 14, 17-20).

Consistent with our earlier experiments, adding translation mix alone (Figure 7C, mock) or unlabeled ppl86 in the absence and presence of SRP did not release luc120 from the membrane (Figure 7C, lanes 16, 10, 12, respectively). Both luc120-RNCs and ppl86-RNCs were labeled to observe prebound and targeting ribosomes at the

24

same time (Figure 7D). Small amounts of ppl86 sediment in the absence of membranes, likely because of aggregation due to the hydrophobic signal sequence (Figure 7D, compare lanes 18 and 22). Ppl86-RNCs did not bind the luc120-saturated membranes in the absence of SRP, consistent with the blocking of targeting by prebound ribosomes (Figure 7D, compare lanes 18 and 22). In the presence of SRP, ppl86 is efficiently targeted to the membrane (Figure 7D, compare lanes 22 and 24). The prebound luc120-RNCs, however, remain stably bound (Figure 7D, compare lanes 22 and 24).

In summary, we have shown that both radiolabeled nontranslating ribosomes or cytosolic RNCs with a short nascent chain (luc120) efficiently bind the protein conducting channel and thereby prevent binding of a secretory RNC (ppl86). In the presence of SRP, however, secretory RNCs can be targeted to Sec61 in the presence of prebound ribosomes. Importantly, prebound ribosomes remain bound during this reaction, strongly suggesting that SRP provides access to new membrane binding sites.

4.3 Characterization of the new binding sites used by the SRP-system

How can SRP generate new binding sites at the membrane? Sec61 is part of the new binding sites, as it was necessary for protease protection of the nascent chain in proteoliposomes (data not shown, Goerlich et al., 1993), excluding formation a new Sec61-independent state of membrane-insertion (Murphy et al., 1997). The ability of the RNC to obtain a Sec61 binding site requires the SRP-receptor (Neuhof et al, 1998). We therefore asked whether SRP-receptor is part of the new ribosome-binding site that is generated.

To this end, ppl86 RNCs were targeted to rough microsomes in the presence of SRP. Subsequently, membranes were solubilized with digitonin, a mild detergent known to preserve membrane-protein-interactions and not interfere with Sec61-dependent translocation (Mothes et al., 1998). Sedimentation of ribosomes and associated proteins showed that Sec61 was bound to ribosomes in all cases (Figure 8A). SRP-receptor was also sedimenting, but this was strongly reduced when unbound RNCs were removed by sedimenting the membranes before solubilization (Figure 8A, circled arrows). Comparing the absence and presence of SRP-dependent targeting (Figure 8A, compare "mock" to "ppl86") revealed no difference in SRP-receptor sedimentation. We also used the nonhydrolyzable GTP-analog GMPPNP in the

targeting reaction, which is known to trap SRP bound to SRP-receptor (Connolly and Gilmore, 1986; Connolly et al., 1991; Song et al., 2000). Also in this case, no difference between the absence and presence of SRP-dependent targeting was observed (Figure 8A, compare "mock/PNP" to "ppl86/PNP"). Protease protection experiments verified that SRP-dependent targeting had occurred both with and without GMPPNP present (Figure 8A, autoradiography; High et al., 1991). These results indicate that SRP-receptor is not a stable component of the novel binding site that is generated for the RNC during SRP-dependent targeting. To exclude that the difference may be too small to be visible, we co-immunoprecipitated Sec61 and SRP-receptor after mild solubilization of membranes. We compared PKRMs, devoid of bound ribosomes, and RMs, which carry both endogenous nontranslating ribosomes and RNCs in an approximate ratio of 1:1 (Adelman et al., 1973). In both cases, no co-immunoprecipitation of Sec61α with SRα was observed (Figure 8B). SRα also did not co-immunoprecipitate with Sec61α in RMs. To exclude that the complex is unstable in detergent, we tried to crosslink Sec61 to SRP-receptor using the homobifunctional, membrane-permeable crosslinker bismaleimidohexane (BMH) in native membranes. We did not observe any crosslink between the two by immunoblotting for Sec61β and SRα (data not shown).
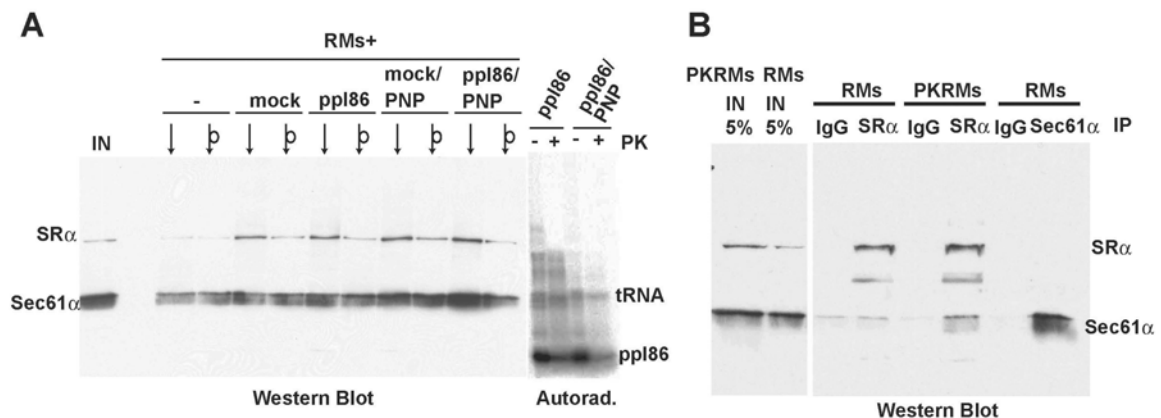
Figure 8: SRP-receptor is not in a stable complex with RNC/SRP during targeting. **A)** Sedimentation of ribosomes and immunoblotting for cosedimenting Sec61α or SRP-receptor α-subunit (SRα). IN: Rough microsomes (RMs) loaded directly. Solubilization was done after targeting (arrows) or after targeting and removal of unbound ribosomes and RNCs (circled arrows). RMs were incubated with buffer (-), unprogrammed rabbit reticulocyte lysate (mock) and ppl86 translation reaction containing SRP. GMPPNP was added in excess over endogenous GTP during the targeting reaction (mock/PNP, ppl86/PNP). The autoradiography shows protease (PK) protection of the nascent chain (ppl86). **B)** Sec61α and SRα do not coimmunoprecipitate. Solubilized RMs and PKRMs (IN) were incubated with antibodies against Sec61α, SRα or an equal amount of rabbit control IgGs (IP). The immunoprecipitates were analyzed by immunoblotting for both proteins.

To investigate in more detail if the SRP-receptor might associate with RNCs after SRP-dependent targeting, we studied the migration of membrane-bound ribosomes through a sucrose gradient. Rough microsomes were incubated with nontranslating ribosomes or ppl86-RNC-SRP complexes and excess ribosomes were removed by sedimentation of the membranes. After mild solubilization with digitonin, the extract was separated by sucrose gradient centrifugation. The fractions were precipitated with chloroform and methanol, followed by extraction of sucrose and detergent with water (Wessel and Flugge, 1984), as digitonin strongly interfered with the attempted TCA-precipitation (data not shown). The fractions were analyzed by immunoblotting for Sec61 and SRP-receptor.
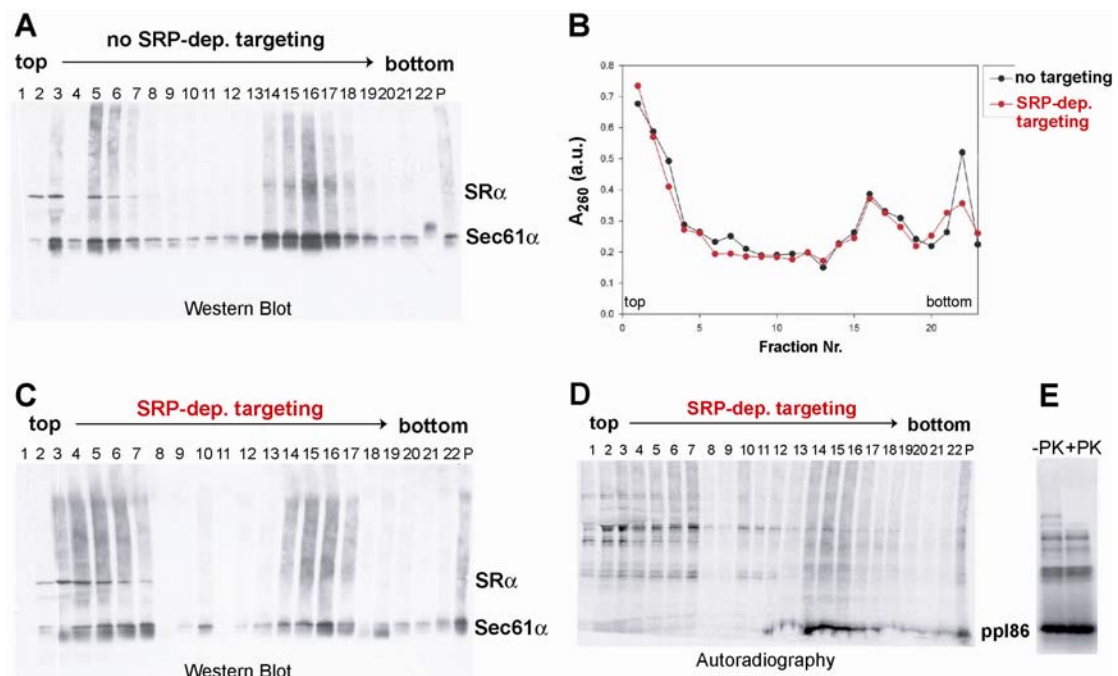
Figure 9: SRP-receptor does not comigrate with RNCs targeted by SRP. Rough microsomes (RMs) were incubated with unprogrammed retic lysate (**A**, no SRP-dep. targeting) or rabbit reticulocyte lysate translating ppl86 (**C**, SRP-dep. targeting). After removing excess ribosomes/RNCs and solubilization, the extract was separated on a sucrose gradient and fractions were taken from top to bottom. Fractions were analyzed by A_{260} (**B**; the high absorbance on top of the gradient is due to BSA; ribosome peak fractions 14-19), immunoblotting for Sec61α and SRα (A, C) and autoradiography of the immunoblot (**D**, ppl86). **E)** A sample of the membranes was used for a protease (PK) protection experiment to control for SRP-dependent targeting.

The majority of Sec61 was found in a complex with ribosomes (Figure 9A, B). The SRP-receptor, however, comigrates with proteins not attached to ribosomes, i.e. BSA (Figure 9A, B). When ppl86 was targeted to RMs in the presence of SRP, the migration pattern of all components remained unchanged (Figure 9C). An

autoradiography of the immunoblot reveals that the nascent chain remains attached to the ribosomes, indicating that the integrity of the RNCs was preserved (Figure 9B,D). A protease protection experiment showed that SRP-dependent targeting had efficiently taken place (Figure 9E). Taken together, the SRP-receptor α-subunit is necessary for SRP-dependent targeting, but unlikely to be a stable part of the new binding site provided for the RNC.

The SRP-receptor is a heterodimer of an α- and a transmembrane-containing β-subunit, which anchors the α-subunit to the membrane (Tajima et al., 1986; Miller et al., 1995). Both subunits have GTPase activities and the β-subunit is thought to make contact with Sec61 and to regulate RNC transfer to the channel (Rapiejko and Gilmore, 1997; Fulga et al., 2001; Helmers et al., 2003; Young et al., 1995). We therefore generated a polyclonal antibody against the purified canine SRP-receptor β-subunit and repeated the cosedimentation experiments. Similar to the α-subunit, the β-subunit could not be found in stable association with Sec61 or the targeted RNCs (data not shown).

In summary, SRP-receptor is necessary for SRP-dependent targeting, but is not detected in a complex with RNC/SRP or Sec61, indicating that it is no stable component of the new binding site. This is consistent with previous observations that have failed to detect a stable complex between RNC, SRP and the SRP-receptor in the presence of Sec61 and point to a more transient role of SRP-receptor, as the complex can be observed in the absence of Sec61 (Rapiejko and Gilmore, 1997; Song et al., 2000). As GTP-hydrolysis is not necessary for the targeting reaction, nonhydrolyzable GTP-analogues do not trap a transfer intermediate (Figure 8A, Connolly et al., 1991; Rapiejko and Gilmore, 1994).

4.4 A free channel population observed after membrane saturation
Surprisingly, solubilization of rough microsomes yielded a fraction of Sec61 that migrated on top of the sucrose gradient, even when an excess of ribosomes had been used for binding (Figure 9A, B). As shown before, rough microsomes did not bind nontranslating ribosomes or RNCs in the absence of SRP (Figure 5C). To confirm this observation, we saturated membranes with nontranslating ribosomes so that targeting of ppl86 became strictly SRP-dependent (Figure 10A) and no more ribosomes could associate with the membrane (Figure 10C). We immediately solubilized the same

membranes and separated ribosome-bound from free Sec61 on a sucrose gradient. Immunoblotting for Sec61α revealed that about 30% was not bound by ribosomes and remained on top of the gradient together with the SRP-receptor (Figure 10B). Longer centrifugation times showed that SRP-receptor and free Sec61 are not associated with each other (data not shown).
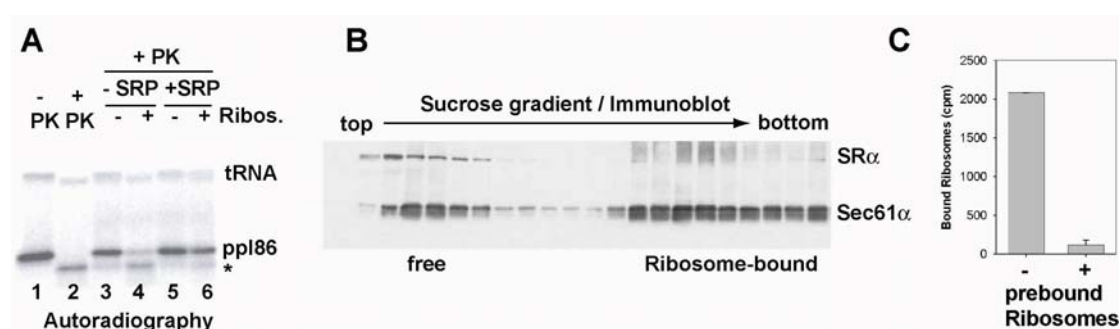
Figure 10: A significant fraction of free channel can be detected under conditions where SRP is necessary for targeting. **A)** PKRMs were used as such (-Rbs) or nontranslating ribosomes were bound and the membranes reisolated (+Rbs). Wheat-germ translated ppl86-RNCs were incubated with the membranes in the absence or presence of SRP. Protease (PK) protection was used for detection of the inserted ppl86. tRNA: ppl86 associated with peptidyl-tRNA. asterisk: nascent chain fragment protected only by the ribosome **B)** The same presaturated PKRMs used in A) were solubilized and separated on a sucrose gradient. Sec61α and SRα were detected by immunoblotting. **C)** Radiolabeled ribosomes were incubated with PKRMs and PKRMs in the absence and presence of prebound ribosomes. The membranes were sedimented and analyzed by scintillation counting. The same saturation conditions as in A) and B) were used.

As we could not exclude that Sec61 was released from the ribosome during solubilization, we devised a method to assess the presence of free channel in an intact membrane. An antibody against the cytosolic C-terminus of Sec61α (Neuhof et al., 1998) is likely to recognize only unbound channel in the membrane, as the bound channel is sterically shielded by the ribosome (Menetret et al., 2000; Menetret et al., 2005). We saturated membranes with nontranslating ribosomes so that targeting of ppl86s became SRP-dependent. Subsequently, anti-Sec61α antibody was added to the intact membranes. After binding and removal of unbound antibody, membranes were solubilized and ribosome-bound and free channel were separated as before. The IgG heavy chain of the Sec61-bound antibody could be detected by immunoblotting.
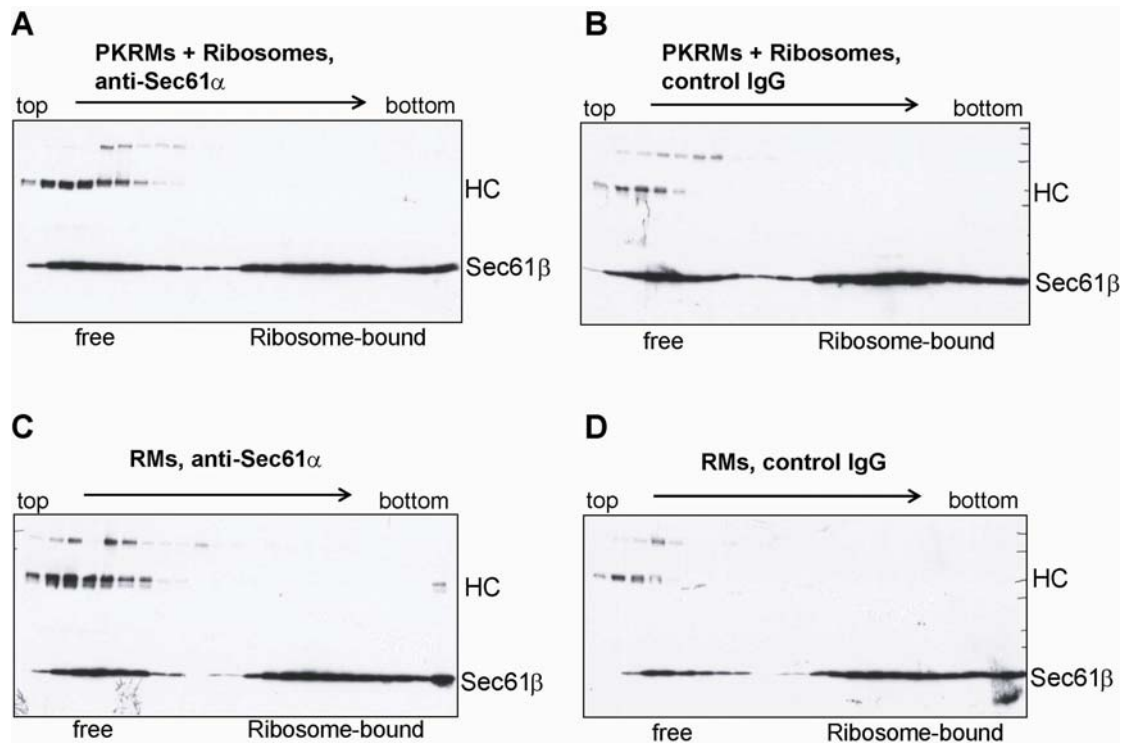
Figure 11: A free Sec61 population detected by antibodies in native membranes. **A)** PK-RMs were pre-saturated with nontranslating ribosomes, and reisolated. The membranes were incubated with an excess of affinity-purified antibodies to Sec61α antibody, re-isolated again by sedimentation, and solubilized in digitonin. The extract was subjected to sucrose gradient centrifugation and fractions were analyzed by immunoblotting for Sec61β and IgG heavy chain (HC). The sedimentation position of the ribosomes is indicated. **(B)** As in **(A)**, but membranes were incubated with the same amount of normal rabbit control IgG. (**C**) As in **(A)**, but using RMs. **(D)** As in **(B)**, but using RMs.

Sec61α-antibodies were found to comigrate exclusively with the free channel population (Figure 11A). Using the same amount of normal rabbit control IgG resulted only in little contamination that was not associated with the free Sec61 fraction (Figure 11B). This indicates that the bound ribosomes prevent the channel from interacting with the antibody as expected, and that a free channel population was detected in the membrane prior to solubilization.

We repeated the experiment using native rough microsomes, that carry endogenous ribosomes and RNCs. Again, anti-Sec61α antibody was absent from the ribosome-bound channels but comigrated with the free channel population (Figure 11C). The same amount of normal rabbit control IgG resulted only in little contamination that was not associated with the free Sec61 fraction (Figure 11D).

We conclude that the observed free channel population is present in intact membranes and no solubilization artefact. Although the binding curve predicts that 90–95 % of the ribosome binding sites should be occupied under the conditions used, and

ribosome binding has been shown to be very stable once formed (Figure 5A), about 30% of Sec61 are devoid of ribosomes (Figure 10).

As the SRP-receptor is known to be necessary for targeting, we asked if it is important for the presence of a free channel population. To this end, we generated proteoliposomes with Sec61 alone and with both Sec61 and SRP-receptor, the minimal system for SRP-dependent targeting (Neuhof et al., 1998). Both preparations were incubated with an excess of ribosomes. Subsequent solubilization and separation of ribosome-bound from free channel on a sucrose gradient revealed that free channel was present in both cases (Figure 12).
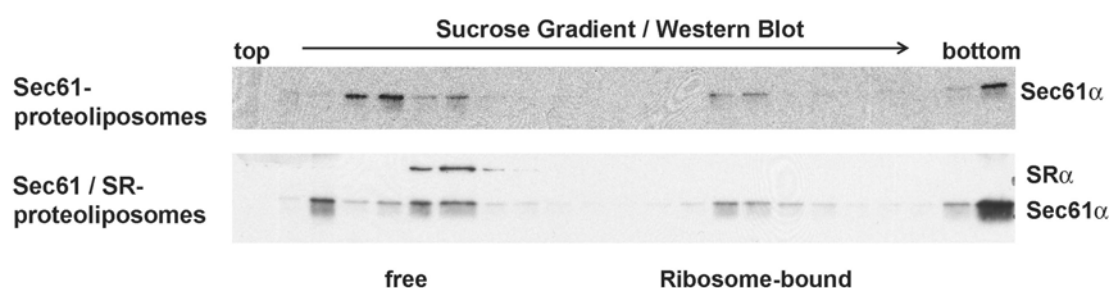
Figure 12: Occurrence of free channel does not depend on the presence of SRP-receptor. Purified canine Sec61 alone or Sec61 and SRP-receptor (SR) were reconstituted into proteoliposomes. Proteoliposomes were incubated with an excess of nontranslating ribosomes, reisolated and solubilized. The extract was separated on a sucrose gradient, Sec61α and SRα were detected by immunoblotting. Ribosome-bound and free fractions are indicated.

This indicates that the SRP-receptor is not required for the presence of a free channel population. Hence, Sec61 alone seems to be able to form a high- and a low-affinity binding site for ribosomes in the membrane.

4.5 Importance of the free channel population for SRP-dependent targeting

We subsequently addressed the importance of the free channel population for SRP-dependent translocation by further increasing the concentration of ribosomes during presaturation. The ribosomes used before were present in excess and concentrated at approximately the concentration that is present freely in the cytosol of a secretory cell (0.3μM; Blobel and Potter 1967; Ramsey and Steele 1967; Barle et al., 1999). Sedimentation of ribosomes and resuspension in a small volume yielded higher concentrations of ribosomes, that were used for ribosome prebinding. After removing excess ribosomes, a sample of the membranes was solubilized, separated on a sucrose gradient and analyzed by immunoblotting for Sec61α (Figure 13A). Another sample

was used to conduct a targeting assay in the absence and presence of SRP. Insertion of the radiolabeled ppl86 into Sec61 was monitored by protease protection (Figure 13B). Increasing the concentration of ribosomes during binding decreased the amount of free channel observed until almost quantitative saturation was achieved at very high ribosome concentrations (Figure 13A, lowest panel). This shows that the free channel population can bind nontranslating ribosomes only at very high ribosome concentrations. The more free channel is present, the more efficient ppl86 targeting becomes, both in the absence and presence of SRP (Figure 13B and C). SRP can promote targeting in all situations, although the efficiency is reduced at unphysiologically high ribosome concentrations (Figure 13C).
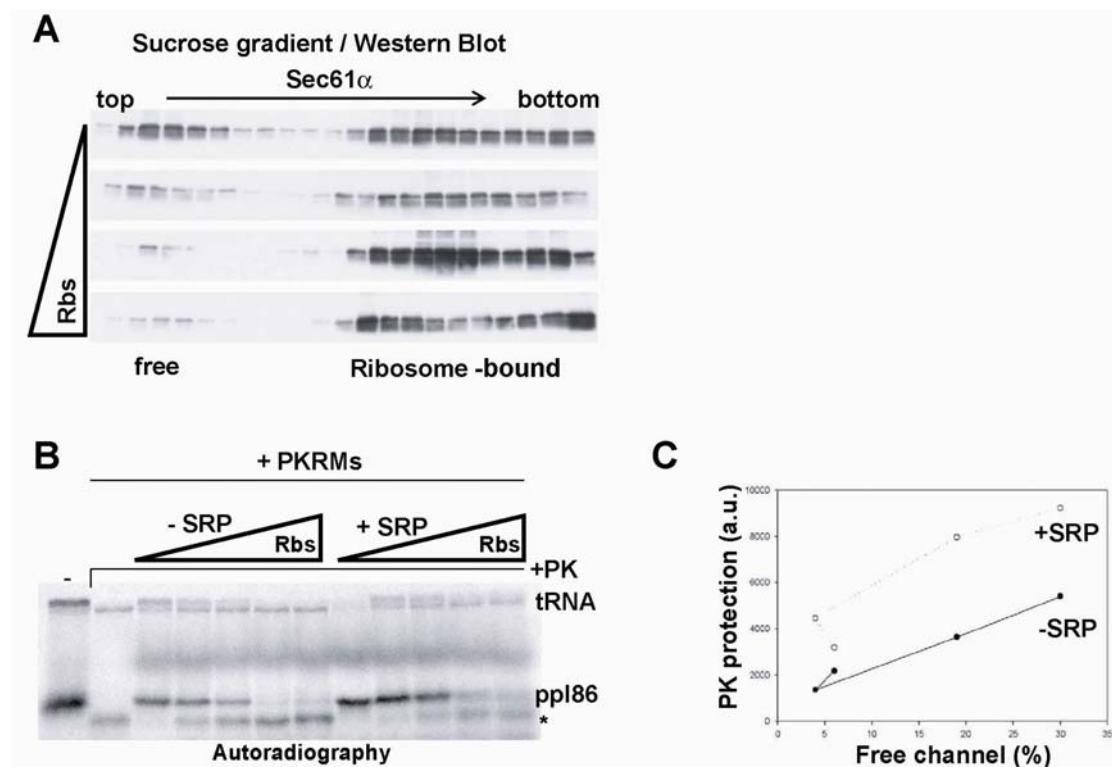
Figure 13: The free channel is capable of binding ribosomes at elevated concentrations. This impairs targeting. **A)** PK-RMs were pre-incubated with increasing concentrations of purified ribosomes (0.3, 0.6, 1.3, and 1.6μM), re-isolated, and solubilized. A detergent extract was subjected to sucrose gradient centrifugation and fractions were analyzed by immunoblotting for Sec61α. Free and ribosome-bound fractions are indicated. **B)** The same membranes analyzed in A) were used for protease (PK) protection experiments to assess targeting. Radiolabeled ppl86 nascent chains were targeted in the absence and presence of SRP. The asterisk indicates a degradation fragment protected by the ribosome alone. tRNA: nascent chain associated with peptidyl-tRNA. **C)** Quantitation of free channel from A) and protease-protected ppl86 from B).

We have shown that the free binding site is not accessible to physiological concentrations of nontranslating ribosomes or RNCs, if SRP is absent (Figure 5C,

Figure 10, Figure 11A,C). If a functional SRP-system is present, targeting of RNCs can be accomplished (Figure 6). It is therefore likely that the free channel population constitutes the initial entry site for SRP-dependent targeting, which would also explain why dissociation of prebound ribosomes is not required. If the free channel population needs to be captured by the membrane-bound RNC/SRP/SR-complex, targeting should be slower if less free channel is present. We therefore investigated the kinetics of SRP-dependent targeting at different concentrations of free channel. The membranes contained identical total amounts and concentrations of Sec61, while the amount of free channel was adjusted by presaturating with increasing concentrations of ribosomes.
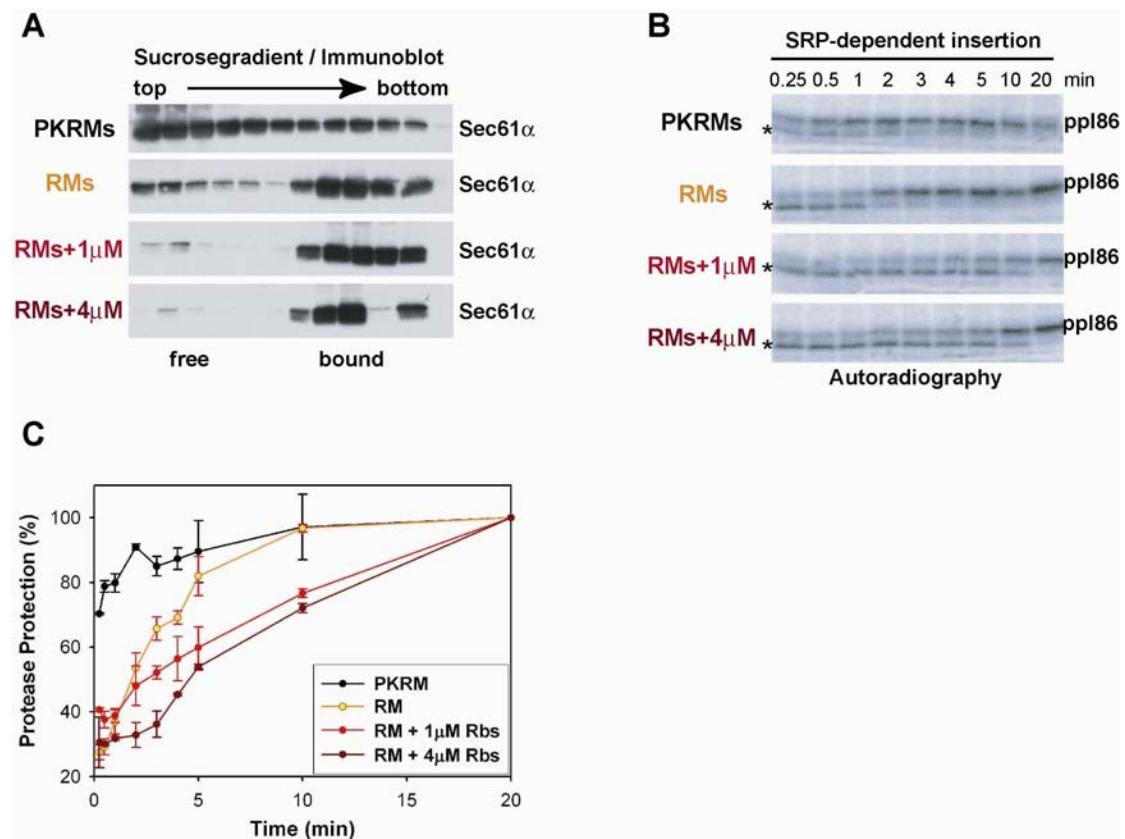
Figure 14: A) Untreated PK-RMs (black), RMs (yellow), or RMs pre-incubated with $1\mu M$ (red) or $4\mu M$ (dark red) purified ribosomes were re-isolated and solubilized. The extract was separated by sucrose gradient centrifugation and analyzed by immunoblotting for Sec61α. **B)** The membranes used in A) were incubated with reticulocyte lysate ppl86mer translated in reticulocyte lysate in the presence of endogenous SRP. All samples were treated with proteinase K at different time points to determine insertion of ppl86 into the channel. The asterisk indicates the nascent chain fragment protected by the ribosome alone. **C)** Quantitation of B). The percentage of protected ppl86 is given.

Ribosome-free PKRMs were compared to ribosome-bearing RMs and RMs additionally incubated with high concentrations of ribosomes. After removal of

unbound ribosomes, a sample was solubilized and analyzed on a sucrose gradient to separate ribosome-bound from free Sec61. Consistent with our earlier observation, the amount of free channel decreased as higher concentrations of ribosomes were used for prebinding (Figure 14A). To measure targeting kinetics, samples of these membranes were incubated with ppl86 in the presence of SRP and the reaction was stopped on ice at different time points (Figure 14B; quantitation in Figure 14C). Protease protection of ppl86 is fastest in PKRMs with full insertion of ppl86 being achieved almost instantaneously (Figure 14A,B,C; black lines). In RMs, there is a clear delay in the appearance of the protease protected fragment when compared to PKRMs (Figure 14A,B,C; yellow lines). If the concentration of free channel is further reduced, ppl86 targeting slows down considerably (Figure 14A,B,C, red and dark red lines).

The kinetic measurements show a correlation between the presence of a free channel population and the rate of SRP-dependent targeting, indicating that the free channel is used as an entry site for translocation. This is consistent with the earlier observation that prebound ribosomes do not dissociate during targeting. The SRP system is not limiting for the reaction, as it is identical in all samples and SRP is binding RNCs and the SRP-receptor with subnanomolar affinity (Flanagan et al., 2003; Gilmore et al., 1982). The insertion kinetics therefore indicate that capturing a free channel is the rate-limiting step in targeting.

4.6 Differences between free and bound Sec61

The affinity of ribosomes to Sec61 predicts that 90–95% of the ribosome binding sites should be occupied when 0.3μM ribosomes are used for saturation. Surprisingly, under these conditions 30-40% of Sec61 are found in an unbound, free population. This argues that two physically different ribosome binding sites might exist. Both have to be formed by Sec61, however, as they can be observed in Sec61-proteoliposomes (Figure 12). Also, the fractions are interconvertible, as the free channel can be forced to bind ribosomes by high ribosome concentrations (Figure 13). Cryo-EM structures of Sec61-ribosome-complexes reveal that the ribosome-bound channel is an oligomer, most likely a tetramer (Menetret et al., 2000; Morgan et al., 2002; Menetret et al., 2005; Figure 15C). The ribosome-bound density contains both Sec61 (Figure 15A, pink mesh) and TRAP (Translocon associated protein complex; Figure 15, green), a protein of unknown function that is part of the translocon

complex but appears to be dispensable for translocation (Menetret et al., 2005, Goerlich and Rapoport, 1993).
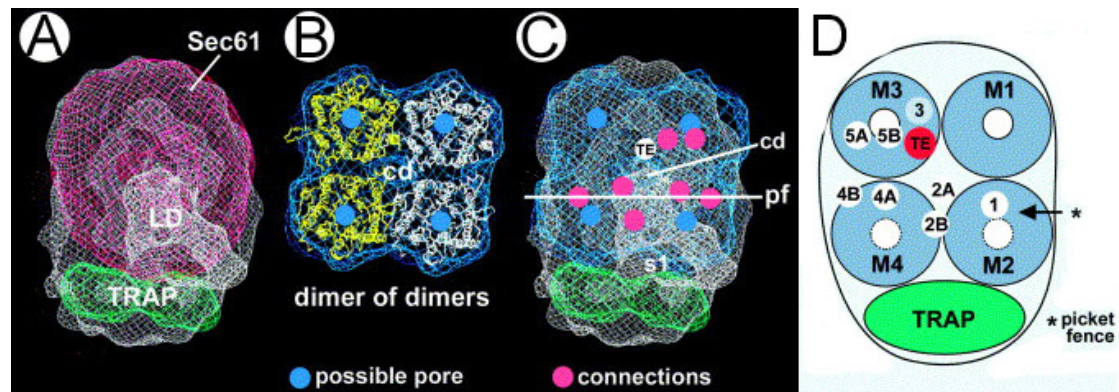
Figure 15: Ribosome-bound channel viewed from the ribosomal side (all pictures from Menetret et al., 2005). **A)** The white mesh shows the channel complex containing Sec61 (pink, Menetret et al., 2000) and TRAP (green mesh: bacteriorhodopsin structure which has the same amount of transmembranehelices as a TRAP-dimer). LD: Lumenal domain of TRAP. **B)** A proposed tetramer of M. janaschii SecYEG channels (van den Berg et al., 2004). cd: central depression; pf: picket fence-like arrangement of ribosome-channel connections. **C)** The volume of two SecYEG dimers correspond reasonably well with the Sec61-part of the native channel structure (white mesh). In pink, connections to the ribosomes are marked. Blue dots indicate the channel pores (van den Berg et al., 2004). TE: End of the ribosomal exit tunnel. **D)** Model of the proposed arrangement of Sec61(blue; M1-4) and TRAP (green) in native membranes. The connections to the ribosome are labeled in white (1, 2A, 2B, 3, 4A, 4B, 5A, 5B). The end of the ribosomal exit tunnel is labeled in red (TE). The asterisk indicates the picket fence of channel-ribosome connections that has been observed.

At 20.5Å resolution (determined by Fourier Shell Correlation cutoff of 0.5, $FSC_{0.5}$), there are 7 contact points between Sec61 and the ribosome visible (Figure 15C, D). While 5-6 contacts are formed with a bona fide Sec61 dimer within the tetramer (Figure 15D, "M3", "M4"), the other dimer obtains only 1-2 connections (Figure 15D, "M1", "M2"). As the binding sites are unevenly distributed, a part of the channel might be able to laterally leave a ribosome-bound complex (for example "M1" in Figure 15D), giving rise to a monomeric or dimeric free channel population. To test this hypothesis, we first investigated if there is an equilibrium between the free and bound Sec61, which would be expected if they are present in different oligomeric states. After solubilization of membranes, we isolated the free and ribosome-bound channel populations and reconstituted them into proteoliposomes (Figure 16 A,D). Figure 16D shows an immunoblot of the reconstituted membranes after sedimentation to remove protein that had not been incorporated into proteoliposomes (Figure 16D, "Rc."). The final preparation sedimented as expected, indicating the presence of intact

vesicles. The Sec61 content of the final proteoliposome preparations was compared to

RMs (Figure 16D, "Rc. product").
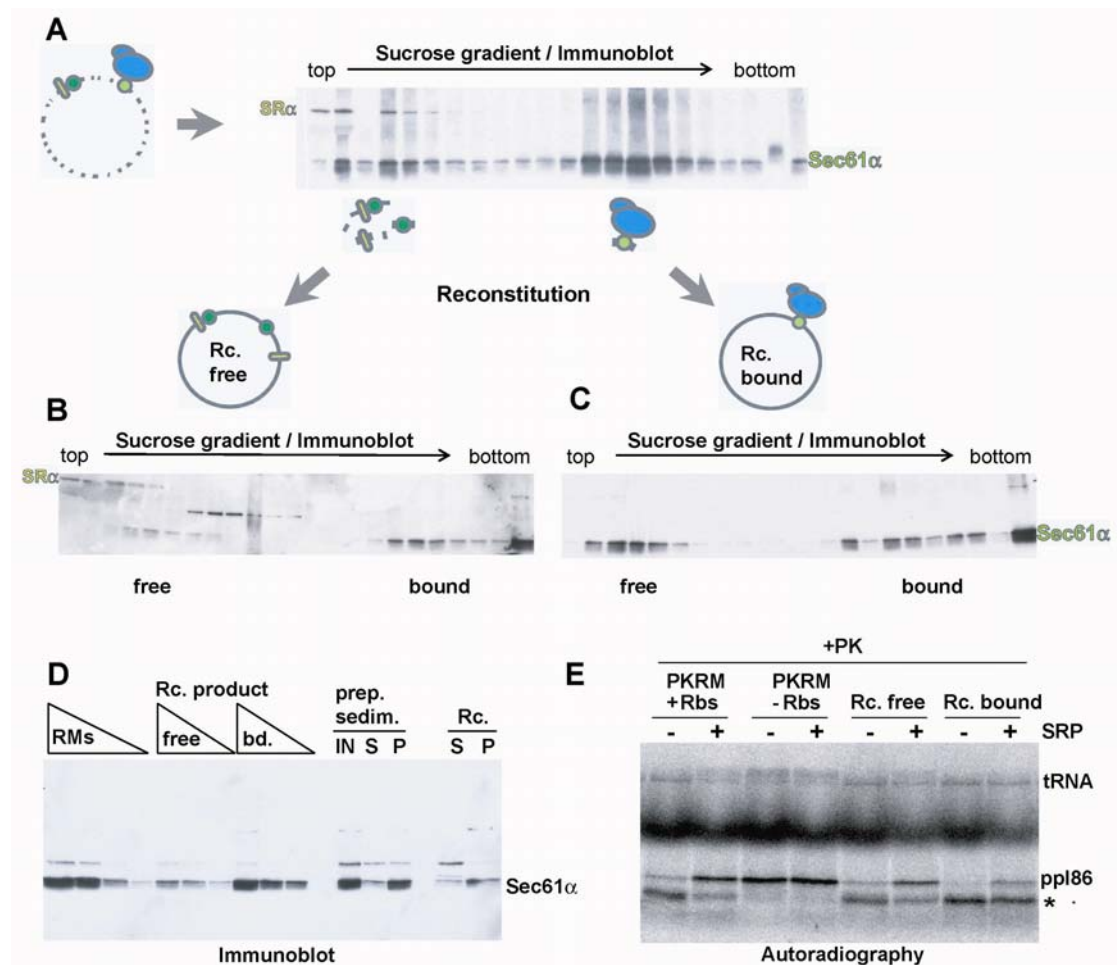
Figure 16: Free and bound channel are interconvertible and in an equilibrium with each other. **A)** Rough microsomes were solubilized in DBC and ribosome-bound channel (light green; Rbs. blue) was separated from free channel (dark green) and other light proteins (i.e. SRP-receptor, yellow) by sucrose gradient centrifugation. An immunoblot for Sec61α and SRα is shown. Isolated free and ribosome-bound channel populations were reconstituted into proteoliposomes (Rc. free and Rc. bound, respectively). **B)** Ribosomes were added to the free channel vesicles and they were solubilized and separated on a sucrose gradient as before. Sec61α and SRα were detected by immunoblotting. Both proteoliposomes give rise to a free and a bound population of Sec61 again. **C)** as B, but without extra addition of ribosomes. **D)** Reconstitution is feasible as assessed by immunoblotting against Sec61α. Rough microsomes (RMs) are loaded next to the final products reconstituted free (Rc. free) and bound (Rc. bound) vesicles. Samples taken during channel preparation (prep. sedim.): IN: starting material solubilized RMs; S: free channel population; P: bound channel population; After reconstitution (Rc), proteoliposomes were sedimented (P): Unincorporated protein remained in the supernatant (S). **E)** Protease (PK) protection experiment using ribosome-free PKRMs (-Rbs), PKRMs with prebound ribosomes (+Rbs) or the reconstituted free (Rc. free) and bound channel (Rc. bound) vesicles. Ppl86 was translated in wheat germ extract and purified canine SRP was added or omitted. The asterisk indicates a degradation fragment protected in the ribosome; tRNA: peptidyl-tRNA-associated ppl86.

The membranes harboring only the free or the bound channel population ("Rc. free" and "Rc. bound", respectively) were used to investigate if they gave rise to two populations again. Ribosomes were added to the reconstituted free fraction under the same conditions used for the initial ribosome binding. Subsequently, both samples were solubilized and separated on a sucrose gradient. Both gave rise to a very similar distribution between free and bound channel as the original native membrane (Figure 16A, B, C). Hence, the reconstituted free channel gains the ability to bind ribosomes, while the bound channel releases Sec61 to reform a free channel population. In a functional SRP-dependent targeting assay, both the reconstituted free and the reconstituted bound channels behaved identical to membranes with prebound ribosomes (Figure 16E).

These results indicate that there is an equilibrium between two physically different states of the Sec61 translocon. The ratio between free and bound Sec61 seems to adjust itself at a given ribosome concentration, indicating that both species are interconvertible.

The oligomeric state of free Sec61 in the membrane has so far remained elusive. Due to the small size of Sec61, electron cryo-microscopy analysis is limited to channels with ribosomes bound. Purified Sec61 in detergent seems to form particles of various dimensions, as judged by negative staining and electron microscopy (Jean-François Ménétret, personal communication). The bacterial homolog SecYEG has been shown to be highly dynamic and present in different oligomeric states in membranes (Bessonneau et al., 2002; Scheuring et al., 2005).

The conformational state of the Sec61p complex can be probed by the reagent bismaleimidohexane (BMH), which will crosslink the single cysteines of two β-subunits if they are in close proximity (Partis et al., 1983; Kalies et al., 1998). RMs were treated with BMH, and solubilized. The extract was separated by sucrose gradient centrifugation and analyzed by immunoblotting. The identity of BMH-dependent crosslinks (Kalies et al., 1998) was verified by probing the same sample and samples from Sec61-proteoliposomes with different antibodies and identifying detection overlaps (data not shown). Immunoblotting against both Sec61α and Sec61β without crosslinking confirmed that free channel is present (Figure 17A). The solubilized ribosome-channel complexes migrate normally in a sucrose gradient

(Figure 17B, black line). Crosslinking did not change the ratio between free and bound channel or the ribosomal migration pattern (Figure 17B, red line).
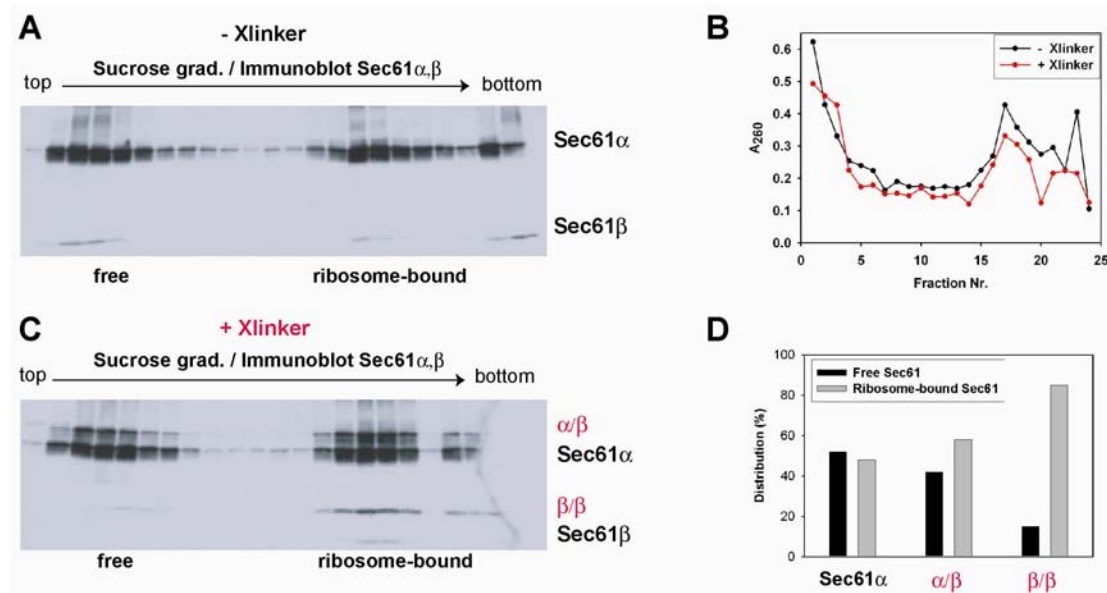
Figure 17: The free and ribosome-bound channel population differ in their conformational states. Rough microsomes (RMs) were treated with buffer or 1mM BMH for 30min on ice, quenched, solubilized and separated on a sucrose gradient. **A)** Immunoblot of buffer-treated RMs detecting both Sec61α and Sec61β in a ribosome-bound and a free form. **B)** A_{260} measurement of the fractions from top to bottom, showing a ribosomal peak (Fractions 15-20) both without (black line) and with crosslinker (red line) treatment. **C)** Immunoblot of BMH-crosslinked RMs detecting both Sec61α and Sec61β in a ribosome-bound and a free form. **D)** Quantitation of the band intensities in C) for Sec61α, the α/β crosslink and the β/β crosslink in both free (black bars) and ribosome-bound channel fraction (grey bars).

Exposure to BMH leads to a Sec61β/β crosslink that is essentially confined to the ribosome-bound fraction (Figure 17C, β/β; quantitation in D), while a Sec61α/β crosslink is present to similar extent in both the free and the bound channel population (Figure 17C, α/β; quantitation, in D). The Sec61β/β crosslink migrates at the expected size for two connected Sec61β molecules. A crosslink between randomly interacting Sec61β in the membrane is unlikely, as the free channel does not give rise to the crosslink. The β/β crosslink could therefore be taken as indicative of oligomerization, a result consistent with structural data available for the ribosome-bound channel (Menetret et al., 2005, Morgan et al., 2002). The free channel, however, fails to display a β/β Xlink and must thus be present in a different conformational state. It is unlikely that the crosslink is absent because of subtle differences in Sec61β arrangement within the oligomer, as the cysteine in Sec61β is 31 amino acids from the membrane on the cytosolic side, which equals a distance of

more than 50Å assuming an α-helical conformation (Mitra et al., 2004). Together with the 16Å spacer arm length of BMH, most Sec61 arrangements should yield a crosslink (Partis et al., 1983). Thus, the results seem to suggest different oligomeric states of the free and bound Sec61. A smaller oligomeric state of Sec61 in the free population, i.e. a Sec61 monomer or dimer, would explain its lower affinity for ribosomes, as it could not form as many contacts with the ribosome as a tetramer can (Menetret et al., 2005). The binding of ribosomes at high concentrations to the free channel could be explained by a higher probability of a spontaneously formed oligomer interacting with a ribosome under these conditions. Alternatively, a weakly bound ribosome could act as a scaffold and assemble a full oligomer (Hanein et al., 1996).

4.7 Biochemical analysis of the ribosome-channel junction

We further investigated if the free and the bound channel populations are interconvertible and different from each other, as suggested by Figures 14 and 16. To this end, we tested whether the ribosome-channel junction is static or dynamic. Aurintricarboxylic Acid (ATA) is a polyanionic, highly conjugated compound that inhibits protein-nucleic acid interactions (Figure 18B; Gonzalez et al., 1980). It has been used to prevent ribosome binding to canine microsomes and does not adversely effect the integrity of ribosomes (Borgese et al., 1974, Fresno et al., 1976). If ribosome-channel binding was static, adding ATA after binding has occurred, should have no effect. If the binding was dynamic, the ribosome-channel contacts would break and reform over time and ATA could prevent their reformation. This should lead to dissociation of prebound ribosomes over time.

We bound radiolabeled ribosomes to dog microsomes, removed unbound ribosomes and split the sample into three portions: One was treated with buffer, one with ATA at 0°C and one with ATA at 28°C. Membranes were sedimented at different time points and analyzed by scintillation counting. While in the presence of buffer no dissociation of prebound ribosomes was observed (Figure 18A, black line), ATA lead to strong dissociation that was complete after five minutes at 28°C (Figure 18A, red line). Even at 0°C, ATA induced dissociation of prebound ribosomes, albeit more slowly and to a lesser degree (Figure 18A, blue line).
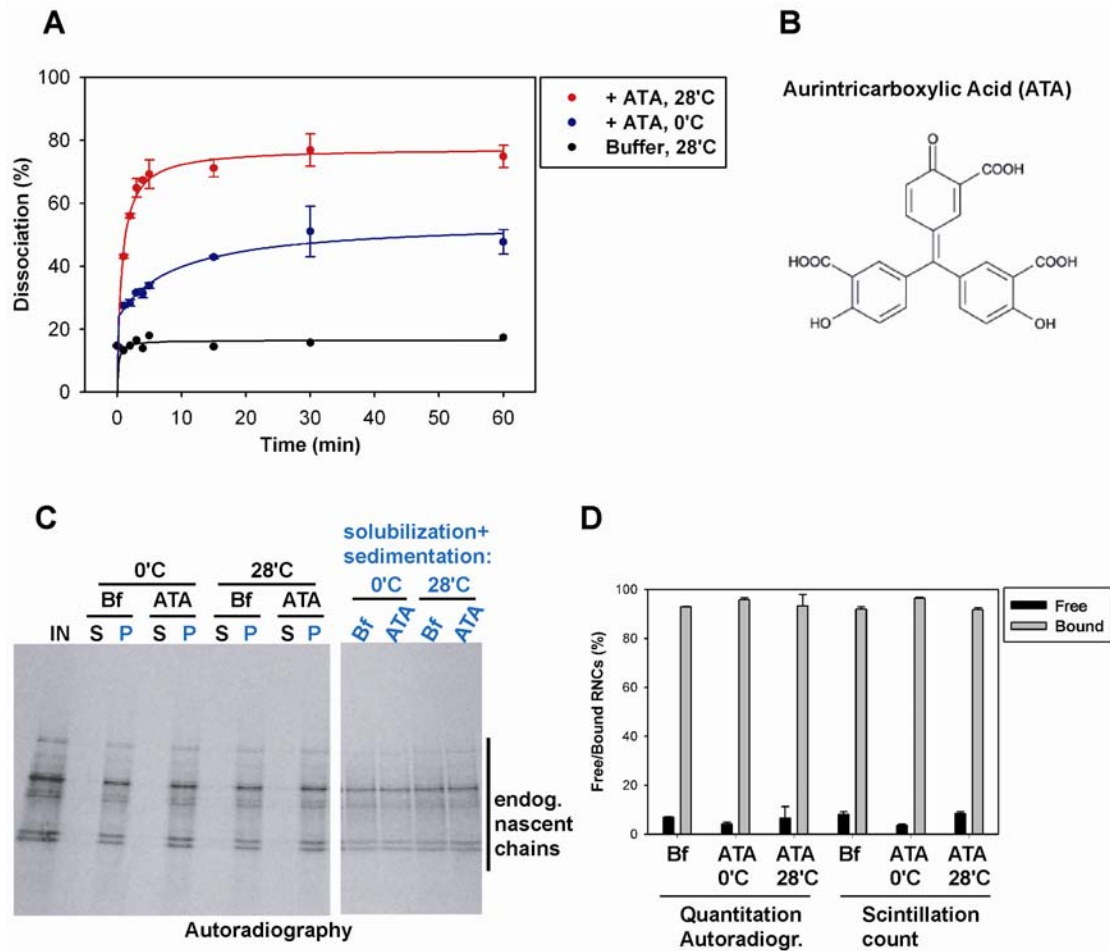
Figure 18: Aurintricarboxylic Acid (ATA) can dissociate prebound ribosomes without disassembling them. **A)** Radiolabeled ribosomes were bound to PKRMs. Samples of the membrane were incubated with buffer (28°C, black line) or 100μM ATA (28°C, red line; 0°C, blue line). Dissociation was assayed by sedimentation of membranes and scintillation count of both supernatant and pellet. **B)** Structure of ATA. **C)** Endogenous nascent chains were radiolabeled in rough microsomes. The purified membranes were incubated with buffer or 100μM ATA at both 0°C and 28°C. Membranes were sedimented and both supernatant (S) and pellet (P) analyzed by autoradiography. Samples of the pellet were solubilized and RNCs sedimented (blue). **D)** Quantitation of the autoradiography shown in C) and a similar experiment using scintillation counting as a readout.

It has been reported that ATA leaves ribosomes intact (Fresno et al., 1976). To ensure that ribosomes are not disassembled by ATA, we investigated the dissociation of labeled RNCs. When membrane-bound RNCs are disassembled, the nascent chain will be set free, either into the lumen or into the cytosol. RMs were incubated with an mRNA-free in vitro translation mixture containing ^{35}S-methionine, labeling the nascent chains of endogenous, RM-bound RNCs (Blobel and Dobberstein, 1975a; Matlack and Walter, 1995). After sedimentation, labeled membranes were incubated with buffer or ATA at both 0°C and 28°C and sedimented (Figure 18C). In all cases, the endogenous nascent chains cosedimented with the microsomes. No release of

40

nascent chains into the supernatant was observed (Figure 18C, "P"). When a sample of the sedimented membranes was solubilized and ribosomes sedimented by ultracentrifugation, radiolabeled nascent chains cosedimented with the ribosomes, indicating that they were still associated. There was no difference between those membranes treated with buffer or ATA (Figure 18C, blue; for quantitation, see D, Autoradiography). Similar results were obtained when samples were analyzed by scintillation counting (Figure 18D, Scintillation count). These experiments confirm that ATA does not interfere with ribosome integrity (Fresno et al., 1976). As prebinding was done in the absence of ATA and the binding is very stable (Figure 5A), a static model for ribosome binding fails to explain the fast and efficient dissociation observed. It is unlikely that ATA functions as an effector and actively disrupts the contact sites between ribosome and channel, as there are seven visible contacts, which all have a different molecular environment (Menetret et al., 2005).

The results can be well explained by assuming that the binding is dynamic, constantly breaking and reforming contacts. Reformation of contacts would be prevented by ATA, and the ribosome would eventually dissociate. This model could also explain the extraordinary stability of ribosome binding to Sec61 (Figure 5), as disruption of one or two contacts at a time would not lead to dissociation. Instead, the ribosome would be held in place by the remaining connections until the contact has reformed. For dissociation, all seven connections would need to be disrupted at the same time, which is unlikely.

While the ATA experiments indicate a dynamic ribosome-channel junction, we could not distinguish between the Sec61 oligomer staying intact while ribosome contacts were breaking and reforming, and Sec61 molecules leaving the complex laterally. The latter option seems possible, as we have observed that the free and the bound channel population are interconvertible and in an equilibrium with each other (Figure 16).

In order to address this question, we used the protease chymotrypsin. Chymotrypsin selectively digests the free channel, while the ribosome-bound channel is protected from degradation (Kalies et al., 1994). Once Sec61 has been treated with chymotrypsin, it loses its ability to bind ribosomes (Raden et al., 2000). If free channel is digested and in exchange with the bound, protected channel population, dissociation of ribosomes might be observed over time.

First, we wanted to ensure that chymotrypsin only digests free channel under the conditions used. The serine protease chymotrypsin cleaves Sec61α at R_{274} and K_{393} (Figure 19A, red; Song et al., 2000). An antibody directed against the C-terminus of Sec61α (Figure 19A, red) recognizes an 8kD (C-terminus to K393; Figure 19A, double asterisk) and a 15kD fragment (C-terminus to R274; Figure 19A, single asterisk) following proteolysis.
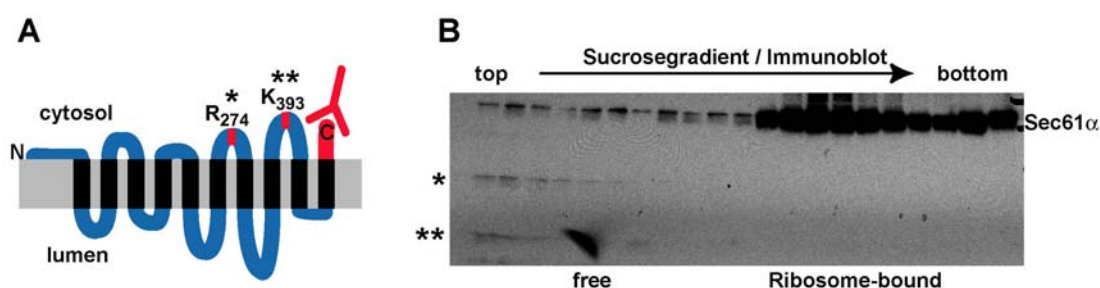
Figure 19: Chymotrypsin selectively digests free channel. **A)** Topology of Sec61α in the ER membrane (grey). Transmembrane segments are shaded black. C-terminal antibody binding is depicted (red) and the chymotrypsin cleavage sites are shown (red; R_{274} and K_{393}; Song et al., 2000). **B)** Rough microsomes have been digested with 50μg/ml chymotrypsin for 1h on ice. After inactivating the protease, membranes were solubilized and separated on a sucrose gradient. Immunoblotting detects full length Sec61α, a 15kD degradation fragment (*) and a 8kD degradation fragment (**) consistent with the predicted cleavage sites (A). Free and ribosome-bound fractions are indicated.

PRKMs with prebound ribosomes were treated with chymotrypsin, solubilized, and the free and the ribosome-bound channel were separated by sucrose gradient centrifugation and analyzed by immunoblotting. The 8kD and 15kD degradation fragments comigrate with the free channel population only (Figure 19B, asterisks), which is consistent with published results (Kalies et al., 1994).

Next, we investigated whether the degradation of free Sec61 influences the equilibrium and leads to dissociation of ribosomes over time. Radiolabeled ribosomes were bound to canine microsomes, excess ribosomes removed and the sample split in half. To one half, buffer was added, whereas the other half was treated with a low concentration of chymotrypsin as in Figure 19B. While no significant dissociation is observed in the buffer control (Figure 20A, black line), chymotrypsin treatment resulted in clear dissociation of prebound ribosomes over time (Figure 20A, red line). This indicates that the selective digestion of unbound Sec61 can influence the stability of prebound ribosomes at the membrane.
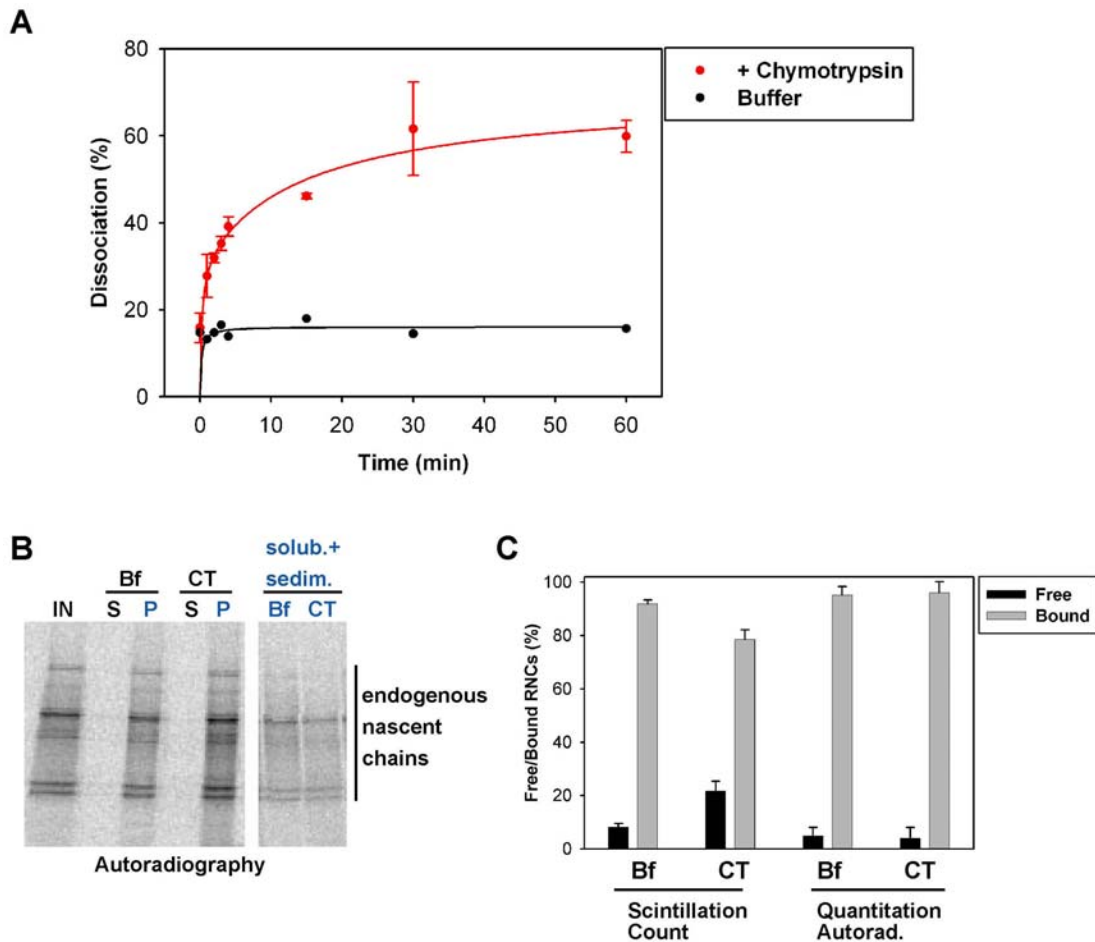
Figure 20: Low concentrations of chymotrypsin can dissociate prebound ribosomes without disassembling them. **A)** Rough microsomes were incubated with buffer (black line) or 50μg/ml chymotrypsin (red line) on ice. The protease was inactivated at different time points and membranes were sedimented. Both supernatant (dissociated ribosomes) and pellet (bound ribosomes) were analyzed by scintillation counting. **B)** 50μg/ml chymotrypsin does not disassemble RNCs. Endogenous nascent chains were radiolabeled in rough microsomes. The purified membranes were incubated with buffer (Bf) or 50μg/ml chymotrypsin (CT) on ice. Membranes were sedimented and both supernatant (S) and pellet (P) analyzed by autoradiography. Samples of the pellet were solubilized and RNCs sedimented (blue). **C)** Quantitation of the autoradiography shown in B) and a similar experiment using scintillation counting as a readout.

We performed control experiments to assess the integrity of membrane-bound ribosomes using the same method as in the ATA experiments. The nascent chains of RM-bound endogenous RNCs were labeled with ^{35}S-methionine and the membranes purified (Figure 20B). Chymotrypsin treatment did not result in endogenous nascent chains being released into the supernatant during membrane sedimentation (Figure 20B,C). Samples of the membrane pellets were analyzed further by solubilizing and sedimenting RNCs by ultracentrifugation (Figure 20B, blue). Buffer-treated and chymotrypsin-treated microsomes showed no difference in nascent chain release and therefore in ribosome disassembly (Figure 20B, lanes 6 vs 7). Figure 20C shows a

43

quantitation of these results and a parallel experiment analyzed by scintillation counting. In the latter case, chymotrypsin leads to a 10% increase in radioactivity in the supernatant, which is only a small fraction of the dissociation observed in Figure 20A. Consistent with the literature, these results indicate that chymotrypsin treatment as performed does not disassemble ribosomes or release significant amounts of RNCs from the membrane (Sabatini and Blobel, 1970; Kalies et al., 1994). Thus, proteolysis of the free channel has an effect on the binding stability of prebound ribosomes. Severed channel molecules cannot be bound by ribosomes (Raden et al., 2000) and may fail to replace Sec61 that is laterally leaving the ribosome-channel complex, leading to dissociation of prebound ribosomes. This is consistent with the observation that free and bound channel are in an equilibrium with each other (Figure 16) and that the ribosome-channel junction is dynamic (Figure 18).

4.8 Working model of SRP-dependent targeting

In summary, we have shown that nontranslating ribosomes bind Sec61 in microsomal membranes very firmly and do barely dissociate (Figure 5A). RNCs carrying a secretory nascent chain fail to bind to these membranes, as all high affinity binding sites are occupied (Figure 5C). They can only bind to the membrane and translocate their nascent chain in the presence of SRP and its receptor (Figure 6). SRP-dependent targeting of RNCs does neither require nor directly result in displacement of prebound ribosomes (Figure 7). Thorough examination of the microsomal membranes revealed that the prebound ribosomes are associated with only a fraction of Sec61 in the membrane (Figure 10). The free channel population binds ribosomes very weakly and cannot be accessed by RNCs in the absence of SRP (Figure 5C). It can form in proteoliposomes containing only purified Sec61 (Figure 12). Kinetic measurements showed that the free channel population is used as an entry site during SRP-dependent targeting (Figure 14). If the free and the ribosome-bound channel population are isolated, they split up in a free and a bound fraction again, showing that they are interconvertible and in an equilibrium with each other (Figure 16). Crosslinking studies showed that the free and the bound Sec61 populations differ in their conformation, likely in their oligomeric state (Figure 17). The ribosome-bound Sec61 is assumed to be a tetramer, maintaining 7 connections with the ribosome (Menetret et al., 2005), while the free Sec61p may be present in a smaller oligomeric state, probably monomeric or dimeric. The connections between oligomeric Sec61 and the

ribosome continuously break and reform, together keeping the ribosome bound (Figure 18). Selective digestion of the free channel leads to dissociation of ribosomes, arguing for an exchange within the two populations and for Sec61 being able to laterally leave the ribosome-channel junction (Figure 20).

Hence, we have the following working model for SRP-dependent targeting (Figure 21): If the channel is freely accessible, ribosomes bind with high affinity and a very slow dissociation rate (Figure 21A). The high affinity binding site is provided by an oligomer of Sec61, most likely a tetramer (Figure 21A, light green). A monomeric or dimeric Sec61 population binds ribosomes only weakly, likely because it cannot form as many connections with the ribosome as a Sec61-tetramer can (Figure 21A, dark green; Menetret et al., 2005). This would make ribosome binding to the free Sec61 very unstable (k_{off} high). The free Sec61 population cannot be directly accessed by RNCs (Figure 21B). RNCs need to take an alternative route, which is provided by the SRP-system. SRP can bind the signal sequence, block the ribosomal Sec61 binding site and target the RNC to the membrane via the SRP-receptor interaction (Figure 21b, red: RNC; yellow: SRP, SRP-receptor). This interaction leads to a conformational change that exposes parts of the Sec61-binding site at the ribosome (Pool et al., 2002; Halic et al., 2006). Interaction with Sec61 will be more probable because diffusion is reduced from three dimensions in solution to two dimensions in the membrane (Figure 21, "2d" vs. "3d"). In addition, the SRP-receptor may play a more active role: After binding the SRP/RNC complex, the transmembrane segment of the SRP-receptor β-subunit may become competent for binding Sec61 and stabilizing the interaction enough so that the nascent chain can start to translocate (Fulga et al., 2001; Helmers et al., 2003). Recognition of the nascent chain by the channel would stabilize the RNC-Sec61 interaction (Jungnickel et al., 1995) and lower the k_{off} rate such that the reaction becomes irreversible. As translocation is ongoing, lumenal chaperones and other foldases will interact with the nascent chain (Kleizen and Braakman, 2004) and thus counteract RNC dissociation from the channel. The complex of SRP and its receptor may not be needed for stabilization beyond the point of signal sequence recognition by Sec61 (Song et al., 2000). After reciprocal activation of GTPase-activity and GTP hydrolysis, SRP dissociates from its receptor (Figure 21B, right panel; Egea et al., 2004).

A: SRP-independent binding
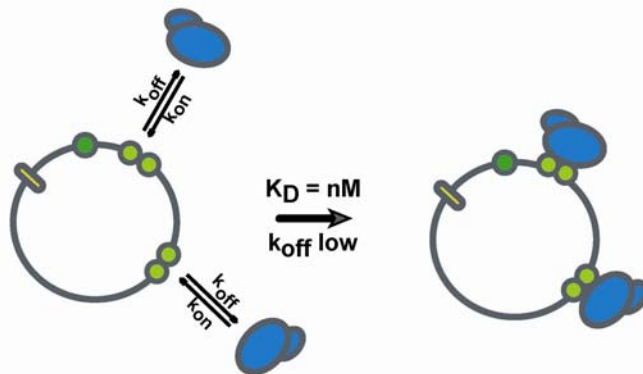
B: SRP-dependent targeting in the presence of competing ribosomes
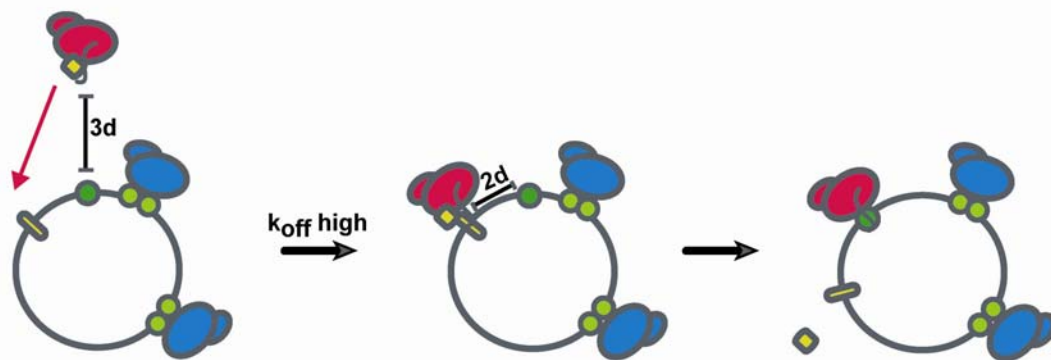
Figure 21: Proposed model for ribosome binding to the ER membrane. **A)** SRP-independent targeting. The protein-conducting channel Sec61 (green) provides high (light green) and low affinity binding sites (dark green). The two binding sites differ in their conformation, likely in their oligomeric state. SRP-independent targeting of both nontranslating ribosomes (blue) and RNCs occurs efficiently to the high affinity binding sites, while the low affinity binding sites remain unbound. **B)** SRP-dependent targeting in the presence of competing ribosomes. If the high affinity binding sites are occupied (as they are in native ER membranes) RNCs (red) cannot bind to the membrane without SRP (k_{off} high). The low affinity binding site can only be accessed when SRP (yellow box) binds the signal sequence and targets the RNC to the membrane via the SRP/SRP-receptor interaction (yellow). This reduces diffusion from three dimensions (3d) to two dimensions (2d). The membrane-bound RNC/SRP/SRP-receptor complex can capture an unbound channel and the RNC can insert its nascent chain. The interaction between the signal sequence and Sec61 stablilizes the complex. SRP and its receptor dissociate from the RNCs, reciprocally stimulate each other's GTPase activity and dissociate. A new cycle can begin.

After the nascent chain has been released from the ribosome, the ribosome may dissociate from the monomeric or dimeric Sec61; alternatively, the membrane-bound ribosome could sequester more free Sec61 molecules over time, so that the binding becomes stable beyond signal sequence cleavage and nascent chain release (not depicted).

4.9 Conditions for dissociation of prebound ribosomes

A question that has not been addressed by our model is how membrane-bound nontranslating ribosomes will dissociate from the channel. There seems to be barely any spontaneous dissociation (Figure 5A) and ribosomes are not displaced by SRP-dependent targeting of translocation substrates (Figure 7). Large subunits have been reported to remain associated with Sec61 after termination of translation (Borgese et al., 1973; Potter and Nicchitta, 2000, 2002).

Interestingly, we were able to observe up to 50% dissociation when incubating the membranes with large amounts of reticulocyte lysate (Figure 22D, "mock"). The effect depends on the amount of reticulocyte lysate added and is saturable (Figure 22A). To obtain 50% dissociation, we needed to use 20 times the amount we have used before for the SRP-dependent targeting experiments (Figure 7). We investigated how much of the dissociating radioactivity was due to ribosomes, as free radiolabel may be present to a small extent (Figure 22B, "total"). After binding to membranes, the unbound radioactivity was analyzed and found to be 50% ribosomal (Figure 22B, "unbound"). After incubating the membranes with a large amount of reticulocyte lysate, the dissociated radioactivity was analyzed by ultracentrifugation. In this case, 90% of the radioactivity was ribosomal (Figure 22B, "bound"). This shows that we are indeed observing dissociation of ribosomes, as the contaminating free label does not bind to membranes and is not affecting the results.

Similar results were obtained when using wheat germ or HeLa-extracts (mitotic extracts and S-phase extracts) instead of reticulocyte lysate. Again, ribosomes did not dissociate when treated with extraction buffer, but up to 50% were released when using HeLa- or wheat germ extract (data not shown). We proceeded by assaying if the dissociation reaction is dependent on translation or translocation. We performed two identical experiments in parallel, with the radiolabel either on the cotranslationally translocated nascent chain (Figure 22C), or on the prebound ribosomes (Figure 22D). We observed translocation of both model substrates preprolactin 86mer (Figure 22C, ppl86) and wildtype preprolactin (Figure 22C, pplwt) by protease protection. As SRP is present in rabbit reticulocyte lysate, translocation was not impaired by the presence of prebound ribosomes (Figure 22C, red +). As a control, a 120mer of the cytosolic firefly luciferase was translated (Figure 22C, luc120). Complete translation inhibition was achieved using cycloheximide (Figure 22C, pplwt+CH).
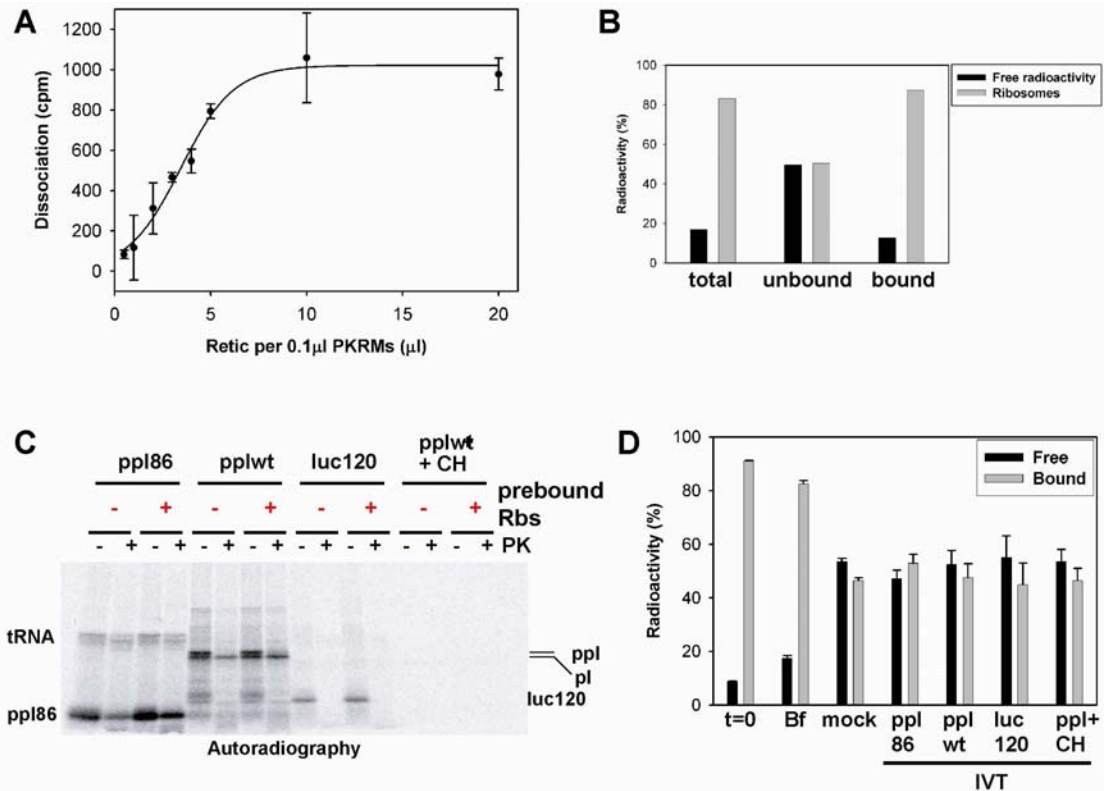
Figure 22: Large amounts of rabbit reticulocyte lysate cause translation-independent dissociation of prebound ribosomes. **A)** The graph shows a quantitation of dissociation using different amounts of reticulocyte lysate (Retic). A plateau was reached at $10\mu l$ Retic per $0.1\mu l$ PKRMs, i.e. $50\mu l$ Retic per eq PKRMs. **B)** The dissociating radioactivity is due to ribosomes. Ribosomes without membranes (total) were sedimented by ultracentrifugation (grey bars), contaminating radiolabel remained in the supernatant (black bars). After binding to membranes and solubilization, 90% of the radiolabel sedimented as ribosomes (bound). The fraction that did not bind to the membranes in the first place contained most of the contaminating radiolabel (unbound). **C)** Protease (PK) protection experiment using different translation substrates ($5\mu l$ Retic/$0.1\mu l$ PKRMs). Ppl86: preprolactin 86mer; pplwt: full length preprolactin; pl: prolactin; luc120: firefly luciferase 120mer; CH: $170\mu g/ml$ cycloheximide **D)** As in C, but using unlabeled IVT and labeled prebound ribosomes. t=0: before incubation; Bf: after incubation with buffer; mock: incubation with reticulocyte lysate.

In parallel, the fate of radiolabeled prebound ribosomes was investigated (Figure 22D). Prebound ribosomes do not significantly dissociate in buffer (Figure 22D, Bf), when compared to the starting point (Figure 22D, t=0). Incubation with a large amount of reticulocyte lysate leads to 50% dissociation (Figure 22C, mock). The amount of dissociation does not change when preprolactin 86mer or full length preprolactin are translocated. Similarly, translation of firefly luciferase 120mer or translation inhibition using cycloheximide has no additional effect on dissociation of prebound ribosomes (Figure 22D, luc120 and pplwt+CH).

In conclusion, it seems that large amounts of cell extracts contain a factor that can dissociate up to 50% of ribosomes from the membrane. Controls showed that the

dissociation is not caused by salts, and independent of translation, translocation or SRP binding to its receptor. We have tried to fractionate reticulocyte lysate to identify the component responsible for dissociation of ribosomes, but were unable to isolate it (data not shown). It is possible that we observe several factors acting together. The fact that only 50% of the radiolabel dissociates, may argue that the observed dissociation is due to release of the small subunit. In fact, it has been shown that the small 40S subunits are in constant exchange with free subunits in the reaction, while the large 60S subunits remain firmly bound (Borgese et al., 1973). Another possibility is that we are observing the effect of the "Detachment Factor", a 50kD proteinaceous component of reticulocyte lysate that has been described to dissociate ribosomes from the membrane (Blobel, 1975). It was shown to reversibly associate with ribosomes, but has not been unambiguously identified (Ionasescu et al., 1981). We have observed SRP-dependent targeting in the absence of cytosol using purified components (Figure 6C), indicating that Detachment Factor is not needed for providing binding sites to the targeting reaction.

Taken together, SRP-dependent targeting does not directly lead to the displacement of firmly bound nontranslating ribosomes. However, dissociation of membrane-bound ribosomes is possible when a large excess of cytosol is present. This is independent of translation and translocation, arguing that SRP-dependent targeting and dissociation of prebound ribosomes may be regulated independently in the cell.

4.10 Structural characterization of ribosome-channel complexes by electron cryo-microscopy

4.10.1 Structure of a eukaryotic ribosome-channel complex

Ribosomes bound to high-affinity binding sites in the ER membrane were previously shown to be associated with a tetramers of Sec61 (Morgan et al., 2002; Menetret et al., 2005). Our biochemical characterization of SRP-dependent targeting, however, revealed that additional, low-affinity binding sites are present at the ER membrane. They might be formed by smaller oligomers of Sec61, most likely monomers or dimers. SRP facilitates the interaction of RNCs with these low-affinity binding sites, so that efficient targeting can occur even in the presence of competing ribosomes. The complex between an RNC and the low-affinity binding site provided by Sec61 is

likely physiologically relevant. However, much of its structure and composition have remained elusive. To characterize this complex, we decided to dissect intermediates of protein translocation by electron microscopy.

Electron cryo-microscopy visualizes unstained and unfixed ribosome particles embedded in vitreous ice. If a homogeneous population of particles is randomly oriented, the three-dimensional structure of an average particle can be determined by single particle reconstruction, which compares a large dataset of selected single particles to computer-generated projections of a reference structure (Frank, 2000). In order to achieve optimal sample homogeneity, we used purified ribosomes or RNCs and purified Sec61 or SecYEG in detergent solution for complex assembly. Sec61 is functional in mild detergents, such as digitonin, and translocation can occur in the absence of membranes (Mothes et al., 1998).

To assemble a eukaryotic ribosome-channel complex, nontranslating wheat germ ribosomes were purified by repeated sedimentation, and a 20x molar excess of purified Sec61 was added. After complex formation, the mixture was frozen on carbon-coated grids. Because only large complexes can be visualized by electron cryo-microscopy, unbound Sec61 did not interfere with the analysis. About 20000 single ribosomal particles were selected and used for structure determination. The angular distribution of particles was sufficiently random, although ribosomes display some preference for binding to the carbon grid via Sec61, as has been reported before (data not shown; Menetret et al., 2005). The structure of the complex between nontranslating wheat germ ribosomes and canine Sec61 could be determined to a resolution of 18 and 28Å, respectively (Figure 23). The resolution was calculated according to the Fourier shell correlation curve with a 0.5 cutoff ($FSC_{0.5}$). Separate resolution curves for the ribosome and the channel were determined by the program EMAN (Ludtke et al., 1999). Consistent with previous results, the resolution of the ribosome is better than that of Sec61, most likely due to conformational flexibility of the ribosome-channel junction and the channel itself (Menetret et al., 2005). The threshold used for depicting the structure was chosen in a way that noise was excluded and the ribosomal density appeared solid. Sec61 is bound close to the tunnel exit at the bottom of the 60S ribosomal subunit (Figure 23, Figure 25G). The density is roughly triangular when viewed from the ribosome or the lumen and has a diameter of approximately 80Å (Figure 23B,E). When viewed from the side, it appears

flattened with a thickness of about 45Å (Figure 23A,C), enough to span the lipid bilayer (Mitra et al., 2004).
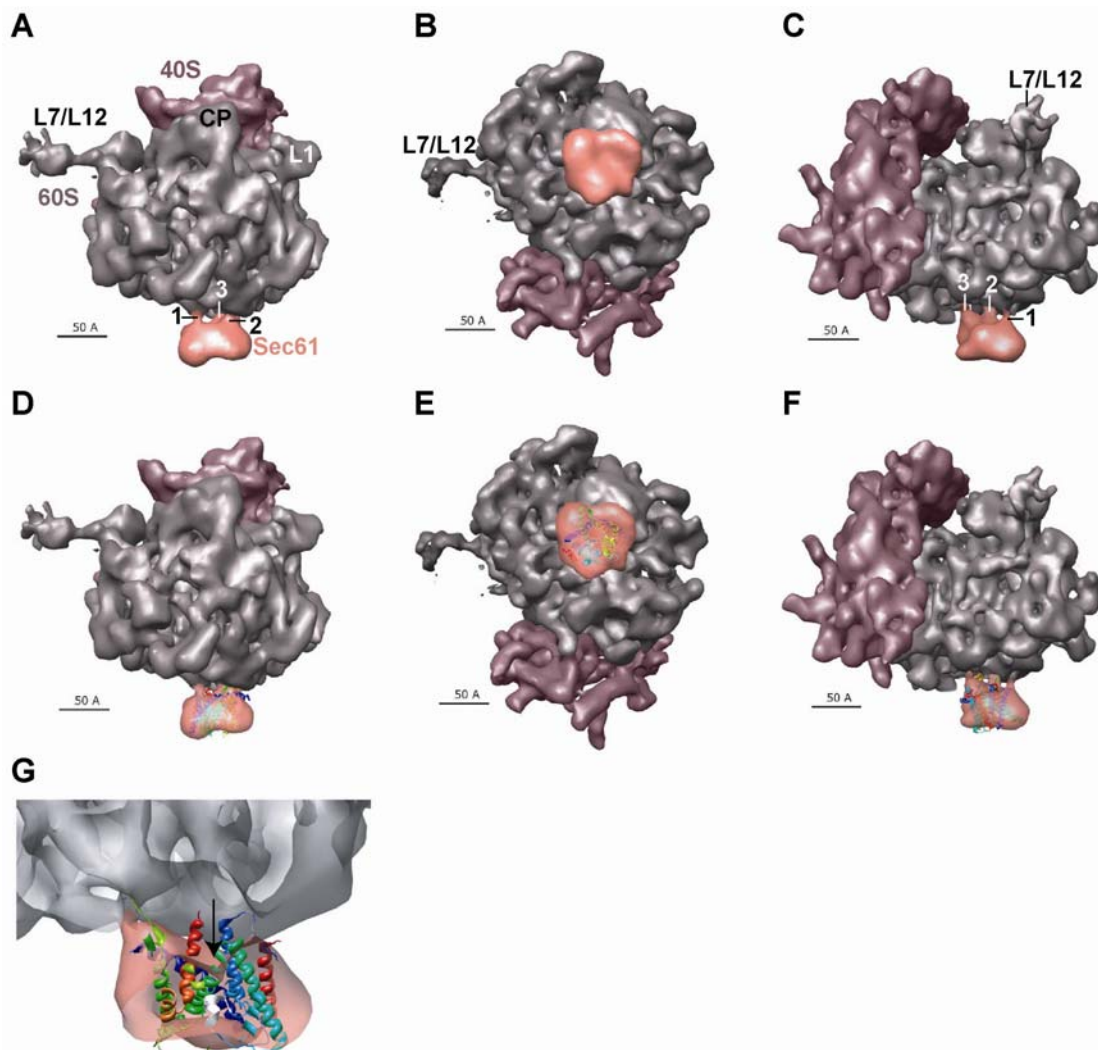
Figure 23: Structure of nontranslating wheat germ ribosomes (Grey: 50S subunit; Purple: 40S subunit) bound to C.f. Sec61 (orange) in detergent. The resolution is 18Å for the ribosome and 28Å for the channel (FSC$_{0.5}$). **A)** Ribosome-channel complex viewed along the plane of the membrane. The location of the large ribosomal subunit proteins L1, L7/L12, and of the central protuberance (CP) is indicated. The three connections between ribosome and Sec61 are labeled (1,2,3). **B)** Ribosome-channel complex viewed from the ER lumen. **C)** View from A) rotated 90° around the vertical axis. **D, E, F)** views as in A, B, C with the X-ray structure of the archaebacterial Sec61-homolog SecYEβ shown (van den Berg et al., 2004). **G)** A cross-section of the structure shown in D-F. The plug domain of SecYEβ is coloured white. The arrow indicates the location of the central depression.

Surprisingly, Sec61 seems to be a monomer, as the X-ray structure of the archaebacterial homolog SecYEβ can easily be accomodated within the density (Figure 23D-G). The toroid shape of the density corresponds well to the X-ray structure filtered to 28Å (data not shown). Some additional density at the edges of Sec61 is likely due to the digitonin micelle surrounding the channel (74kD; Hubbard,

1954). The Sec61 monomer forms three distinct contacts with the ribosome (Figure 23A,C). Consistent with this, a maximum of three contacts between the ribosome and one Sec61 molecule is observed in ribosome-channel complexes derived from native membranes (Menetret et al., 2005). The cytosolic loops 6 and 8 of Sec61α are important for ribosome binding and likely to contribute two of the connections (Raden et al., 2000), which will be discussed in more detail later (Figure 25). Viewed from the ribosomal side, the Sec61 density shows a central funnel-shaped depression (Figure 23G). When the X-ray structure of the archaebacterial Sec61-homolog SecYEβ is docked into the density according to the best fit of cytosolic loops 6 and 8 with the connections between ribosome and channel, the indentation is aligned with the plug domain of SecYEβ (Figure 23G, white). This indicates that the central depression could correspond to the closed pore observed in the X-ray structure (van den Berg et al., 2004). The pore would open during translocation and allow the nascent chain to pass (Tam et al. 2005, Cannon et al., 2005).

While membrane-bound ribosomes were shown to be associated with tetramers of mammalian Sec61 (Menetret et al., 2005), only one copy of purified Sec61 is bound to ribosomes in detergent (Figure 23). This shows that the ribosome can associate stably with a single Sec61 molecule, and probably identifies the highest-affinity binding site for a Sec61 monomer on the ribosome. In membranes, an interaction of ribosomes with Sec61 tetramers is favoured as they provide a higher affinity; a subpopulation of ribosomes bound to smaller oligomeric states of Sec61 might be present, but cannot be separated from ribosomes bound to tetrameric Sec61. The use of detergent seems to prevent tetramer formation and thereby enables us to study the association of smaller Sec61 oligomers with the ribosome.

4.10.2 Structure of a eukaryotic ribosome-channel complex engaged in translocation

Having investigated Sec61 binding to nontranslating ribosomes, we were interested in the oligomeric state of Sec61 when bound to ribosomes carrying a secretory nascent chain. To determine the structure of such complexes by electron cryo-microscopy, we established a method to purify stalled ribosome-nascent-chain complexes (RNCs). The N-terminally HA-tagged bovine preprolactin (ppl), a secretory protein, was used as a model substrate. A sequence coding for 86 amino acids was transcribed omitting

the stop codon (ppl86mer). In vitro translation of this truncated mRNA, which lacks a stop codon, resulted in stalled RNCs carrying the HA-ppl86mer nascent chain. These RNCs were purified by anti-HA affinity chromatography and eluted with HA-peptide (Figure 24A; Beckmann et al., 2001). Consistent with previous results, the yield was relatively low (5%) and seemed to be limited by the binding efficiency to the anti-HA beads, most likely because of sterical constraints contributed by the ribosome (Beckmann et al., 2001). The purification resulted in an enrichment of the peptidyl-tRNA in the eluate (Figure 24A), but as most of the peptidyl-tRNA hydrolyzes during gel electrophoresis in the buffer system used, no quantitative conclusion about nascent chain association with the ribosome can be drawn. The eluate contained ribosomes, as indicated by absorbance measurements (data not shown).

Ribosome-associated ppl86mer is recognized by Sec61 and forms a stable complex (Jungnickel et al., 1995). This can be recapitulated in detergent solution, where addition of Sec61 leads to insertion of nascent ppl86mer into the channel, making it protease-resistant (Mothes et al., 1998). Adding a 20x molar excess of purified C.f. Sec61 to the purified HA-ppl86mer RNCs in digitonin led to protection of 60% of the nascent chains (Figure 24B), indicating that they had inserted into the channel. In the absence of Sec61, only a short fragment of the nascent chain was protected by the ribosomal exit tunnel (Figure 24B, asterisk; Malkin and Rich, 1967). For structure determination, purified Sec61 in digitonin was added to the affinity-purified HAppl86mer-RNCs under the same conditions and the mixture was directly frozen on carbon-coated grids. Unbound Sec61 was invisible because of its small size. 20000 single ribosomal particles were selected and the three-dimensional structure was determined using the program EMAN (Ludtke et al., 1999). The Fourier Shell correlation curves were calculated for half-volumes of the density for both ribosome and channel, and a resolution of 16Å for the ribosome and 25Å for Sec61 was determined ($FSC_{0.5}$). The threshold used for depicting the structure was chosen in a way that noise was excluded and the ribosomal density appeared solid.

The peptidyl-tRNA is clearly visible at the interface of 40S and 60S subunit, indicating that the nascent chain is associated with the ribosome (Figure 24C, red). In addition, weaker density for E-site tRNA can be seen (data not shown). Consistent with previous results, the nascent chain itself cannot be visualized in the ribosomal exit tunnel, most likely because of conformational flexibility (Beckmann et al., 2001).
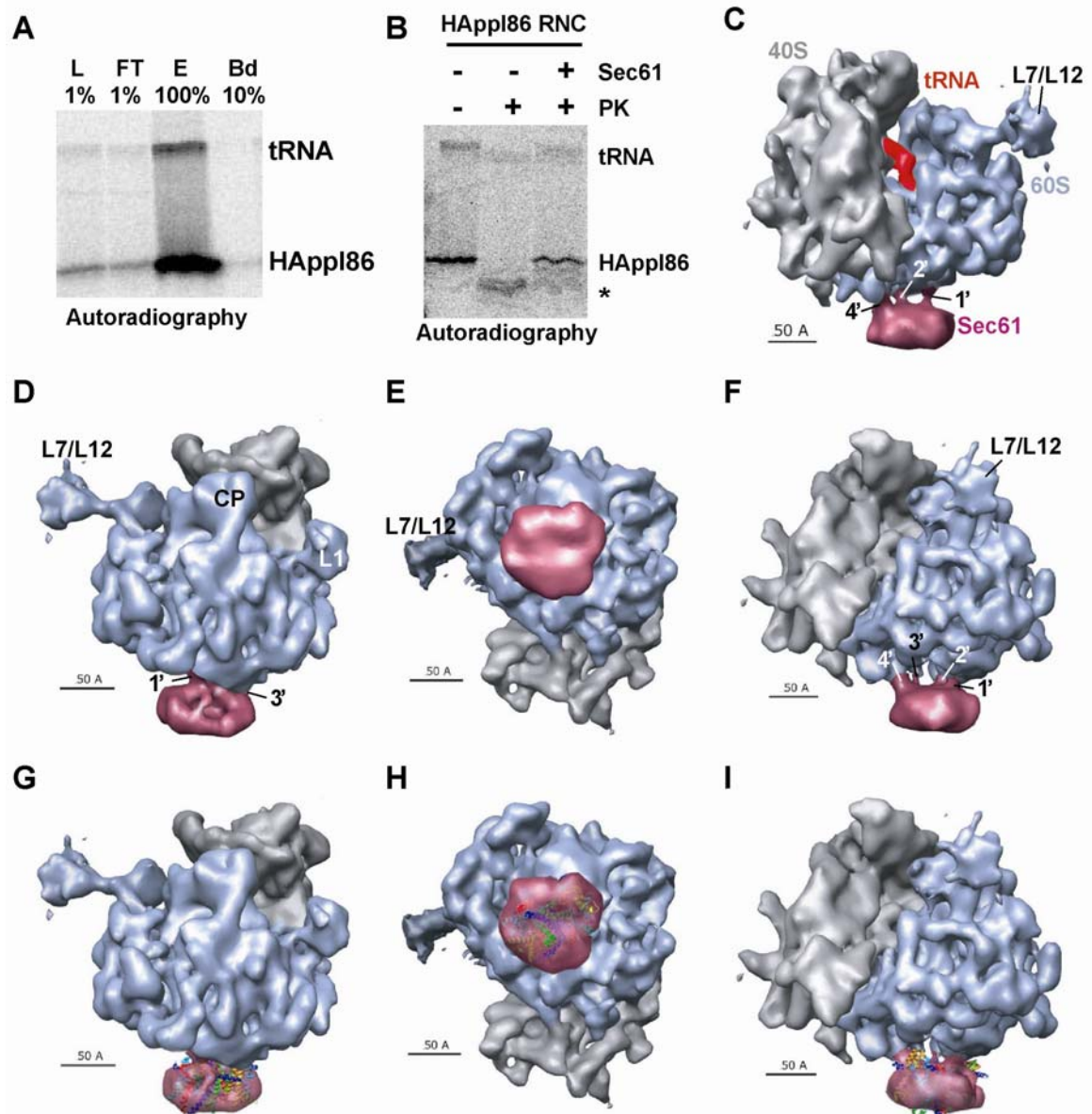
Figure 24: Purification, characterization and structure determination of wheat germ HAppl86mer-RNCs bound to C.f.Sec61 in detergent. **A)** Purification of HAppl86mer-RNCs by affinity chromatography of an in vitro translation reaction (L). FT: flowthrough, E: eluate; Bd: protein remaining bound after elution. The indicated fractions were analyzed by SDS-PAGE and autoradiography. tRNA: ppl86mer associated with its peptidyl-tRNA after SDS-PAGE. **B)** Purified HAppl86mer-RNCs were treated with and without Proteinase K (PK) after incubation in the absence or presence of a 20x molar excess of purified C.f.Sec61 in detergent. tRNA: ppl86mer associated with its peptidyl-tRNA after SDS-PAGE. Asterisk: position of a fragment protected solely by the ribosome. **C)** Structure of a complex between wheat germ RNCs carrying a secretory nascent chain (HAppl86) and C.f. Sec61. The resolution is 16Å for the ribosome and 25Å for the channel (FSC$_{0.5}$). The large ribosomal subunit (60S) is shown in light blue, the small ribosomal subunit (40S) in grey and Sec61 in magenta. The location of the large ribosomal subunit proteins L7/L12 is indicated. The ppl86mer-associated peptidyl-tRNA (tRNA) is visible in the peptidyltransferase center of the ribosome (red). Three of the four connections between the channel and the RNC (1', 2', 3', 4') can be seen in this view (1', 2', 4'). **D)** RNC-channel complex viewed along the plane of the membrane. The location of the large ribosomal subunit proteins L1, L7/L12, and of the central protuberance (CP) is indicated. **E)** RNC-channel complex viewed from the ER lumen. **F)** View from D) rotated 90° around the vertical axis. **G, H, I)** views as in D, E, F with a dimer of the archaebacterial Sec61-homolog SecYEβ accomodated in the channel density for illustration (van den Berg et al., 2004).

54

Sec61 is associated with the large ribosomal subunit close to the tunnel exit (Figure 24C-I). When viewed along the plane of the membrane, Sec61 appears extended with a thickness of approximately 45Å. When viewed from the lumen, the channel density is roughly circular with an approximate diameter of 100Å. Thus, Sec61 bound to RNCs appears larger and more irregular than the Sec61 bound to nontranslating ribosomes (for comparison, see Figure 29A,B). When looking towards the large ribosomal subunit, one side of the channel displays cavities (Figure 24D). These could be due to conformational flexibility after channel opening, which would reduce the density observed, so that they appear empty at the threshold chosen. Sec61 bound to RNCs is most likely a dimer, as two copies of the archaebacterial SecYEβ X-ray structure can be accommodated in the channel density (Figure 24G-I). The SecYEβ-dimer is depicted in a back-to-back orientation, as it is arranged in two-dimensional crystals (Collinson et al., 2001). However, the orientation of the Sec61 molecules relative to each other cannot be deduced from the structure due to the low resolution of the channel. For the same reason, the signal sequence of the nascent chain cannot be seen, although it is known to intercalate between helices 7 and 2b of Sec61 (Plath et al., 1998). The putative Sec61-dimer forms four connections with the large subunit of the RNC (Figure 24C, F, I). A detailed comparison of the connections that are formed between nontranslating ribosomes or RNCs and the channel is shown in Figure 25. While the Sec61 monomer bound to nontranslating ribosomes forms three connections close to the exit site (Figure 25, Nr. 1,2 and 3), the Sec61 dimer bound to RNCs is larger, laterally extended and forms four connections (Figure 25A-C, Nr. 1',2',3' and 4'). Both structures were aligned in three dimensions, so that the exit tunnel and the canyon of the peptidyl transferase centers are superimposed (Figure 25). The location and intensity of ribosome-channel contacts Nr. 1 and 2, which are closest to the ribosomal tunnel exit (TE), is conserved in both structures (Figure 25, G vs. H, F,I). Connection Nr. 3 is the strongest connection in the Sec61 monomer bound to nontranslating ribosomes (Figure 25A,D), but is strongly diminished in the Sec61 dimer (Figure 25G vs H), suggesting a conformational change during dimerization. Its residual presence might be due to some nontranslating ribosomes present in the RNC preparation. Instead, the dimer forms a new contact (Nr. 4') distant from the

ribosomal tunnel exit, that buries 250Å^2 and seems to be the strongest contact formed by the dimer (Figure25B, H).
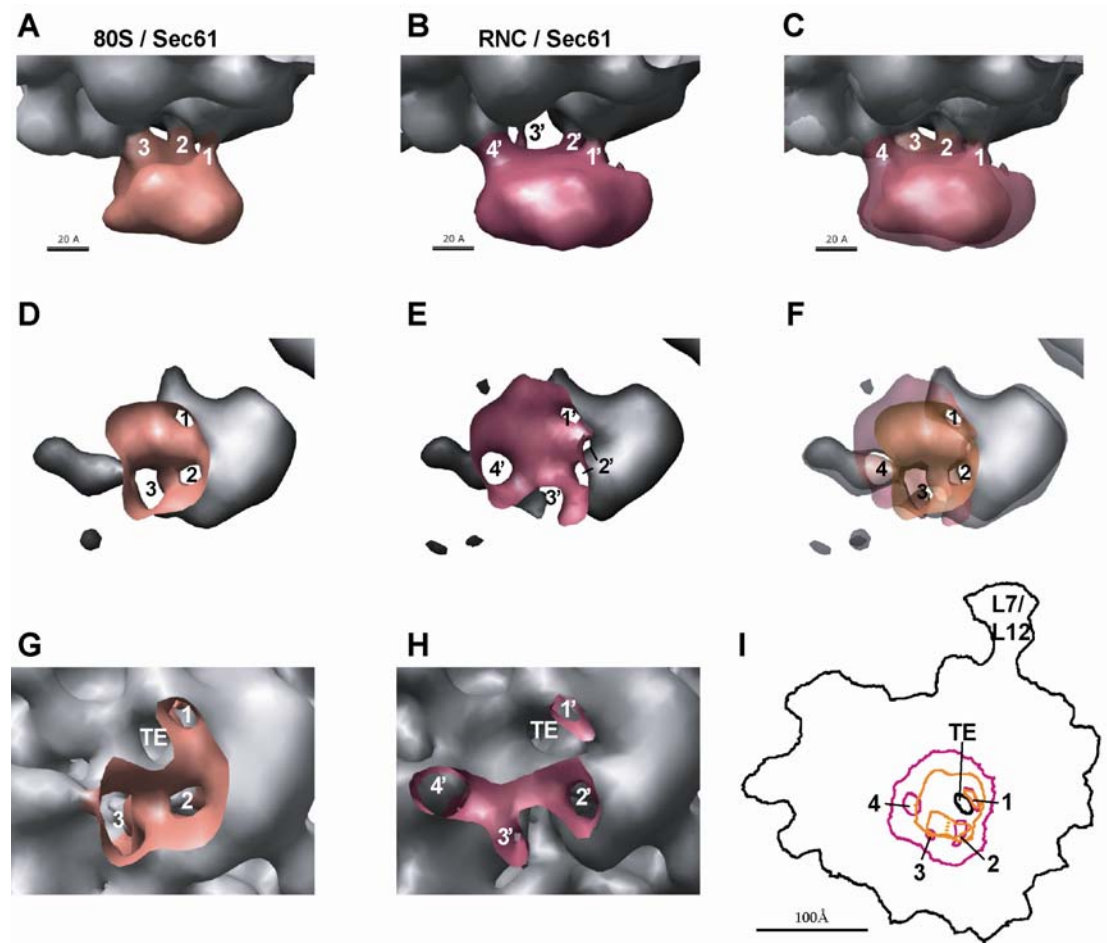
Figure 25: Comparison of ribosome-channel contacts. Sec61 bound to a nontranslating ribosome is shown in orange, Sec61 bound to a HAppl86mer-RNC is shown in magenta. Contacts between the ribosomal large subunits (grey) and the channel are labeled 1-3 for the nontranslating ribosome and 1'-4' for the translating ribosome. **A)** A close-up of the channel bound to nontranslating ribosomes. **B)** A close-up of the channel bound to HAppl86mer-RNCs. **C)** Alignment of both complexes showed in A and B so that the ribosomal exit tunnel is superimposed. **D, E, F)** A, B, C viewed from the ER lumen. Only the channel-ribosome interface is shown, the rest of the density has been removed for clarity. **G, H)** Lumenal views of Sec61 bound to nontranslating (G) or translating (H) ribosomes. The ribosomal tunnel exit (TE) is shown, some Sec61 density has been removed for clarity. **I)** Both ribosome-channel complexes viewed from the lumen were aligned so that their exit tunnel (TE) is superimposed. The outline and generalized ribosomal contact points (1-4) of Sec61 are indicated (orange: bound to a nontranslating ribosome; magenta: bound to a RNC). Contacts 2 and 3 of Sec61 bound to nontranslating ribosomes appear merged (separated by a dashed line), as a different cutting plane has been used here. The location of the large ribosomal proteins L7/L12 is given.

In summary, while two contacts remain the same, the third one formed by the Sec61 monomer largely breaks when a dimer is bound and is replaced by a fourth strong contact distant from the ribosomal tunnel exit. It is therefore likely, that one Sec61

molecule within the dimer binds the ribosome as the Sec61 monomer does, while the second molecule binds more distant from the ribosomal tunnel exit close to contact Nr. 4'. The binding of the second Sec61 molecule reduces formation of contact Nr. 3', which could mean that the loops forming contact Nr. 3 are involved in interaction with the additional Sec61 molecule or undergo conformational changes in response to its binding. As both complexes were prepared using identical conditions, except for the presence of a nascent chain, it is likely that the nascent chain leads to recruitment of the second Sec61 molecule. It is possible that the nascent chain directly interacts with the second copy of Sec61, using it for translocation. Alternatively, translocation of the nascent chain could lead to conformational changes in Sec61 that increase the affinity for a second Sec61. The removal of contact Nr. 3 might increase the conformational freedom of the translocating channel, supporting lateral opening during translocation. At the same time, the translocon would be secured at the ribosome by the strong contact 4' formed by the second Sec61 molecule.

Taken together, we provide evidence that nontranslating ribosomes can bind Sec61 monomers in detergent solution. This likely identifies the highest-affinity binding site for a Sec61 monomer on the ribosome. The presence of a secretory nascent chain leads to the recruitment of a second copy of Sec61, so that a dimer is bound to the ribosome. The binding sites for the monomer and the dimer are overlapping. Sec61 dimers are sufficient for the insertion of the nascent chain, as judged by protease protection experiments. Consistent with our biochemical results that suggest that RNCs are targeted to a monomeric or dimeric channel population, the RNC-Sec61 structure might resemble an initial translocation intermediate after SRP-dependent targeting has occurred. It is possible that the membrane-bound ribosomes sequester more copies of Sec61 over time, leading to the assembly of a Sec61 tetramer underneath the ribosome (Hanein et al., 1996; Menetret et al., 2005). We show for the first time that a Sec61 tetramer is not necessary for nascent chain insertion into eukaryotic Sec61, but may stabilize the complex at a later stage. Together with our previous results, this strongly suggests that the regulation of Sec61 oligomerization plays an important role in translocation.

4.10.3 Structure of a bacterial ribosome-channel complex

To address the evolutional conservation of nascent-chain mediated oligomerization, we analyzed structural intermediates of translocation in bacteria. The bacterial inner

membrane is equivalent to the eukaryotic ER and harbours the SecYEG channel complex, that it homologous to the Sec61p complex. Most secretory proteins are exported posttranslationally by a cytosolic ATPase unique to eubacteria, SecA, while inner membrane proteins are translocated cotranslationally in an SRP-dependent fashion (Ulbrandt et al., 1997). The bacterial SRP-system is essential and consists only of the SRP54-like Fifty-four-homolog (Ffh) in complex with one 4.5S RNA (ffs), and the SRα-homolog FtsY (Phillips and Silhavy, 1992).

To ensure comparability, we established a procedure to purify E.c. SecYEG analogous to C.f. Sec61 (Goerlich and Rapoport, 1993). SecYEG was solubilized and purified in digitonin. In the last step, the detergent was exchanged to DeoxyBigChap (DBC; Figure 26A). For structure determination of a bacterial ribosome-channel complex, E.c. 70S ribosomes were purified by repeated sucrose gradient centrifugation and a 20x molar excess of E.c. SecYEG was added in DBC. After complex formation, the mixture was frozen on perforated carbon grids, so that the sample was captured in holes without touching the carbon film, preserving the channel in an unperturbed conformation (Menetret et al., 2005). 15000 single particles were selected and a three-dimensional map of the complex was calculated using the program EMAN (Ludtke et al., 1999; Figure 26B-E). Using the half-volume method, the resolution was determined to be 15Å for the ribosome and 25Å for SecYEG at $FSC_{0.5}$. The threshold for depicting the structure was determined by docking the X-ray structure of the E.coli ribosome into the density (Schuwirth et al., 2005). SecYEG binds the large subunit close to the tunnel exit site, similarly to the eukaryotic complex (Figure 26B-E). When viewed along the plane of the membrane, the density is extended and has a thickness of about 35-45Å, enough to span the membrane (Mitra et al., 2004). When viewed from the periplasm, the SecYEG-density looks roughly triangular, being slightly less rounded than the eukaryotic structure, with a diameter from 70 to 100Å (Figure 26C,E; compare to Figure 23B,E). The density was compact and homogeneous even at higher threshold (data not shown), and showed a lot of detail. The bound SecYEG is likely a monomer, as the X-ray structure of the archaebacterial homolog SecYEβ provides a good fit for the density (Figure 26D-G). Some density at the perimeter of SecYEG is probably due to the three additional helices present in the eubacterial complex and the detergent micelle.
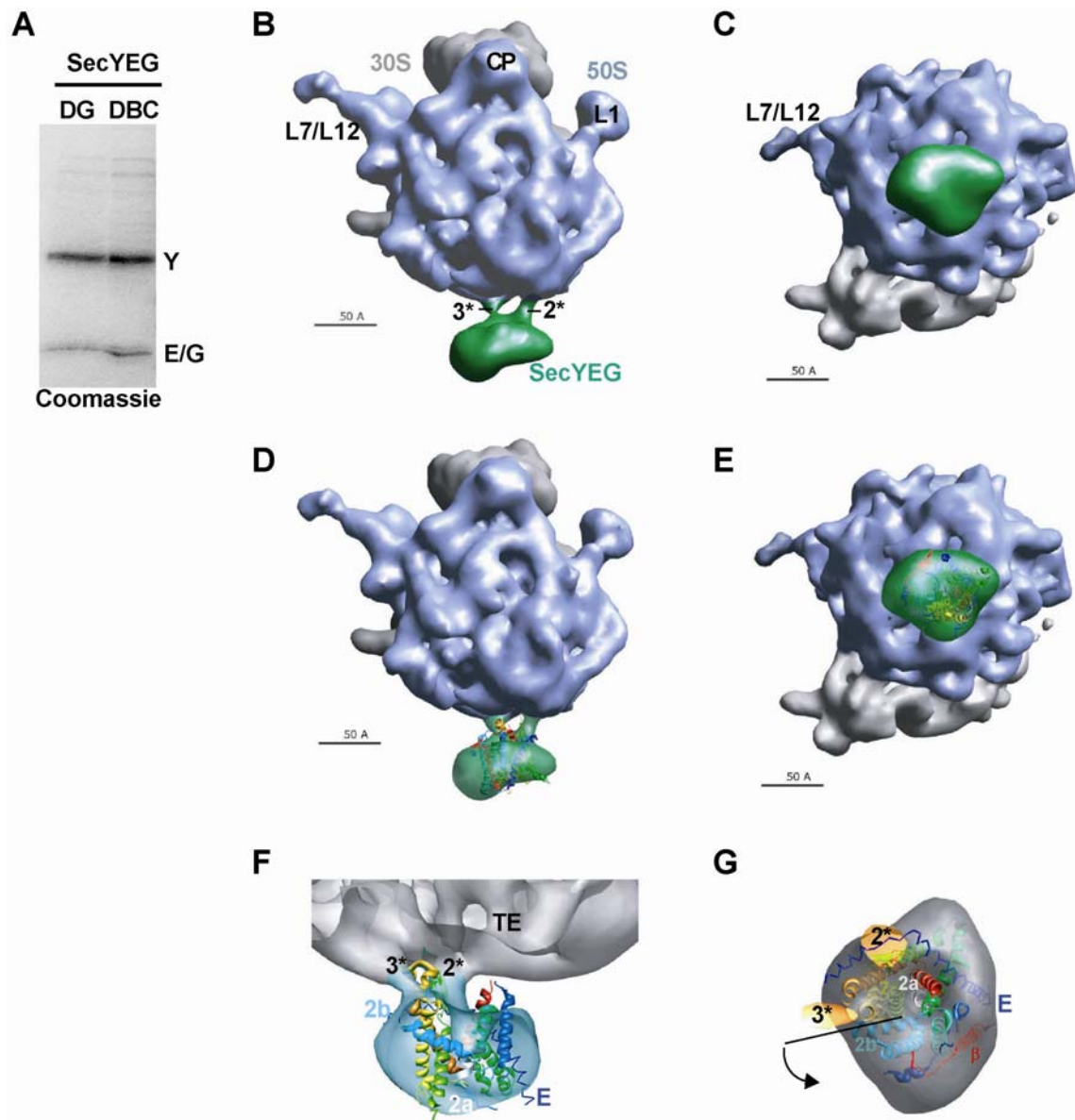
Figure 26: Structure of a bacterial ribosome-channel complex. **A)** E.c. SecYEG was purified in Digitonin (DG), the detergent exchanged to DBC, and analyzed by SDS-PAGE and Coomassie Blue staining. **B)** Structure of E.c. SecYEG (green) in DBC bound to nontranslating E.c. ribosomes (blue: large subunit, 50S; grey: small subunit, 30S) viewed from within the ER membrane. The resolution is 15Å for the ribosome and 25Å for the channel ($FSC_{0.5}$). The location of the large ribosomal proteins L1, L7/L12, and of the central protuberance (CP) is indicated. The two connections formed between SecYEG and the ribosome are marked as 2* and 3*, as they are in similar locations as the contacts 2 and 3 in the eukaryotic structures. **C)** Structure of an E.c. ribosome-channel complex viewed from the ER lumen. **D, E)** as in B, C, but with the X-ray structure of the archaebacterial SecYEG-homolog SecYEβ docked into the density (van den Berg et al., 2004). The cytosolic loops 6 and 8 of SecY were aligned with the two ribosome-channel contacts. **F)** Cross-section of the ribosome-channel complex. The ribosomal exit tunnel (TE) and the two contacts aligned with loops 6 and 8 of SecYEβ are marked (2*, 3*). The plug-domain of SecYEβ (helix 2a; white) and one of the helices forming the lateral gate of SecYEG (2b; cyan) is indicated. SecE (E) is depicted as a blue ribbon. **G)** as in F, but viewed from the cytosol. The ribosomal density has been removed except for the connections to SecYEG (orange, 2*, 3*). The black arrow indicates the location and direction of opening for the lateral gate.

To exclude detergent artefacts, another structure of the E.c. ribosome-SecYEG complex in DDM was determined, showing a very similar SecYEG-monomer bound to the ribosome (data not shown). In the structure depicted, two connections are formed between the channel and the ribosome, opposite of the ribosomal tunnel exit (Figure 26B, D, F). They are located at similar positions as the connections Nr. 2 and 3 in the eukaryotic ribosome-Sec61 complex (Figure 25; for comparison, see Figure 29). Connection Nr. 1, that has been observed juxtaposed to the tunnel exit in the eukaryotic complex, is absent in the bacterial structure at the threshold chosen (Figure 25I, Figure 29). The cytosolic loops 6 and 8 of SecY are important for ribosome binding (Raden et al., 2000) and align well with the two connections between the ribosome and SecYEG. This allows docking of the X-ray structure into the SecYEG density and indicates how SecYEG may be oriented relative to the ribosome (Figure 26F,G). The lateral gate of SecYEβ would be adjacent to contact 3*, leading the translocated nascent chain away from the tunnel exit (Figure 26G). When viewed from the ribosome, the SecYEG density displays a central cavity (Figure 26F,G), that is perfectly aligned with the plug domain within SecYEG (Figure 26F,G; white). It is therefore likely that we observe the funnel-shaped opening that has been reported for the closed state of SecYEG (van den Berg et al., 2004).

Taken together, the structure of E.c. SecYEG bound to nontranslating ribosomes in detergent solution reveals that SecYEG binds as a monomer, forming two contacts with the ribosome at the threshold chosen. This likely identifies the highest-affinity binding site for a SecYEG monomer on the ribosome, which seems to be conserved between prokaryotes and eukaryotes. The connections formed likely include the cytosolic loops 6 and 8 of SecY, which can be aligned with the density, revealing the orientation of a SecYEG monomer relative to the ribosome. A central cavity in the density is blocked on the lumenal side, very likely by the central plug domain observed in the X-ray structure (van den Berg et al., 2004).

4.10.4 Structure of a bacterial ribosome-channel complex engaged in translocation

To investigate how an actively translocating ribosome-SecYEG complex is constituted, we established a procedure to purify bacterial RNCs. The bacterial inner membrane protein FtsQ, which was used as a model substrate, is translocated

cotranslationally. A nascent chain length of 77 amino acids permitted efficient interaction of the transmembrane anchor sequence with SecY (van der Laan et al., 2001; Urbanus et al., 2001). An N-terminal HA-tag was added to FtsQ and linear DNA was produced by PCR, including a supercoiling-insensitive tac-promoter. The stop codon was omitted. HAFtsQ77mer was generated by a coupled transcription / translation reaction of the truncated template in bacterial extract. The produced E.c. HAFtsQ77mer-RNCs were affinity-purified and eluted with HA-peptide (Figure 27B). As in the wheat germ HAppl86-RNC purification, the yield was relatively low (3%) and seemed to be limited by the RNC-binding to the affinity matrix, most likely because the ribosomes sterically hinder binding of the nascent chain (Beckmann et al., 2001). The purification resulted in an enrichment of the peptidyl-tRNA in the eluate, but no quantitative conclusions about the association of the nascent chain with the ribosome can be drawn, as most of the peptidyl-tRNA hydrolyzes during gel electrophoresis in the buffer system used (Figure 27B). The eluate contained ribosomes, as indicated by absorbance measurements (data not shown). A low-resolution structure of the purified HAFtsQ77-RNCs determined by electron cryo-microscopy showed a 70S bacterial ribosome with a visible peptidyl-tRNA, indicative of the presence of a nascent chain (data not shown). Unlike in the wheat germ system, structure determination of an RNC-SecYEG complex initially failed, as the addition of SecYEG resulted in aggregation of the sample (data not shown). We therefore used a 20x molar excess of purified E.c. SecYEG (Figure 27A) for binding in detergent and further purified the RNC-SecYEG complex by sucrose gradient centrifugation (Figure 27C). While the intact RNC-SecYEG complex migrated at 70S (Figure 27C), unbound SecYEG remained on top of the gradient and aggregates sedimented (data not shown). The 70S peak fractions were pooled, the sucrose was removed by gelfiltration and the sample was concentrated. After freezing on carbon-coated grids, the mixture was largely monodisperse and homogenous, indicating a high degree of purity and successful removal of aggregates (data not shown). SecY is present in the complex in approximately equimolar amounts, as indicated by silver staining and quantitative immunoblotting of the purified product (Figure 27D,E). As protease protection experiments in detergent were not feasible with bacterial RNC-YEG complexes (data not shown), we used a crosslinking assay to investigate if the nascent chain had inserted into the channel (Cannon et al., 2005).
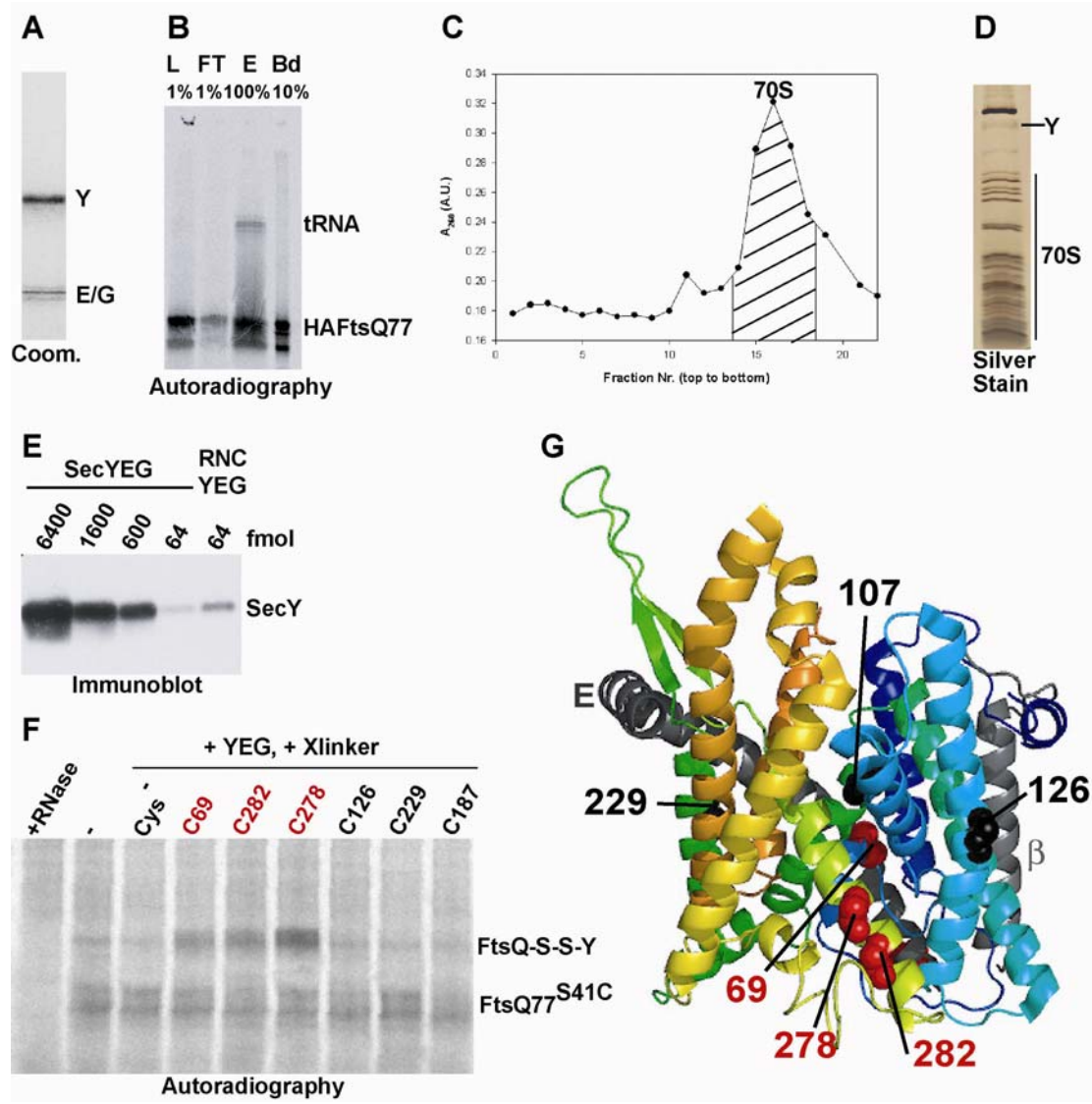
Figure 27: Purification of a bacterial RNC-channel complex. **A)** Purified E.c. SecYEG in DDM used for complex formation was analyzed by SDS-PAGE and Coomassie Blue staining. **B)** Purification of radiolabeled E.c. HAFtsQ77mer-RNCs by affinity chromatography of an in vitro translation reaction (L). Fractions are indicated for the starting material (L), flow through (FT), eluate (E) and material that did not elute (Bd). The samples were analyzed by SDS-PAGE and autoradiography. tRNA denotes FtsQ77mer associated with its peptidyl-tRNA after SDS-PAGE. **C)** Sucrose gradient centrifugation of the complex between HAFtsQ77mer-RNCs and E.c. SecYEG in DDM. The shaded area was pooled and used for structure determination. **D)** The preparation used for structure determination was analyzed by SDS-PAGE and silver staining. The location of the ribosomal proteins (70S) and of SecY (Y) is indicated. **E)** Quantitative immunoblotting for SecY. In lanes 1-4, purified E.c. SecYEG was loaded. In lane 5, 64 fmol (determined by A_{260} of the RNCs) of the purified RNC-channel complex were loaded. **F)** Crosslinking experiment between peptidyl-tRNA-associated FtsQ77^{S41C} and SecYEG mutants containing single cysteines in different locations of SecY (C69, C282, C278, C126, C229, C187). As controls, RNase was used to hydrolyze the peptidyl-tRNA, a reaction without SecYEG and crosslinker (-) was performed and a cysteine-free SecYEG (Cys⁻) was used for crosslinking. The position of the crosslinked band is indicated (FtsQ-S-S-Y). red: pore-lining cysteines (Cannon et al., 2005); black: control cysteines **G)** Position of the cysteines used for crosslinking. The homologous residues in the X-ray structure of the archaebacterial SecYEβ have been highlighted as red (crosslinking pore-lining cysteines 69, 282 and 278) and black (non-crosslinking control cysteines 126, 229 and 187) spheres. SecE and Secβ are shown in grey (E, β).

To this end, a cysteine point mutation (S41C) was introduced into the transmembrane anchor of HAFtsQ77mer, and complexes were formed with purified SecYEG-mutants in detergent. The SecYEG-mutants contained single pore-lining cysteines in SecY, that had been shown to crosslink with a cysteine in a translocating nascent chain, or control cysteines outside of the pore (Cannon et al., 2005). Following complex formation between radiolabeled HAFtsQ77[S41C]-RNCs and SecYEG-mutants in detergent, we observed crosslinks between FtsQ and the pore-lining residues (Figure 27F,G; red), but not between FtsQ and control residues outside of the pore (Figure 27F,G; black). Crosslinks were only observed with the tRNA-associated nascent chains, indicating that released nascent chains do not form crosslinks with SecYEG (data not shown). Taken together, this strongly argues that we could form and purify functional complexes between HAFtsQ77mer-RNCs and E.c. SecYEG in detergent.

For structure determination, complexes between E.c. HAFtsQ77-RNCs and E.c. SecYEG were purified as described and frozen on carbon-coated grids. 46000 single particles were selected and the three-dimensional structure was determined using the program EMAN (Ludtke et al., 1999). Separate Fourier-shell-correlation curves were calculated for the 70S ribosome and SecYEG using the half-volume method. The resolution was determined to be 10Å for the ribosome and 17Å for the channel ($FSC_{0.5}$). The threshold used for depicting the structure was chosen in a way that the threedimensional map of the ribosome matched the X-ray structure of the 70S ribosome filtered to 11Å resolution (Schuwirth et al., 2005). SecYEG binds to the large ribosomal subunit close to the tunnel exit (Figure 28). The density is oval when viewed from the periplasmic side, with a diameter of 85-100Å, and seems to be larger than SecYEG bound to nontranslating ribosomes (Figure 28C; for comparison, see Figure 29). When viewed along the plane of the membrane, the channel seems to be larger and more tightly connected to the 50S subunit, than when bound to a nontranslating ribosome (Figures 26, 28). Unlike when bound to nontranslating ribosomes, SecYEG shows internal cavities in the membrane-spanning region (Figure 28C, Figure 29D). The cavities become more pronounced at higher threshold levels (Figure 28G), and are not due to distortion of SecYEG by interaction with the carbon film, as they are absent in ribosome-SecYEG complexes frozen under the same conditions without a nascent chain (data not shown). Similar cavities are observed in the eukaryotic RNC-Sec61 complex (Figure 29B).
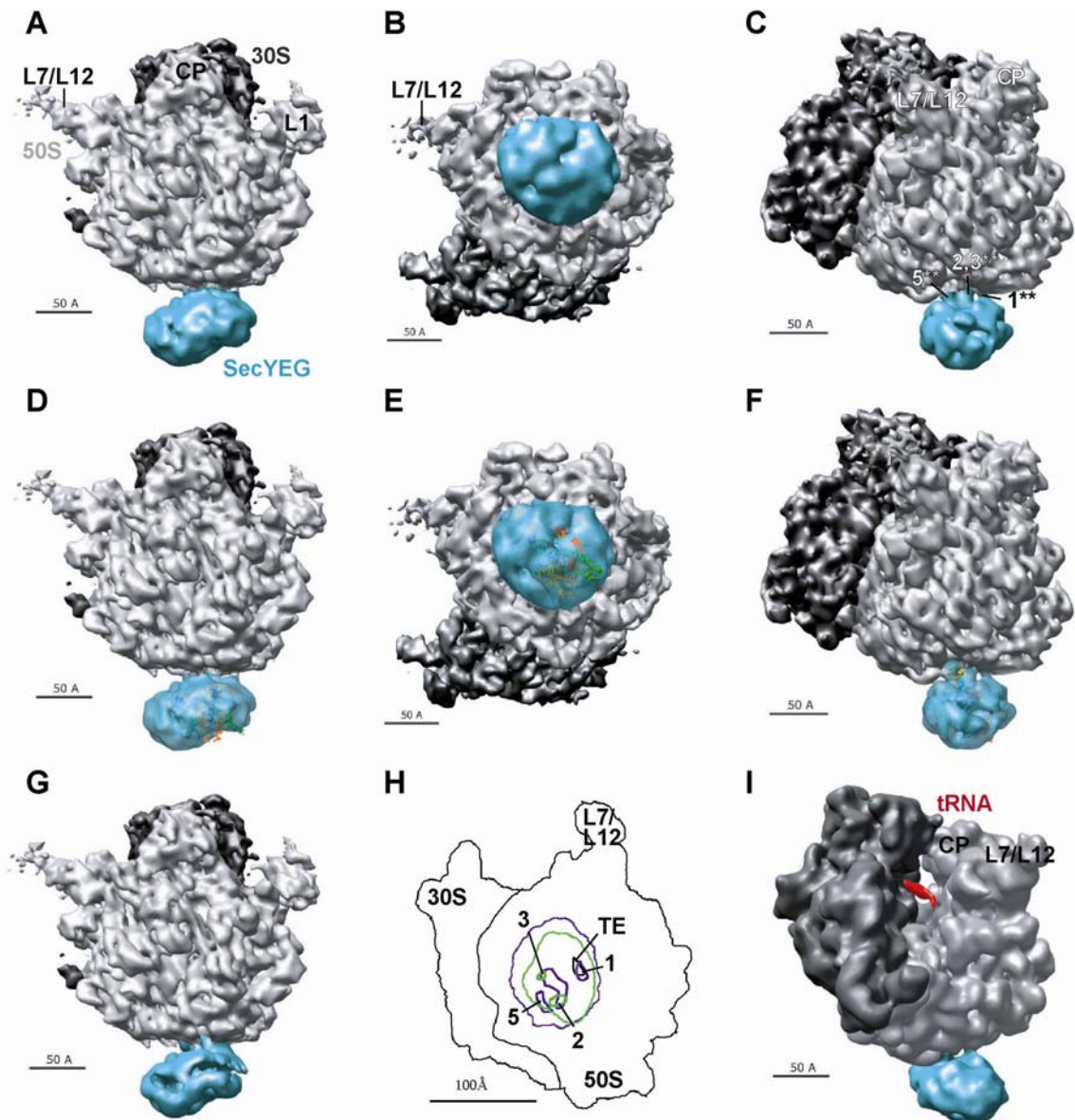
Figure 28: Structure of an E.c. RNC-SecYEG complex assembled in detergent at a resolution of 10Å for the ribosome and 17Å for SecYEG ($FSC_{0.5}$). SecYEG is shown in turquoise, the large ribosomal subunit (50S) in light grey and the small ribosomal subunit (30S) in dark grey. The location of the large ribosomal proteins L1, L7/L12 and the central protuberance (CP) is indicated. **A)** Bacterial RNC-channel complex viewed along the plane of the membrane. **B)** Bacterial RNC-channel complex viewed from the periplasm. **C)** View from A) rotated 90° around the vertical axis. The contacts between RNC and SecYEG are labeled 1**, 2** and 3** according to their similar location to contacts 1-3 in previous structures. No homolog to contact 4 is present, but one novel contact is formed (5**). **D, E, F)** as in A, B, C, with the X-ray structure of the archaebacterial SecYEG-homolog SecYEβ accomodated within the density for illustration. **G)** View as in A) using a higher threshold for depicting the SecYEG density. **H)** Both bacterial ribosome-channel complexes viewed from the periplasm were aligned so that their exit tunnel (TE) is superimposed. The outline and ribosomal contact points (1-5) of SecYEG are indicated (green: bound to a nontranslating ribosome; dark blue: bound to a RNC). Contact 4 is absent in bacterial complexes. The location of the large ribosomal proteins L7/L12 and the outline of the large (50S) and small subunit (30S) is given. **I)** The peptidyl-tRNA (tRNA; red) is visible in the peptidyltransferase center at the interface of large and small ribosomal subunit.

64

While SecYEG displays two distinct connections to nontranslating ribosomes (Figure 28H, green), these contacts merge and form a ridge when SecYEG is bound to RNCs (Figure 28H, dark blue). In addition, two new contacts are formed, one of which is directly juxtaposed to the tunnel exit (Figure 28H). The other new contact is most distant from the tunnel exit (Figure 28H). The central cavity that has been observed in the closed SecYEG (Figure 26F) is absent in the RNC-YEG complex. The peptidyl-tRNA is visible in the peptidyltransferase center (PTC) at the interface between 30S and 50S subunit and displays the characteristic L-shape (Figure 28I; red). The peptidyl-tRNA density is, however, weaker than in the wheat germ RNC structure (Figure 24C) and it is unclear how many ribosomes have retained their nascent chain. The reported structure could therefore also be derived from a mixture of ribosome-channel complexes with and without a nascent chain. This might explain why the SecYEG density is smaller than the Sec61 density bound to RNCs.

However, the extended connections between the ribosome and SecYEG and the internal cavities are reproducibly unique to SecYEG or Sec61 bound to RNCs (Figure 29), and are absent in all other structures determined (data not shown). The observed change in SecYEG density could therefore be due to the nascent chain, possibly representing the opening of the channel. This might explain why the central depression in SecYEG bound to nontranslating ribosomes has disappeared and given rise to larger cavities. The peptidyl-tRNA may display conformational variability within the PTC, as has been suggested before (Menetret et al., 2000).

Comparing the prokaryotic and the eukaryotic ribosome-channel contacts reveals that contact Nr. 1 close to the tunnel exit exists in both eukaryotic structures and in the bacterial SecYEC-RNC complex; contacts Nr. 2 and 3 are conserved between prokaryotes and eukaryotes, while contact Nr. 4 is only formed if a Sec61 dimer is bound (Figure 29, Figure 25I vs 28H). In both cases, the interaction between the channel and the RNC seems to be more extensive than the interaction with nontranslating ribosomes (Figure 29). In eukaryotes, this is accomplished by oligomerization of Sec61 (Figure 24); in prokaryotes, SecYEG might change its conformation without changing its oligomeric state (Figure 28). As it is unclear how many ribosomes carry a nascent chain, the prokaryotic RNC-YEG structure could also represent a mixture of nontranslating ribosomes bound to monomeric SecYEG and RNCs bound to dimeric SecYEG.
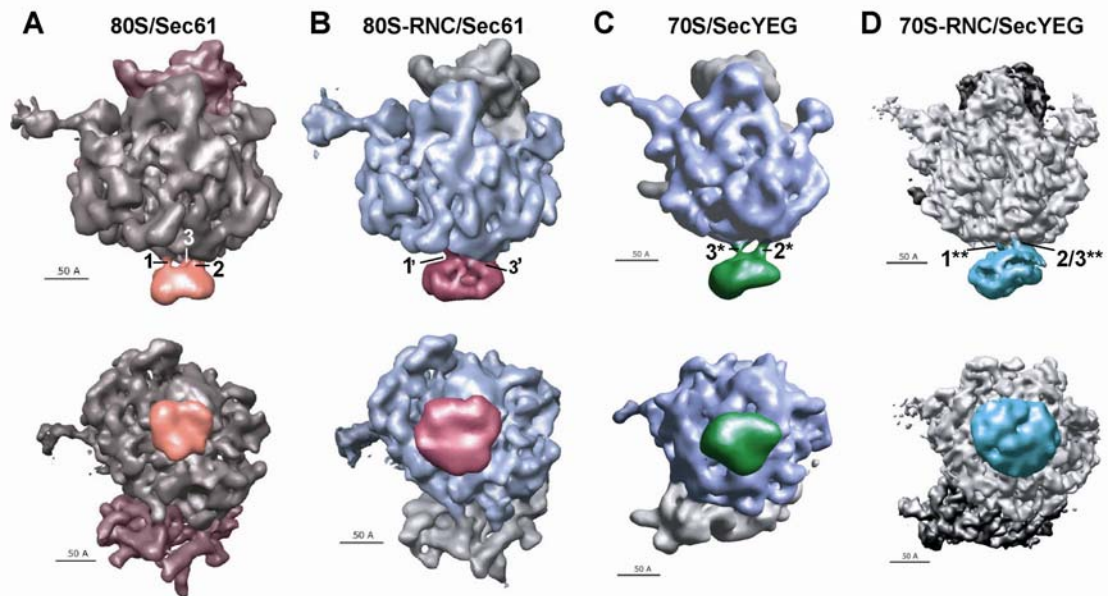
Figure 29: Comparison of eukaryotic ribosome-channel complexes with (80S-RNC/Sec61, **B**) or without (80S/Sec61, **A**) a nascent chain to prokaryotic ribosome-channel complexes with (70S-RNC/SecYEG, **D**) and without (70S/SecYEG, **C**) a nascent chain. Bottom row: lumenal / periplasmic view; For details, see Figures 21,22,24 and 26. Visible contact points are labeled.

In both eukaryotes and prokaryotes, the presence of a nascent chain leads to the appearance of cavities, that break up the channel density (Figure 29). This suggests an increase in conformational flexibility within the translocon, that could be due to channel opening mediated by the nascent chain.

4.10.5 Binding of bacterial ribosomes to bacterial and eukaryotic membranes

The ribosome-channel complexes described have been assembled in detergent. If ribosomes are bound to intact mammalian membranes and then solubilized, they carry a Sec61 tetramer, held in place by seven connections (Menetret et al., 2005). This suggests that the structures in detergent may represent early stages of oligomerization. There is no structural data for ribosome-SecYEG complexes from native bacterial membranes, but in detergent, ribosome-bound SecYEG seems to be monomeric or dimeric (our data and Mitra et al., 2005). To test whether a higher oligomeric state of the channel leads to a higher binding affinity, we compared the binding of bacterial ribosomes to intact bacterial and mammalian membranes.

Radiolabeled E.c. ribosomes were bound to bacterial inner membrane vesicles (IMVs) or mammalian ER membranes (PKRMs) and the respective binding curves were determined using a sedimentation assay (Figure 30A). PKRMs and IMVs were sedimented quantitatively (data not shown).
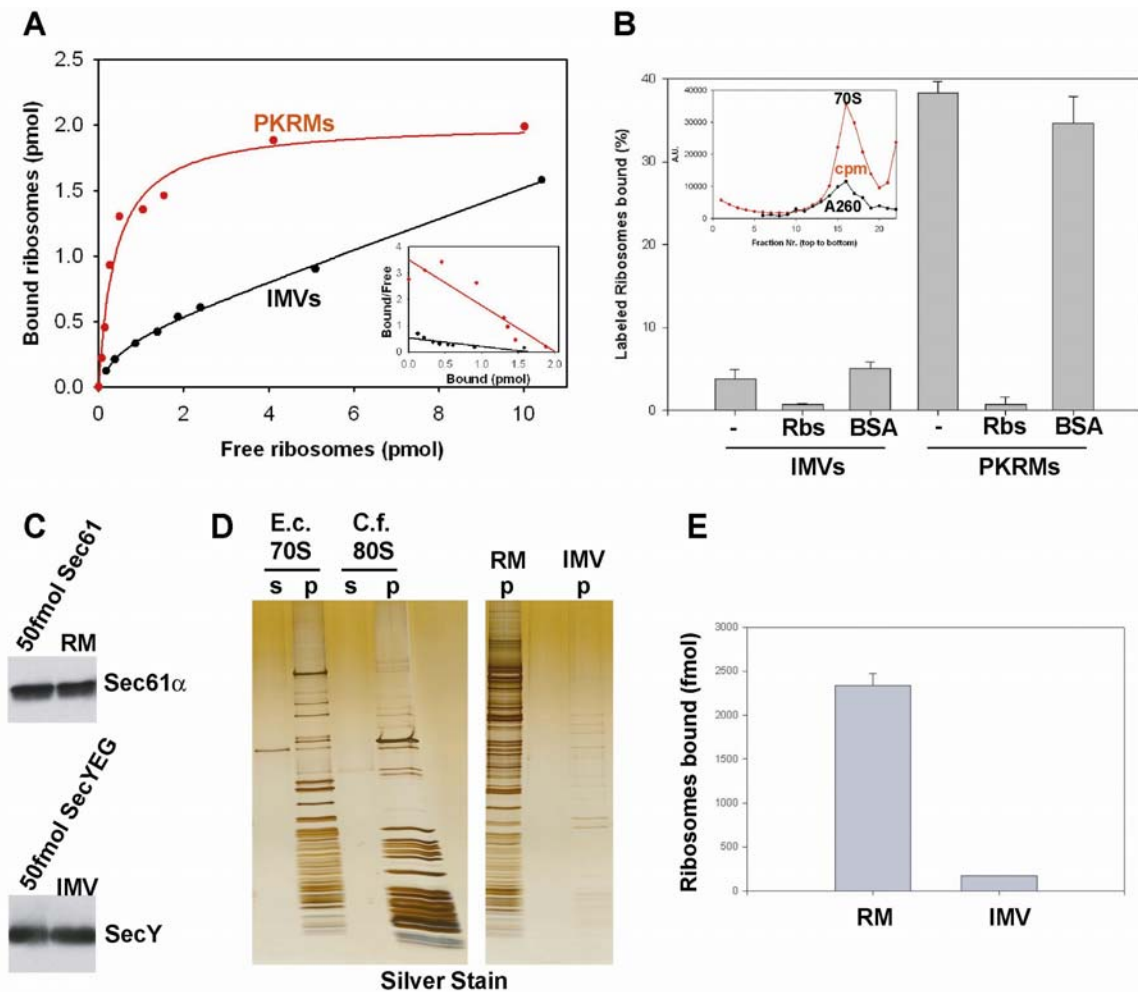
Figure 30: Ribosome binding to the translocon is weaker in bacteria than in eukaryotes. **A)** Binding of radiolabeled nontranslating ribosomes to canine ER membranes (PKRMs; red) or bacterial inner membranes (IMVs; black). A sedimentation assay was used to separate free from bound ribosomes. Inset: Scatchard-plot of the data. **B)** Ribosome binding to IMVs and PKRMs is specific. Unlabeled ribosomes or equal amounts of BSA were used for incubation with the membranes, before radiolabeled ribosomes were bound. Membrane-bound ribosomes were separated from free ribosomes. by sedimentation. Inset: Sucrose gradient centrifugation of radiolabeled E.c. ribosomes. Fractions were analyzes by A_{260} (black) and scintillation counting (red). The location of the 70S peak is indicated. **C)** Quantitative immunoblotting of RMs and IMVs in comparison with 50fmol purified Sec61 or SecYEG. Immunoblotting was performed for Sec61α and SecY. **D)** Bacterial inner membranes and eukaryotic ER membranes containing an identical amount of channel were used for extracting membrane-bound ribosomes by solubilization with DDM and sedimentation (RM p, IMV p). Purified E.c. 70S ribosomes and C.f. 80S ribosomes quantitatively sedimented (s: supernatant; p: pellet). **E)** Quantitation of solubilization experiments as in D.

While the binding of E.c. ribosomes to PKRMs was as strong as the binding of eukaryotic ribosomes to PKRMs (Figure 4B), the binding of E.c. ribosomes to IMVs was significantly weaker. The binding to IMVs was consistent with binding to two classes of sites, a class of high-affinity sites that is present in very small amounts and a more abundant class of low affinity binding sites (Figure 30A). IMVs and PKRMs

contained the same amount of SecY/Sec61, as determined by quantitative immunoblotting. Experiments with different batches of IMVs and salt- or urea-washed IMVs lead to the same result (data not shown). Control experiments showed that the ribosomes migrated at 70S in a sucrose gradient and contained the radiolabel (Figure 30B, inset). Binding of ribosomes to IMVs and PKRMs was specific, as it could be efficiently competed by unlabeled ribosomes, but not by BSA (Figure 30B). If the binding of E.c. ribosomes to bacterial inner membranes was stronger in vivo, we would expect that bacterial inner membranes retained their bound ribosomes after purification, as has been reported for mammalian rER membranes (Adelman et al., 1973). We therefore purified IMVs and rER membranes (RMs) under physiological conditions and assayed their SecY/Sec61 content by quantitative immunoblotting (Figure 30C). Membranes containing identical amounts of SecY/Sec61 were solubilized, the ribosomes quantitatively sedimented by ultracentrifugation and analyzed by SDS-PAGE and silver staining (Figure 30D). Bacterial IMVs had considerably less ribosomes bound than mammalian RMs (Figure 30D, right panel; quantitation in Figure 30E), indicating that the binding of E.c. ribosomes to SecYEG is considerably weaker than the binding to Sec61. The 6% of ribosomes cosedimentation that occurs in IMVs (relative to 100% in RMs) could be due to binding to a small number of high affinity ribosome binding sites, likely higher oligomers of SecYEG (Scheuring et al., 2005).

5 DISCUSSION

We have investigated how protein translocation can occur at the endoplasmic reticulum membrane, which harbours the protein-conducting channel Sec61 and is saturated with nontranslating ribosomes. We found that under these conditions, which resemble the situation in vivo, the SRP-system becomes essential for targeting of ribosome-nascent-chain (RNC) complexes to the membrane.

Interestingly, ribosomes prebound to Sec61 are not displaced by SRP-dependent targeting of RNCs. Instead, SRP facilitates the interaction of RNCs with a specific population of Sec61, that cannot easily associate with nontranslating ribosomes. This population of Sec61 is probably present in a lower oligomeric state than the tetrameric Sec61 occupied by nontranslating ribosomes. Both populations are interconvertible and in an equilibrium with each other. We determined the structures of ribosome-channel complexes assembled in detergent solution by electron cyro-microscopy. In eukaryotes, a Sec61 monomer is bound to nontranslating ribosomes, while a Sec61 dimer is bound to RNCs carrying a secretory nascent chain. In prokaryotes, a monomer is bound in the absence of a nascent chain. This indicates that ribosomes can not only bind tetrameric Sec61, but also smaller oligomeric forms of the protein-conducting channel. We propose that the structures of these ribosome-channel complexes may represent early stages in targeting, after the RNC has been transferred from the SRP/SR complex to Sec61.

5.1 Why is SRP needed for targeting?

Although SRP is needed in vivo, translocation can occur efficiently in vitro in the absence of SRP (Jungnickel et al., 1995). Indeed, in the absence of SRP-receptor, SRP impairs RNC binding to Sec61, as it occludes the Sec61 binding site on the ribosome (Goerlich et al., 1993; Halic et al., 2004). Most experiments aimed at elucidating the mechanism of translocation were performed by adding secretory RNCs to membranes devoid of bound ribosomes. However, SRP becomes necessary when competing ribosomes are present at the ER membrane, which corresponds to the situation in vivo (Neuhof et al., 1998, Raden et al., 1998). It is well documented that the rough endoplasmic reticulum (rER) of mammals is studded with ribosomes, roughly half of which are translocating (Adelman et al., 1973). These ribosomes remain bound after termination of translation (Borgese et al., 1973; Seiser and Nicchitta, 2000). We

showed that under these conditions, SRP facilitates RNC binding to a population of Sec61 monomers or dimers which cannot associate with nontranslating ribosomes or RNCs on their own. Therefore, the SRP-system does not only seem to function by bringing RNCs to the right compartment, but by enabling them to efficiently compete with nontranslating ribosomes for translocon binding.

5.2 The mechanism of SRP-dependent targeting

Our work provides an explanation for how RNCs formed in the cytoplasm can gain access to binding sites at ER membranes saturated with nontranslating ribosomes. Two classes of ribosome binding sites are present in the ER membrane: high-affinity binding sites are constituted by a Sec61 tetramer, and low-affinity binding sites likely consists of a Sec61 monomer or dimer. The SRP/SR system facilitates interaction of RNCs with the low-affinity binding sites provided by Sec61. As the binding of RNCs to the low-affinity binding site is unstable, the transfer of RNCs to Sec61 needs to be highly regulated. With this in mind, we propose a new mechanism of SRP-dependent targeting, that is consistent with published data on both SRP and the SRP-receptor (Figure 31).

The eukaryotic SRP system contains three GTPases, that together regulate RNC targeting to the ER membrane: SRP54, SRα and its transmembrane anchor SRβ. The SRP-family of GTPases is structurally more related to ATPases than to other GTPases (Montoya et al., 2000), and its members display only low affinity for nucleotides, requiring no guanine exchange factor (GEF). The SRβ GTPase is a transmembrane protein unique to eukaryotes and resembles Ras-GTPases (Miller et al., 1995).

Upon signal sequence binding, SRP54 displays an increased affinity for GTP (Bacher et al., 1996). In its GTP-bound form, SRP54 can associate with GTP-loaded SRα, that is anchored to the membrane by GDP-bound SRβ (Legate et al., 2000). The association of SRP54 and SRα leads to conformational change and to the exposure of parts of the Sec61 binding site at the ribosome (Pool et al., 2002; Halic et al., 2006). A recent three-dimensional structure of a RNC-SRP-SR complex reveals that the exposed binding site could harbour a maximum of two Sec61p complexes (Halic et al., 2006). This supports our model of Sec61 monomers or dimers being employed in SRP-dependent targeting, as a Sec61 tetramer would be too large to fully interact with the ribosome. The SRP/SR complex might act as a scaffold, that keeps the RNC

stably bound until it has sequestered a Sec61 complex. The bound ribosome prevents SRβ from binding GTP, unless contact with the translocon is established (Fulga et al., 2001). It is possible that the ribosome interacts with the β-subunit of Sec61, which is known to bind ribosomes and to act as a GEF for SRβ (Levy et al., 2001; Helmers et al., 2003). At that time, the RNC is partially bound to Sec61 but likely also to SRβ, which obtains a high affinity for ribosomes upon GTP-binding (Bacher et al., 1999). In addition, GTP-binding of SRβ triggers signal sequence release of SRP54 (Fulga et al., 2001), and the nascent chain could interact with the recruited Sec61 while the complex is stabilized by the interaction of the ribosome with SRβ. The time window for nascent chain transfer would be, however, short, as an SRβ-bound ribosome functions as a GAP for SRβ and is released once SRβ is in its GDP-bound form (Bacher et al., 1999). Once the signal sequence has established contact with Sec61, the RNC is firmly anchored to the ER membrane (Jungnickel et al., 1995). After release of the nascent chain, SRP54 and SRα act as each other's GTPase activating protein (GAP), hydrolyze GTP and dissociate (Powers and Walter, 1995).
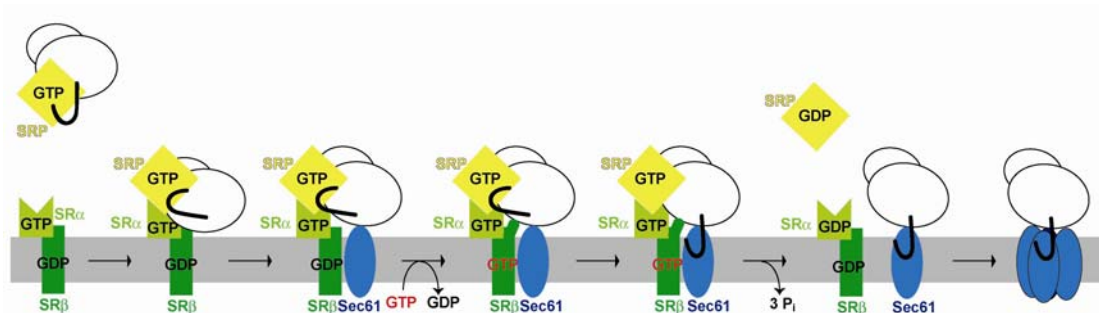
Figure 31: Proposed mechanism for SRP-dependent targeting. SRP recognizes the emerging signal sequence (black) and binds GTP, becoming competent for SRα-binding. Conformational change exposes the Sec61 binding site on the RNC while blocking the GTP-binding site of SRβ. Sec61-binding by the RNC (white) leads to nucleotide exchange in SRβ, which in its GTP-bound form has a high affinity for the ribosome and triggers signal sequence release by SRP54. The signal sequence is recognized by Sec61 and and the ribosome activates the GTPase activity of SRβ and is subsequently released. SRα and SRP reciprocally stimulate each other's GTPase activity and dissociate. At a later stage of translocation, a Sec61 tetramer may form.

The SRP system thus seems to sequentially stabilize transition states during the transfer of an RNC to a low affinity binding site, minimizing accidental RNC dissociation from Sec61. This model is consistent with the structural data we have obtained. Without a nascent chain, a Sec61 monomer is bound, possibly representing the "foothold" the RNC takes on Sec61 while still being associated with the SRP/SR complex. Insertion of the nascent chain leads to the association of a second Sec61

molecule, which might accomodate the nascent chain. Alternatively, translocation of the nascent chain could remove the central plug from the pore and change the conformation of Sec61 (Tam et al., 2005). This could favour the association of more Sec61 molecules, which might stabilize the conformationally dynamic, translocating Sec61. Consistent with this, membrane-bound ribosomes are associated with tetramers of Sec61 (Menetret et al., 2000). This indicates that they may have recruited more Sec61 molecules over time, assembling a tetramer underneath the ribosome (Hanein et al., 1996). The idea of gradual stabilization of the translocation complex is also supported by the nascent chain being required for initial binding of RNCs to Sec61 (Neuhof et al., 1998), while being dispensable at a later stage (Adelman et al., 1973).

This model needs to be further substantiated, ideally by structural characterization of the intermediates during RNC transfer to Sec61. This is, however, hampered by the lack of trapping methods for the different stages of transfer, as GTP binding and not hydrolysis seems to be the decisive step for all GTPases involved. To gain insight into this highly regulated process, new approaches beyond the usual techniques for GTPase investigation need to be found.

5.3 Evolutional conservation in prokaryotes

In bacteria, the SRP system is essential and consists only of SRP54 (Ffh) and a SRα-homolog (FtsY) (for review, see Herskovits et al., 2000). There is no known homolog for SRβ and it is still unclear if there is a membrane receptor for FtsY (Herskovits et al., 2001; Zelazny et al., 1997). There is some evidence that FtsY and SRα might be able to bind ribosomes in detergent solution (Herskovits et al., 2002; Mandon et al., 2003) and at least transiently interact with SecYEG (Angelini et al., 2005). The protein-conducting channel in the bacterial inner membrane is to a large extent associated with the ATPase SecA, which catalyzes posttranslational translocation, is unique to eubacteria, and appears not to interfere with ribosome binding (Zito and Oliver, 2003). Ribosome binding to bacterial membranes is known to occur (Prinz et al., 2000, Herskovits et al., 2000), but it is unclear to what extent. We compared the amount of endogenous ribosomes bound to rER and bacterial inner membranes relative to the SecYEG/Sec61 content, and found that bacterial membranes carry only very few ribosomes relative to their eukaryotic counterparts. Consistent with this, we

observed that ribosome binding to SecYEG is much weaker than ribosome binding to Sec61. The binding curve is consistent with binding to two sites, a high-affinity binding site that has been described (Prinz et al., 2000) and a much more abundant low-affinity binding site so far uncharacterized. According to our hypothesis, the high affinity binding sites would be provided by a SecYEG oligomer, while the low affinity binding sites would consist of SecYEG monomers or dimers. Freeze-fracture experiments show that SecYEG exists in a concentration-dependent equilibrium between monomers, dimers and tetramers in E.coli membranes (Scheuring et al., 2005). In wildtype cells, only 1% of the SecYEG is present as a tetramer, while 40% is dimeric and 60% monomeric. As oligomerization is concentration-dependent, overexpression of SecYEG leads to an accumulation of higher oligomeric states (Bessonneau et al., 2002), which may explain why high affinity binding sites can be observed (Prinz et al., 2000) and why SecYEG forms ring-like structures in B.subtilis membranes (Meyer et al., 1999).

While there is no such data available for prokaryotes, ribosomes derived from mammalian rER membranes seem to be bound to a Sec61 tetramer (Menetret et al., 2005). In order to remove these ribosomes from the Sec61-tetramer, the release of the nascent chain by puromycin together with subsequent high salt treatment is necessary (Adelman et al., 1973). In bacteria, however, puromycin treatment on its own leads to dissociation of nearly all membrane-bound ribosomes (Smith et al., 1977; Smith et al., 1978). This indicates that the ribosome-channel binding in bacteria is weaker than in eukaryotes, and is consistent with our findings that only few high affinity binding sites are present in vitro and in vivo at E.coli membranes.

Structural studies in detergent solution have shown that a SecYEG monomer is bound to bacterial ribosomes without and perhaps also with a nascent chain present (our data), but there are also reports of SecYEG dimer binding to RNC complexes (Mitra et al., 2005). In the latter structure with an average resolution of 15Å, a total of two SecYEG dimers is bound, one at the ribosomal exit site and one at the mRNA exit site at the interface of 30S and 50S ribosomal subunit, occupying a nonphysiological binding site. The SecYEG density at the ribosomal exit site does not correspond to the expected shape of a SecYEG dimer (Breyton et al., 2002); a large conformational change was required in order to produce a reasonable fit (Mitra et al., 2005). The resolution of the channel is unclear, and there is no evidence that the nascent chain productively interacts with SecYEG. The resolution of the channel is known to be

generally worse than the resolution of the ribosome, most likely because of conformational flexibility, incomplete occupancy of the ribosome with the channel, and the dominance of the large ribosomal density in the computational alignment of the particles (Menetret et al., 2005). As the different oligomeric states of SecYEG are governed by a concentration-dependent equilibrium in detergent (Bessonneau et al., 2002), it is possible that the results obtained depend on the exact conditions used for complex formation.

Taken together, ribosome binding to the bacterial inner membrane is considerably weaker than ribosome binding to the rER, and less pronounced in vivo. We propose that in comparison to Sec61, the oligomerization equilibrium of SecYEG is shifted towards monomeric and dimeric states, resulting in more low-affinity binding sites at the membrane. It is possible that tetramer formation is not favoured in the bacterial membrane (Bessonneau et al., 2000). This might explain why SRP is essential in bacteria, while eukaryotes can survive, although with significant growth defects, in the absence of SRP (Brown and Fournier, 1984; Phillips and Silhavy, 1992; Amaya et al., 1990; Hann and Walter, 1991).

5.4 Differences in structures determined from membranes and in detergent

Mammalian ribosome-channel complexes, that were assembled on membranes and then solubilized, contain a tetramer of Sec61 (Menetret et al., 2000; Morgan et al., 2002; Menetret et al., 2005). Similar complexes assembled in detergent reveal a monomer or dimer of Sec61 bound to the ribosome (our data). It is possible, that the interactions for maintaining the Sec61-tetramer cannot be preserved without the prebound ribosome as a stabilizing factor. This would be consistent with oligomeric rings of Sec61 only forming after addition of ribosomes to membranes (Hanein et al., 1996). For the tetrameric structures, nontranslating ribosomes were bound to ribosome-stripped ER membranes, thereby preferably targeting high-affinity binding sites (Morgan et al., 2002). We therefore assume that Sec61 tetramers constitute the high-affinity binding sites, while Sec61 monomers or dimers represent the low-affinity binding sites in the rER membrane, which will remain largely unbound. A mixture of ribosome-channel complexes of different oligomeric states would likely lead to the appearance of a tetramer, as the high-affinity binding sites are more abundant in eukaryotes and their larger size would mask contributions of smaller oligomers in the final structure. This could be reflected by the uneven density

distribution within the channel oligomer (Beckmann et al., 1997; Menetret et al., 2000; Beckmann et al., 2001).

We assume that the monomers and dimers, that we observed by electron cryo-microscopy, represent nucleation states of Sec61 oligomerization. Low oligomeric states of Sec61 should thus be present in only a small fraction of ribosome-channel complexes at the membrane.

5.5 The nature of the pore

Using electrophysiological and fluorescence quenching methods, the protein-conducting channel Sec61 was observed to form aqueous pores in the rER (Simon et al., 1989; Simon and Blobel, 1991; Wirth et al., 2003; Crowley et al., 1994). Consistent with protease protection data, the channel opens when the secretory nascent chain has reached a length of about 70-80 residues (Crowley et al., 1994; Jungnickel et al., 1995). During translocation, ion permeability of the channel is low, but increases when the nascent chain is released by puromycin. The pore remains open until the ribosome is dissociated (Simon and Blobel, 1991). The diameter of the open pore was estimated to be between 6 and 60Å (Hamman et al., 1997; Wirth et al., 2003). Structures of ribosome-channel complexes determined by electron cryo-microscopy show an oligomer of Sec61 with a central indentation (Menetret et al., 2000), that is close to the ribosomal exit site and was therefore interpreted as the protein-conducting pore (Beckmann et al., 1997). In contrast, the X-ray structure of the archaebacterial Sec61-homolog SecYEβ is shaped like an hourglass with a central plug domain (van den Berg et al., 2004), that is opened during translocation, as indicated by crosslinking experiments and molecular modeling (Harris and Silhavy, 1999; Tam et al., 2005; P. Tian and Andriocioaei, 2006; Gumbart and Schulten, 2006). Crosslinking experiments between different pairs of cysteines in the translocation substrate and in SecYEG showed that nascent chains contact the central pore region of SecYEG during translocation (Cannon et al., 2005). These data do not exclude that Sec61 oligomerization leads to fusion of pores, which could form the central indentation observed in ribosome-channel structures. Our ribosome-channel structures determined by electron cryo-microscopy now firmly establish that the central indentation is not necessary for protein translocation, as a Sec61 dimer was

shown to be sufficient for protease protection of the nascent chain in detergent solution.

In E.coli, a SecYEG monomer was observed and crosslinks between the nascent chain and pore-lining residues in SecYEG indicated that the translocation substrate was transported through the pore. We also observed a central cavity in the SecYEG and Sec61 monomers, that seems to represents the closed pore. It is therefore likely that a single Sec61 molecule can translocate the nascent chain, although channel formation by fusion of pores within two Sec61 or SecYEG molecules cannot strictly be excluded.

5.6 Ribosome dissociation from the ER membrane

Mammalian rER membranes are densely decorated with bound ribosomes, but only 50% are actively translocating (Adelman et al., 1973). Nontranslating ribosomes have a high affinity for Sec61 (Borgese et al., 1974; Prinz et al., 2000), and dissociate only very slowly. In addition, translocating ribosomes seem to remain bound once they have terminated translation and lost their nascent chain (Borgese et al., 1973; Seiser and Nicchitta, 2000).

As ribosome binding to the high affinity binding sites in the rER membrane seems to be extraordinarily stable, an important questions arises: How do ribosomes eventually dissociate from the membrane? As SRP-dependent targeting leads to ribosome binding to the low-affinity binding sites, ribosomes bound to the high-affinity binding site are not immediately displaced. We have shown that the binding to the high-affinity binding site is dynamic, as individual connections constantly break and reform, while several of them together keep the ribosome bound. The tetrameric Sec61 appears to be in an equilibrium with smaller oligomeric forms, and we showed that Sec61 molecules can interchange between the two populations. It is thus possible, that SRP-dependent targeting will eventually deplete the pool of low-affinity binding sites and thereby induce the conversion of high- into low-affinity binding sites. Sec61 could laterally leave the ribosome-channel junction, leading to dissociation of nontranslating ribosomes over time, as progressively fewer connections keep them membrane-bound. This model of interconnected equilibria implies that SRP-dependent targeting indirectly leads to dissociation of prebound ribosomes by influencing the equilibrium between different oligomeric forms of Sec61.

Alternatively, cytosolic factors could catalyze the dissociation of prebound ribosomes, as has been suggested for a "Detachment Factor" isolated from reticulocyte lysate (Blobel, 1975). Consistent with that, we could dissociate prebound ribosomes using large amounts of reticulocyte lysate. However, this effect was negligible in our SRP-dependent targeting assays. It has also been proposed, that reinitiation of translation is possible using membrane-bound ribosomes, which leads to ribosome dissociation if the nascent chain lacks a signal sequence (Potter et al., 2000).

5.7 Different oligomeric states of Sec61 in the ER membrane

Why are different oligomeric states of Sec61 present? Nontranslating ribosomes can bind to Sec61 with high affinity, dissociate only slowly and are present in excess in vivo. Thus, when the translation of translocation substrates begins, the high-affinity binding sites at the membrane are already occupied. In a situation, in which a competitor binds first and quasi irreversibly, the only way for RNCs to translocate their nascent chains is to use a channel population that cannot be accessed by competitors. Such a "reserved" Sec61 population could be generated by lowering the oligomeric state, so that it cannot be bound by nontranslating ribosomes or RNCs. The SRP-system, being only available to RNCs carrying a secretory nascent chain, can facilitate the interaction between RNC and a Sec61 monomer or dimer, so that translocation can occur. We found that the fraction of unbound Sec61 depends on the concentration of ribosomes in the cytosol, and that free and bound Sec61 are in an equilibrium with each other. This equilibrium ensures the presence of free channel even at high ribosome concentrations, i.e. during growth phases. It therefore represents a regulatory mechanism that can be maintained throughout a variety of conditions and ensures translocation of substrates, even when their abundance is very small in comparison to the competitors.

Still, the question why nontranslating ribosomes bind to Sec61 tetramers in the first place remains unanswered. Is this an consequence of the fact that tetramers may need to form underneath the ribosome at a later stage of translocation, to further stabilize the complex? Do Sec61-tetramers bound by nontranslating ribosomes represent a storage form, that could be accessed via the equilibrium between different oligomeric states of Sec61, when high translocation activity is needed? If Sec61 has a role in retrotranslocation, as has been suggested (Kalies et al., 2005; Meusser et al., 2005), ribosomes that finished translocation may also reserve Sec61 for this purpose and

keep the channel in its open conformation (Simon and Blobel, 1991), so that retrotranslocation substrates can be transported from the lumen to the cytosol.

Alternatively, nontranslating ribosomes could be used for initiation of translation and translocation at the membrane, as has been suggested (Potter et al., 2001). In this model, mRNAs would interact with membrane-bound large ribosomal subunits and emerging nascent chains with a signal sequence would be translocated through the bound Sec61, while nascent chains lacking a signal sequence would lead to RNC dissociation from the membrane (Potter et al., 2000). As there is no evidence that secretory mRNAs catalyze their own targeting to the ER without being translated, mRNA binding to membrane-bound ribosomes would be completely random. Hence, the efficiency of translocation would strongly depend on the ratio between secretory and cytosolic proteins that is synthesized at a given time, a clear disadvantage to the cell. This model could, however, be relevant in conjunction with the notion that most translocating ribosomes are present in polysomes in vivo (Nikonov et al., 2002). While the first RNC would be generated in the cytosol and targeted to the ER membrane by the SRP pathway, the mRNA emerging during ongoing translocation could interact with neighbouring membrane-bound large ribosomal subunits and trigger initiation of translation. This would make polysomal translocation very effective, as the SRP-dependent targeting reaction would be quickly amplified at the membrane.

6 MATERIALS AND METHODS

6.1 Molecular Biology

6.1.1 Bacterial strains

Escherichia coli TOP10 (Invitrogen): F' mcrA D(mrr-hsdRMS-mcrBC) f801lacZDM15 DlacX74 deoR recA1 araD139 D(ara-leu)7697 galU galK rpsL (StrR) endA1 nupG

Escherichia coli JM109 (Promega): F' traD36 proA+B+ lacIq delta(lacZ)M15/ delta(lac-proAB) glnV44 e14- gyrA96 recA1 relA1 endA1 thi hsdR17

Escherichia coli JM109(DE3) (Promega): *end*A1, *rec*A1, *gyr*A96, *thi, hsd*R17 (r_k^-, m_k^+), *rel*A1, *sup*E44, λ–, Δ(*lac-pro*AB), [F′, *tra*D36, *pro*AB, *lac*I^{q}ZΔM15], lDE3.

Escherichia coli C43(DE3) -*ompT gal hsdS* (rm) *dcm lon* λDE3

6.1.2 Bacterial growth

Bacteria were cultivated in LB liquid medium (1% bactotryptone (Difco), 0.5% yeast extract (Difco), 1% NaCl) or on agar plates (1.5% Agar in LB, Merck). If using selective media, the following antibiotics were used: Ampicillin (Sigma) 100 μg/ml, Carbenicillin (Sigma) 100 μg/ml, Kanamycin (Sigma) 30 μg/ml, Tetracyclin (Sigma) 25 μg/ml.

6.1.3 Preparation of CaCl$_2$-competent E.coli cells

A single colony was inoculated in 50ml LB medium and rotated over night at 37°C. 2ml were used to inoculate 200ml LB medium, which was aerated at 37°C until an OD$_{600}$ of 0.5 was reached. Cells were cooled on ice for 15min and pelleted (3000rpm, 4°C, 10min, Heraeus). The pellet was resuspended in 80ml Tfb1 (30mM KOAc (Merck), 100mM RbCl$_2$ (Sigma), 10mM CaCl$_2$ (Merck), 50mM MnCl$_2$ (Sigma), 15% (v/v) glycerol (Merck), pH6.5) and incubated on ice for 15min. Cells were pelleted again and resuspended in 8ml Tfb2 (10mM MOPS (Sigma), 75mM CaCl$_2$ (Merck), 10mM RbCl$_2$ (Sigma), 15% (v/v) glycerol (Merck), pH 6.5) and incubated for 15min

on ice. 50μl aliquots of the suspension were snap-frozen in liquid nitrogen and stored at -80°C.

6.1.4 Transformation of CaCl₂-competent cells

Purified plasmid DNA was transformed into CaCl₂-competent cells using a heat shock procedure (Cohen et al., 1972): 50μl of a bacterial suspension was mixed with 0.4μg DNA and incubated on ice for 30min, followed by a 42°C heat pulse of 90s (45s for TOP10 cells). 250μl LB-medium was added and cells recovered for 2-4h at 37°C before plating on selective media.

6.1.5 Plasmid purification

Plasmids were purified using the Mini-Prep or HiSpeed Maxi-Prep Kits (Qiagen) according to the manufacturer's instructions.

6.1.6 DNA/RNA precipitation

H_2O was added to the sample to a final volume of 150μl. The solution was vortexed with 150μl of Phenol/Chloroform/Isoamylalcohol 25:24:1 for 1min at room temperature. The sample was centrifuged for 1min at 14000rpm (Eppendorf tabletop centrifuge). The aqueous layer was isolated and DNA precipitated with 2.5 volumes 100% ethanol and 0.1 volumes of 3M NaAc, pH 4.8 for 20min at -20°C. RNA was precipitated with 0.6 volumes of 100% ethanol and 0.1 volumes of 3M NaAc, pH 4.8 for 20min at -20°C. The precipitate was pelleted by centrifugation at 20000g for 15min at 4°C. The pellet was rinsed with cold 70% ethanol, centrifuged again, air dried and resuspended in H_2O.

6.1.7 Cloning

Vectors: pCRII-TOPO (Invitrogen), pALTER-Ex1 (Promega), pCS2 (Novagen)

6.1.7.1 Polymerase chain reaction (PCR)

50μl PCR reactions contained 10ng template DNA, 0.2mM dNTP-Mix (Roche), 10pmol of each Primer and 1x pfu-buffer/5U Pfu polymerase (Stratagene) or 1x Taq-buffer/1U Taq polymerase (Novagen). PCR was conducted using the following protocol: 2 min 95°C (30sec 95°C, 30sec 50°C, 1-2 min 72°C)$_{30}$ 6 min 72°C.

6.1.7.2 TA-overhang cloning

TA-overhang cloning of PCR-products was performed according to the manufacturer's instructions (Invitrogen). The PCRII-Topo-Kit (Invitrogen) was used and TOP10 cells were transformed with the products.

6.1.7.3 Restriction digest

Restriction digests were performed with 1U enzyme (NEB) per μg DNA according to the manufacturer's instructions (NEB).

6.1.7.4 Ligation

The molar ratio of vector to insert was 1:3. Both restricted vector and insert were purified from an agarose gel with the Gel Purification Kit (Qiagen) according to the manufacturer's instructions. Ligations were conducted with 4U T4Ligase (Invitrogen) per reaction in ligase buffer according to the manufacturer's instructions.

6.1.7.5 Agarose gelelectrophoresis

Agarose gels were made of 1% (w/v) Agarose (Biomol) and 0.1 mg/ml Ethidiumbromide (Sigma) in TE-Buffer (10mM Tris/HCl, pH 7.5, 1mM NaEDTA). Samples were loaded in TE buffer, 8% sucrose, 0.05% bromphenolblue and electrophoresis was conducted at a constant voltage of 8V/cm electrode distance. The stained DNA was vizualized under UV light (366nm).

6.2 Purification of microsomes, proteins and reconstitution

6.2.1 Preparation of microsomes

Rough microsomes (RM) from canine pancreas were prepared as described (Walter and Blobel, 1983). For preparation of puromycin-high salt treated microsomes (PKRM), a suspension of RM containing 3.5 equivalents per μl (eq; 1eq/μl = 50 A_{280}, Walter, et al., 1981) was mixed with an equal volume of buffer B (100mM HEPES/KOH pH 7.6, 200mM sucrose, 300mM KOAc, 10mM Mg(OAc)$_2$, 3mM DTT, 0.2mM GTP, protease inhibitors (10μg/ml leupeptin, 5μg/ml chymostatin, 3μg/ml elastatinal, 1μg/ml pepstatin), 3mM puromycin; Neuhof et al., 1998). After

homogenization, the mixture was incubated for 1h at 0°C, followed by 10min at 37°C and 10min at room temperature. The sample was centrifuged in a Beckman TLA100.3 rotor for 30min at 100000rpm at 2°C. The pellet was resuspended at 10eq/μl in buffer C (50mM HEPES/KOH pH7.6, 500mM sucrose, 800mM CsCl, 15mM Mg(OAc)$_2$, 3mM DTT, protease inhibitors) and mixed with an equal volume of a buffer C containing 1.95M sucrose. The total volume was determined and additional CsCl was added to a final concentration of 700mM. The sample was overlaid with 1ml buffer D (50mM HEPES/KOH pH7.6, 800 mM sucrose, 700mM CsCl, 15mM Mg(OAc)$_2$, 3mM DTT, protease inhibitors) and 0.6ml buffer B in a 13x51mm polycarbonate tube. After centrifugation in a TLA100.3 rotor for 1h at 100000rpm at 20°C, the top 0.2ml were discarded and the following 2-2.5ml, which contained the membranes, were collected. This fraction was diluted 1:4 in 50mM HEPES/KOH pH7.6, 1mM DTT, protease inhibitors, and centrifuged in a TLA100.3 rotor for 30min at 100000rpm at 2°C. The pellet was resuspended in buffer A (50mM HEPES/KOH pH7.6, 250mM sucrose) containing 1mM DTT and protease inhibitors. The membranes were washed twice by resuspension and centrifugation and finally taken up at 2-3eq/μl in buffer A containing 1mM DTT.

6.2.2 Purification of c.f. Sec61, SRP and SRP-receptor

Sec61 was purified from canine microsomes on the basis of its association with the ribosome and by affinity chromatography (Goerlich et al., 1993). SRP was purified from canine rough microsomes as described (Walter and Blobel, 1983b). SRP-receptor was purified from canine rough microsomes by affinity chromatography as described (Goerlich et al., 1993).

6.2.3 Overexpression and purification of E.c. SecYEG

A His-tagged SecYEG construct was transformed into C43(DE3) and aerated in 25ml selective medium over night. 12l of LB medium were inoculated with the starter culture and aerated in a shaker at 37°C until an OD_{600} of 0.6 was reached. Induction was performed with 2mg/ml arabinose for 4h at 37°C. Cells were harvested by centrifugation and pellets were frozen at -80°C.

Pellets were resuspended in 240ml resuspension buffer (20mM Tris/HCl pH7.5, 300mM NaCl, 10% glycerol, 1mM PMSF, EDTA-free complete protease inhibitor mix (Roche)) and lysed by passing twice through a microfluidizer (Microfluidics

Co.). Membranes were pelleted by centrifugation (Ti44, Beckman; 42000rpm, 1h, 4°C) and resuspended in resuspension buffer containing 0.1% DDM (Anatrace) using a douncer. Debris was pelleted (Ti44, Beckman; 30min, 4°C) and the supernatant was incubated with 10ml Ni-NTA-beads (Qiagen) for 1h at 4°C on a roller. The beads were washed in a column with 250ml resuspension buffer with 0.03% DDM (Anatrace) and 20mM Imidazole (Sigma). The bound protein was eluted with 20mM Tris/HCl, pH7.5, 100mM NaCl, 10% glycerol, 300mM imidazole, 0.03% DDM. The eluate was concentrated to 10ml using a Centricon Plus 20 concentrator (Millipore, 30kD cutoff). The next step of purification was either gelfiltration or ion exchange chromatography of the eluate.

Gel filtration:

The gelfiltration column (HiLoad 16-60, Superdex200 prep grade, Amersham) was equilibrated for 2h at 2ml/min using an automated system (Akta, Amersham) in 20mM Tris/HCl, pH7.5, 100mM NaCl, 10% glycerol, 0.03% DDM. The eluate was loaded on the column and gelfiltration was performed at 2ml/min. Absorbance at 260 and 280nm and conductivity was continuosly measured, fractions were collected and the peak was analyzed by gelelectrophoresis and staining.

Ion exchange:

The ion exchange column (HiTrap HP SP, Amersham) was equilibrated with 50mM HEPES/KOH pH7.6, 150mM KOAc, 5 mM Mg(OAc)$_2$, 2.5mM β-mercaptoethanol, complete EDTA-free proteaseinhibitor mix (Roche), 0.03% DDM, 5% glycerol, using an automated system (Akta, Amersham). Elution was performed with a gradient of 150-500mM KOAc in equilibration buffer. The eluate was adjusted to 150mM KOAc by dilution and subsequent concentration (Centricon, Millipore).

If digitonin (Sigma) was used as a detergent instead of DDM, 1% digitonin was used both for solubilization and purification of SecYEG. Solubilization was performed for 2h on ice. DeoxybigCHAP (DBC, Calbiochem) was used at a concentration of 0.3%.

6.2.4 Reconstitution of proteoliposomes

Proteoliposomes were reconstituted as described (Goerlich et al., 1993) from a mixture of lipids: L-α-Phosphatidylcholine (soybean, Sigma) : L-α Phosphatidyl-ethanolamine (soybean, Sigma) : L-α-Phosphatidylserine (soybean, Sigma) : L-α-Phosphatidylinositol (soybean, Sigma) = 100 : 25 : 3 : 12.5 in 50 mM HEPES/KOH

pH7.5, 15% glycerol, 20mM DTT, 2% DBC (Calbiochem). The lipid concentration was 20mg/ml. If necessary, trace amounts of Rhodamine-Phosphatidylethanolamine (Avanti Polar Lipids) were included. The ratio of protein volumes to lipid volumes for reconstitution was 8:6. The same total volume of SM2 Biobeads (Biorad) equilibrated in Buffer was used to remove the detergent over night at 4°C on a shaker. The proteoliposomes were recovered from the supernatant by dilution with the double volume of cold H_2O and ultracentrifugation (TLA 100.3, Beckman, 100000rpm, 4°C, 30min). The pellet was resuspended in RBB buffer (50mM HEPES/KOH, pH7.5, 150mM KOAc, 5mM Mg(OAc)$_2$, 2mg/ml BSA Fr.V (lipid-free), 1mM DTT), aliquots were snap-frozen in liquid nitrogen and stored at -80°C. Protein content of proteoliposomes was assessed by quantitative immunoblotting.

Reconstitution of ribosome-bound and free Sec61p was performed after solubilization of RMs in 1% DBC, with the endogenous lipids for free Sec61p and the synthetic lipid mixture described above for ribosome-bound Sec61p.

6.3 Analytical Methods

6.3.1 Polyacrylamide-Gelelectrophoresis and staining

The Criterion precast gel system (Biorad) was used. Gelelectrophoresis was performed in the Tris/HCl buffer system (Running Buffer: 25mM Tris, 192mM Glycine, 1% (w/v) SDS) at a constant current of 55mA per gel for 1h. The acrylamide concentrations in the gels were 10-20% or 4-10%. Samples were loaded in HU Buffer (Knop et al., 1998: 8M Urea, 5% SDS, 200mM Tris/HCl pH6.8, 1mM EDTA, Bromphenolblue, 1.5mM DTT). Gels were stained with Coomassie (Simple Blue, Invitrogen) or Silver Stain (SilverQuest Kit, Invitrogen) according to the manufacturer's instructions.

6.3.2 Autoradiography

After gelelectrophoresis, gels were equilibrated for 30 min at room temperature in Gel Drying solution (Biorad) and dried on filter paper (Whatman) using a heated vacuum-based gel dryer system (Model 583, Biorad). The dried gel was exposed over night using a imaging plate (Fuji) and analyzed with a phosphoimager (BAS 5000, Fuji). The software Image Gauge 3.0 (Fuji) was used for quantification of bands.

6.3.3 Immunoblotting and Antibodies

After gelelectrophoresis, proteins were transferred from gels to nitrucellulose membranes (HyBond, Amersham) using a Semi-Dry Blotting apparatus (Hoefer). Transfer was accomplished in transfer buffer (20mM Tris, 144mM Glycine, 0.01% NaSDS, 20% Methanol) by a constant current of 180mA per Criterion Gel (Biorad) for 70min at room temperature. The membrane was stained with Ponceau S solution (0.3% Ponceau S (Merck), 5% Acetic Acid) and destained with PBS (20mM Na_2HPO_4/KH_2PO_4 pH7.4, 137mM NaCl (Sigma)). The membrane was blocked for 30min at room temperature with 4% skim milk powder, 0.1% Tween-20 (Sigma) in PBS. The primary antibody was added in blocking solution over night at 4°C. After washing 3x 4min with blocking solution at room temperature, the secondary antibody was added in blocking solution for 1-2h at room temperature. The membrane was washed 3x 4min with blocking solution and 3x 4min with PBS. ECL-solution (Western Lightning, Pierce) was added and incubated for 1 min at room temperature, the membrane was transferred into an imaging cassette and different exposures were taken on Biomax MR film (Kodak).

Primary Antibodies:

rabbit anti C.f.Sec61α peptide CKEQSEVGSMGALLF (Neuhof et al., 1998), used 1:10000 (40ng/ml);

rabbit anti c.f. Sec61β peptide PGPTPSGTNC (Kalies et al., 1994), used 1:50000;

rabbit anti C.f. SRα (Neuhof et al., 1998) used 1:3000;

rabbit anti C.f. SRβ (this study; polyclonal against recombinant, His-tagged C.f. Sec61β was raised in rabbits by Zymed Laboratories) used 1:1000;

rabbit anti C.f. SRP54 used 1:2500;

Secondary Antibodies:

donkey anti-rabbit IgG (Jackson Immuno Research)

ProteinA-HRP (Sigma)

anti-HA-HRP (Roche)

6.3.4 Scintillation counting

A total volume of 150μl sample was mixed with 3ml Optifluor Scintillation fluid for aqueous solutions (Perkin Elmer) in a 6ml glass vial. A Beckman LS6000SE scintillation counter was used for analyzing the samples.

6.3.5 Concentration determination

The concentration of DNA and RNA was determined by absorbance measurements ($1A_{260}=50\mu g/ml$ or $40\mu g/ml$, respectively). Ribosome concentrations were determined by absorbance ($1A_{260}=16nM$ or $80\mu g/ml$ for eukaryotic ribosomes and $21nM$ or $74\mu g/ml$ for prokaryotic ribosomes; Hanein et al.,1996). Protein concentration was determined by the BCA protein assay kit (Pierce) or after denaturation in 8M Urea by absorbance measurements at 280nm using Lambert-Beer's law. Protein concentrations in native membranes were determined by quantitative immunoblotting.

6.4 In vitro transcription / translation

6.4.1 In vitro transcription

PCR product from a 50μl reaction (using a SP6 or T7 Primer) was purified by ethanol precipitation as described and dissolved in 15μl water. 15μl rNTP-Mix, 15μl SP6 or T7 buffer, 7.5μl SP6 or T7 enzyme mix and nuclease-free water was added to a total volume of 150μl (SP6 or T7 Ribomax-Kit, Promega). In vitro transcription was performed over night at 37°C and the mRNA was precipitated with EtOH/NaOAc as described.

6.4.2 In vitro translation

6.4.2.1 Reticulocyte lysate system

In vitro translation using RNase-treated rabbit reticulocyte lysate (Promega) was performed according to the manufacturer's instructions. 7μl reticulocyte lysate, 0.2μl 1mM amino acid mix (-Methionine), 0.2μl ^{35}S-Methionine (IVT grade, Amersham, 15μCi/μl), 0.2μl mRNA (2mg/ml) and nuclease-free water up to 10μl were combined. For cotranslational targeting, membranes were included. In vitro translation was performed for 20min at 28°C and stopped by addition of 2μM edeine. When an

unlabeled product was desired, the ^{35}S-Methionine was left out and a complete amino acid mix (1mM, Promega) was used.

6.4.2.2 Wheat germ extract system

The extract was prepared from wheat germ as described (Erickson and Blobel, 1983). Buffer conditions (KOAc, Mg(OAc)$_2$, Spermidine) was optimized for translation for each batch of wheat germ extract. 4μl wheat germ extract, 1μl 10x Saltmix (1M KOAc, 2mM Mg(OAc)$_2$, 6mM Spermidine), 0.2μl 1mM amino acid mix (-Methionine), 0.2μl ^{35}S-Methionine (IVT grade, Amersham, 15μCi/μl), 0.3μl energy mix (0.1M ATP, 0.02M GTP, 0.6M Creatine phosphate, 8mg/ml Creatine phosphokinase), 0.2μl mRNA (2mg/ml) and nuclease-free water up to 10μl were combined. For cotranslational targeting, membranes were included. In vitro translation was performed for 20min at 26°C and stopped by addition of 2μM edeine. When an unlabeled product was desired, the ^{35}S-Methionine was left out and a complete amino acid mix (1mM, Promega) was used.

6.4.2.3 E.coli S30 extract system

E.coli S30 extract for linear templates (Promega) was used according to the manufacturer's instructions. 4μl Premix, 3μl S30 Extract, 1μl 1mM amino acid mix (-Methionine), 0.2μl ^{35}S-Methionine (IVT grade, Amersham, 15μCi/μl), 0.2μl linear DNA (4mg/ml; purified PCR product), 4U RNase Inhibitor (Protector, Roche), 0.2μl 50μM tmRNA-antisense oligonucleotide (ON10, Hanes and Plueckthun, 1997) and nuclease-free water up to 10μl were combined. For cotranslational targeting, membranes were included. The in vitro translation was performed for 20min at 37 °C and stopped by addition of 2μM edeine. When an unlabeled product was desired, the ^{35}S-Methionine was left out and a complete amino acid mix (1mM, Promega) was used.

6.4.2.4 Isolation of RNCs

RNCs were isolated from in vitro translation reactions by sedimentation through a sucrose cushion (500mM sucrose, 50mM HEPES/KOH pH7.5, 150mM KOAc, 5mM Mg(OAc)$_2$, 1mM DTT) in a Beckman TLA100 rotor at 100000rpm for 30min at 4°C. The samples were resuspended in the orignal volume of RBB buffer (50mM

HEPES/KOH, pH7.5, 150mM KOAc, 5mM Mg(OAc)$_2$, 2mg/ml BSA Fr.V (lipid-free), 1mM DTT).

6.4.2.5 Labeling of endogenous RNCs in RMs

6eq RMs were labeled in a total volume of 10μl reticulocyte lysate in vitro-translation reaction in the presence of ^{35}S-methionine and in the absence of additional mRNA by incubation at 30°C for 15min. Membranes were sedimented or solubilized and RNCs sedimented as described.

6.5 Targeting reactions and ribosome binding experiments

For a standard targeting reaction, 10μl of a translation mixture (0.3μM ribosomes/RNCs) or the same amount of 0.3μM purified ribosomes in RBB buffer were used to presaturate 1 equivalent (eq; 1eq/ul = 50A$_{280}$, Walter and Blobel, 1983a) PKRMs for 30 min on ice. After dilution in 200μl RBB buffer, PKRMs were sedimented by centrifugation (Beckman TLS-55, 7x20mm tubes, 5min, 55000rpm, 4°C) and resuspended in membrane buffer (50mM HEPES/KOH pH7.5, 150mM KOAc, 10mM Mg(OAc)$_2$, 250mM sucrose, 1mM DTT). For each reaction, 0.2eq of these PKRMs were incubated on ice for 15min and at 28°C for 5min with 0.5μl ppl86 in vitro translation, which had been pre-incubated with 50fmol purified SRP or an equal amount of buffer for 5min at 28°C. To assess protease protection of the nascent chain, samples were treated with 0.5mg/ml proteinase K for 1h on ice and the protease was inactivated with 10mM phenylmethylsulfonylfluoride (PMSF) for 10min on ice. The samples were dissolved in urea-containing sample buffer (HU-Buffer; Knop and Schiebel, 1998) and analyzed by SDS-PAGE and autoradiography. To determine co-sedimentation of ribosomes with membranes, the samples were diluted in 200μl cold membrane buffer, and the membranes sedimented (Beckman TLS-55, 7x20mm tubes, 5min, 55000rpm, 4°C). The pellets were analyzed by SDS-PAGE and autoradiography or by scintillation counting of both supernatant and pellet.

6.6 Radiolabeling of ribosomes and dissociation experiments

Wheat germ ribosomes were purified from wheat germ extract (Erickson and Blobel, 1983) by sedimentation through a 2ml sucrose cushion (50mM HEPES/KOH pH7.5, 0.5M sucrose, 150mM KOAc, 5mM Mg(OAc)$_2$) for 45min at 100000rpm (Beckman

TLA 100.3). Ribosomes were resuspended in 0.4ml RBB. This was repeated two more times. Purified ribosomes were radiolabeled with ^{35}S-labeling reagent (t-Boc-[^{35}S]methionine-N-hydroxy-succinimidylester, Amersham) following the manufacturer's instructions, except that 50mM HEPES/KOH pH 7.8, 150mM KOAc, 5mM Mg(OAc)$_2$ was used as buffer and labeling was performed for 1h on ice. The radiolabeled ribosomes were purified by gel filtration through a P-30 Micro Bio Spin column (Biorad) and by sedimentation through a sucrose cushion as before. Purified ribosomes were resuspended in RBB and analyzed by sucrose gradient centrifugation. For measuring dissociation kinetics, 0.4pmol radiolabeled ribosomes per eq PKRMs were bound for 30min on ice, diluted 100x in pre-warmed RBB buffer, and incubated at 28°C. Samples containing 0.2eq PKRMs were sedimented as described. When 100μM ATA or 50μg/ml chymotrypsin were used to test dissociation, dilution was omitted and the samples were sedimented directly (ATA) or after inhibiting chymotrypsin with 10mM PMSF for 2min on ice. To investigate dissociation of pre-bound ribosomes during RNC targeting, radiolabeled ribosomes were used for PKRM presaturation and ppl86 was translated in the presence of unlabeled methionine. The targeting reaction was performed and the membranes sedimented as before.

6.7 Solubilization of membranes and sucrose gradient centrifugation

5eq of membranes were solubilized with 1.5% digitonin in a total volume of 50μl in RBB Buffer for 30min on ice. The extract was cleared by centrifugation (1min, 14000rpm, Eppendorf tabletop centrifuge) and loaded on top of a 10-40% sucrose step gradient in 50mM HEPES/KOH pH7.5, 150mM KOAc, 5mM Mg(OAc)$_2$, 1mM DTT, 0.5% digitonin. The step size was 5% sucrose. Centrifugation was performed for 105min at 55000rpm and 4°C in a TLS-55 rotor (Beckman. 11x34mm tubes). The gradient was fractionated from top to bottom and fractions were precipitated according to Wessel and Fluegge, 1984. The precipitates were denatured in HU sample buffer (Knop and Schiebel, 1998) for 10min at 65°C, followed by SDS-PAGE and immunoblotting with affinity-purified antibodies to Sec61α, Sec61β, and SRα.

6.8 Crosslinking and antibody-binding experiments

12eq RMs were treated with 1mM BMH (Sigma) in a final volume of 35μl of buffer (50mM HEPES/KOH pH7.5, 100mM KOAc, 5mM Mg(OAc)$_2$, 250mM sucrose) for

30min on ice. BMH was quenched with 100mM β-mercaptoethanol for 5min on ice, followed by addition of 1.5% digitonin for solubilization and sucrose gradient centrifugation. For antibody binding experiments, 8eq RMs or ribosome-saturated PKRMs were incubated with 2μg affinity-purified Sec61α-antibody or normal rabbit control IgG (Santa Cruz Biotechnology) for 1h on ice. Each sample was diluted with 0.2ml cold membrane buffer, the membranes were sedimented (Beckman TLS-55, 7x20mm tubes, 5min, 55000 rpm, 4°C), and analyzed by solubilization and sucrose gradient centrifugation.

Disulfide crosslinking of FtsQ77^{S41C} was performed as described in Cannon et al., 2005. Per lane, RNCs purified from 2μl in vitro translation reaction by sedimentation were incubated with 6μg SecYEG-mutant in a total volume of 5.5μl in 50mM HEPES/KOH pH7.5, 50mM KOAc, 5mM Mg(OAc)$_2$, 0.5mg/ml acetylated BSA. After incubation for 15min at 37°C, 0.3μl 10mM Tetrathionate (Sigma) was added for 10min at 37°C. The reaction was stopped with 0.5μl 200mM NEM for 5min on ice. Loading Buffer (MES, Invitrogen) was added, the samples were denatured for 3min at 40°C, and analyzed by MES-buffered SDS-PAGE (MES NuPAGE, Invitrogen).

6.9 Co-immunoprecipitation

20eq membranes were solubilized with 1.5% digitonin (Sigma) in RBB in a total volume of 50μl. The extract was cleared by centrifugation (1min at 14000rpm in an Eppendorf tabletop centrifuge) and the supernatant was incubated with 4μg of affinity-purified antibody or normal rabbit control IgG (Santa Cruz Biotechnology) overnight at 4°C. The reaction was diluted to 300μl with RBB including 0.5% digitonin and incubated with 20μl Protein G sepharose (Roche) for 1h on a roller at 4°C. The beads were sedimented at 1000g for 3min at 4°C and washed five times with 300μl RBB, 0.5% digitonin. The beads were dried with a syringe, eluted with HU sample Buffer (Knop and Schiebel, 1998) and analyzed by SDS-PAGE and immunoblotting. ProteinA-HRP (Sigma) was used for detection after probing with primary antibodies.

6.10 Electron Cryo-Microscopy of Ribosome-Channel Complexes

6.10.1 Preparation of 70S-SecYEG and 80S-Sec61 complexes

Wheat germ ribosomes were purified as described in 6.6. Bacterial ribosomes were kindly provided by W. Clemons and purified from E.coli MRE600 as in Clemons et al., 2001. Complexes were formed by incubation of ribosomes with a 20x molar excess of purified C.f.Sec61 or E.c.SecYEG for 30min on ice in 50mM HEPES/KOH pH7.5, 100mM KOAc, 10mM Mg(OAc)$_2$.

6.10.2 Preparation of eukaryotic RNC-Sec61 complexes

Wildtype preprolactin (ppl) was N-terminally HA-tagged and the SP6 promoter, the HA-tag and 86 amino acids of ppl were amplified by PCR and translated in a total volume of 2ml of wheat germ extract system as described. Translation was stopped with 10µg/ml cycloheximide and ribosomes were sedimented through a 2ml cushion (50mM HEPES/KOH pH7.5, 500mM sucrose, 100mM KOAc, 10mM Mg(OAc)$_2$, 1mM DTT) in a Beckman TLA100.3 rotor (100000rpm, 1h, 4°C). Ribosomes were resuspended in 400µl resuspension buffer (50mM HEPES/KOH pH7.5, 150mM KOAc, 10mM Mg(OAc)$_2$, 2mg/ml BSA, 1 pill/10ml complete EDTA-free protease inhibitor (Roche), 0.2U/µl RNase inhibitor (Protector, Roche), 0.1% DBC (Calbiochem)). The suspension was incubated with 50µl anti-HA affinity matrix (3F10, Roche) overnight at 4°C on a roller. The beads were washed three times with 0.5ml resuspension buffer and two times with resuspension buffer containing 300mM KOAc. The beads were dried with a syringe and eluted three times for 30min on a shaker at 37°C with resuspension buffer containing 1mg/ml HA peptide (Roche) and 300mM KOAc. The unified eluates were sedimented through a 100µl sucrose cushion as before using a Beckman TLA100 rotor (100000rpm, 30min, 4°C) and resuspended in 15µl resuspension buffer. 3pmol purified RNCs were preincubated with 50µl ribosome-free wheat germ extract (supernatant after sedimentation in Beckman TLA100, 100000rpm, 45min, 4°C) for 5min on ice, adjusted to 1% digitonin and a 20fold molar excess purified C.f.Sec61 was added for 15min on ice and 20min at 28°C. The RNC-Sec61 complexes were sedimented through a sucrose cushion as before (Beckman TLA100, 100000rpm, 30min, 4°C), resuspended in 10µl RBB containing 1% digitonin and used for electron cryo-microscopy.

6.10.3 Preparation of prokaryotic RNC-SecYEG complexes

N-terminally HA-tagged FtsQ was subcloned into pALTER-Ex1 and the tac-promoter, the HA-tag and 77 amino acids of FtsQ were amplified by PCR and translated in a total volume of 2ml of E.c. S30 extract system as described. Translation was stopped with 10µg/ml cycloheximide and ribosomes were sedimented through a sucrose cushion (50mM HEPES/KOH pH7.5, 500mM sucrose, 100mM KOAc, 10mM Mg(OAc)$_2$, 1mM DTT) in a Beckman TLA100.3 rotor (100000rpm, 1h, 4°C). Ribosomes were resuspended in 400µl resuspension buffer (50mM HEPES/KOH pH7.5, 100mM KOAc, 10mM Mg(OAc)$_2$, 2mg/ml BSA, 1 pill/10ml complete EDTA-free protease inhibitor (Roche), 0.2U/µl RNase inhibitor (Protector, Roche), 0.1% DesoxyBigCHAP (DBC, Calbiochem)). The suspension was incubated with 50µl anti-HA affinity matrix (3F10, Roche) overnight at 4°C on a roller. The beads were washed three times with 0.5ml resuspension buffer and two times with resuspension buffer containing 200mM KOAc. The beads were dried with a syringe and eluted three times for 30min on a shaker at 37°C with resuspension buffer containing 1mg/ml HA peptide (Roche) and 200mM KOAc. Micro Bio-Spin columns (P-30, Biorad) that had been equilibrated in 50mM HEPES/KOH pH7.5, 100mM KOAc, 10mM Mg(OAc)$_2$ were used for gelfiltration of the eluates. The unified eluates were concentrated to 8µl using a Biomax Ultrafree concentrator (Millipore, 50kD cutoff), adjusted to 0.05% DDM (Anatrace) and incubated with a 20fold molar excess of purified E.c. SecYEG for 30min on ice. Aggregates were removed by centrifugation (1min, 14000rpm in an Eppendorf tabletop centrifuge) and the supernatant was separated on a 10-40% sucrosegradient as described, except that it contained 100mM KOAc and 0.05% DDM was used as a detergent. Ribosome-containing fractions were identified by absorbance measurements, pooled, diluted 1fold and concentrated in a Biomax Ultrafree concentrator (Millipore, 30kD cutoff). Dilution and concentration was repeated until no sucrose was detectable in the flowthrough by refractometry. The purified RNC-SecYEG complexes were concentrated to a final volume of 8µl and used for electron cryo-microscopy or analyzed by SDS-PAGE and silver staining or immunoblotting.

6.10.4 Electron Cryo-Microscopy

Suspensions were loaded onto continuous or perforated carbon film support. The specimens were blotted and plunged into liquid ethane (Dubochet et al., 1988) in a humid environment at 4°C (>85% relative humidity). A Gatan cryo-transfer system and cryo-holder (model 626-DH) were used to transfer grids into a Tecnai TF20 FEG (Field Emission Gun) transmission electron microscope equipped with a cryo-blade type anti-contaminator. All electron micrographs were recorded at 200kV, under minimal dose conditions, using a defocus range of -1.0 to -1.5μm. Micrographs were recorded at 50,000x magnification on KODAK SO163 film and developed for 12min in full strength D19 developer (KODAK). In some cases, images were recorded with the specimen tilted at 20° using a dynamic defocus spot scan.

6.10.5 Three-Dimensional Image Processing and Analysis

Micrographs displaying minimal astigmatism and drift by optical diffraction were chosen for processing. Negatives were digitized on a CreoScitex EVERSMART scanner using a 4.54μm raster, binned to 13.6μm (corresponding to 2.73Å/pixel for maximum expected resolution of ~7Å) or 27.3μm (corresponding to 5.46Å/pixel for maximum expected resolution of ~15Å) and converted to SPIDER format. Image processing was done using the SPIDER software package (Frank et al., 1996) and/or the EMAN software package (http://ncmi.bcm.tmc.edu/EMAN; Ludtke et al., 1999). Particle picking was done with BOXER of EMAN. Particles were then aligned using the *refine* command of EMAN. If it was necessary to correct for the loss of channel during preparation, the *multirefine* command of EMAN was used to remove ribosomes without channel from the dataset. The purified dataset could then be refined further. The resolution of the whole complexes was calculated with the *eotest* of EMAN by comparing half-volumes made from the even and odd numbered particles. The "even" and "odd" volumes were then each separated using *qsegment* of EMAN into ribosome and channel volumes. Comparing the "even-ribosome" and "odd-ribosome" volumes gave us the resolution of the ribosome. Comparing the "even-channel" and "odd-channel" volumes gave us the resolution of the channel.

The threshold representing 100% of the ribosomal volume was chosen on the basis of calculated and experimentally measured partial specific volumes and the known mass of ribosomal protein and RNA. The 100% volume used in this work was $3.3 \times 10^6 \text{Å}^3$ and $5.6 \times 10^6 \text{Å}^3$ for the E.coli and wheat germ ribosomes, respectively. For graphic

representation of the data, the programs Chimera (http://www.cgl.ucsf.edu/chimera) and Adobe Photoshop were used.

7 REFERENCES

Adelman MR, Sabatini DD, Blobel G (1973). Ribosome-Membrane Interaction.Nondestructive Disassembly of Rat Liver Rough Microsomes into Ribosomal and Membranous Components. *J Cell Biol.* **56**, 206-220

Amaya Y, Nakano A, Ito K, Mori M (1990). Isolation of a yeast gene, SRH1, that encodes a homologue of the 54K subunit of mammalian signal recognition particle. *J Biochem (Tokyo)* **107**, 457-63

Andrews DW, Walter P, Ottensmeyer FP (1985).Structure of the signal recognition particle by electron microscopy. *Proc Natl Acad Sci U S A.* **82**, 785-9

Andrews PG, Kole R (1987). Alu RNA transcribed in vitro binds the 68-kDa subunit of the signal recognition particle. *J Biol Chem.* **262**, 2908-12

Angelini S, Deitermann S, Koch HG (2005). FtsY, the bacterial signal-recognition particle receptor, interacts functionally and physically with the SecYEG translocon. *EMBO Rep.* **6**, 476-81

Bacher G, Luetcke H, Jungnickel B, Rapoport TA, Dobberstein B (1996). Regulation by the ribosome of the GTPase of the signal-recognition particle during protein targeting. *Nature* **381**, 248-251

Bacher G, Pool M, Dobberstein B (1999).The ribosome regulates the GTPase of the beta-subunit of the signal recognition particle receptor. *J Cell Biol.* **146**, 723-30

Barle H, Essen P, Nyberg B, Olivecrona H, Tally M, McNurlan MA, Wernerman J, Garlick PJ (1999). Depression of liver protein synthesis during surgery is prevented by growth hormone*. Am J Physiol Endocrinol Metab* **276**, 620-627

Batey RT, Rambo RP, Lucast L, Rha B, Doudna JA (2000). Crystal structure of the ribonucleoprotein core of the signal recognition particle. *Science* **287**,1232-9

Beckmann R, Bubeck D, Grassucci R, Penczek P, Verschoor A, Blobel G, Frank J (1997). Alignment of conduits for the nascent polypeptide chain in the ribosome-Sec61 complex. *Science* **278**, 2123-2126

Beckmann R, Spahn CM, Eswar N, Helmers J, Penczek PA, Sali A, Frank J, Blobel G (2001). Architecture of the protein-conducting channel associated with the translating 80S ribosome. *Cell* **107**, 361-72

Bessonneau P, Besson V, Collinson I, Duong F (2002). The SecYEG preprotein translocation channel is a conformationally dynamic and dimeric structure. *EMBO J.* **21**, 995-1003

Blobel G (1976). Extraction from Free Ribosomes of a Factor Mediating Ribosome Detachment from Rough Microsomes. *Biochem Biophys Res Commun.* **68**, 1-7

Blobel G, Dobberstein B (1975a). Transfer of proteins across membranes. I. Presence of proteolytically processed and unprocessed nascent immunoglobulin light chains on membrane-bound ribosomes of murine myeloma. *J Cell Biol.* **67**, 835-51

Blobel G, Dobberstein B (1975b). Transfer of Proteins across Membranes: II. Reconstitution of Functional Rough Microsomes from Heterologous Components. *J. Cell Biol.* **67**, 852-862

Blobel G, Potter VR (1967). Ribosomes in rat liver: an estimate of the percentage of free and membrane-bound ribosomes interacting with messenger RNA in vivo. *J Mol Biol.* **28**, 539-42

Borgese N, Blobel G, Sabatini D (1973). In vitro Exchange of Ribosomal Subunits between Free and Membrane-Bound Ribosomes. *J. Mol. Biol.* **74**, 415-438

Borgese N, Mok W, Kreibich G, Sabatini D (1974). Ribosomal-Membrane Interaction: In vitro Binding of Ribosomes to Microsomal Membranes. *J. Mol. Biol.* **88**, 559-580

Breyton C, Haase W, Rapoport TA, Kuhlbrandt W, Collinson I (2002).Three-dimensional structure of the bacterial protein-translocation complex SecYEG. *Nature* **418**,662-5

Brown S, Fournier MJ (1984). The 4.5 S RNA gene of Escherichia coli is essential for cell growth. *J Mol Biol.* **178**, 533-50

Cannon KS, Or E, Clemons WM Jr, Shibata Y, Rapoport TA (2005). Disulfide bridge formation between SecY and a translocating polypeptide localizes the translocation pore to the center of SecY. *J Cell Biol.* **169,** 219-25

Cheng Z, Jiang Y, Mandon EC, Gilmore R (2005). Identification of cytoplasmic residues of Sec61p involved in ribosome binding and cotranslational translocation. *J Cell Biol.* **168**, 67-77

Clemons W, Brodersen D, McCutcheon J, May J, Wimberly B, Carter A, Morgan-Warren R, Ramakrishnan V (2001). Crystal structure of the 30S ribosomal subunit from Thermus thermophilus I. Purification, crystallization and structure determination. *J. Mol. Biol.* **310**, 827-43

Clemons WM Jr, Gowda K, Black SD, Zwieb C, Ramakrishnan V (1999). Crystal structure of the conserved subdomain of human protein SRP54M at 2.1 A resolution: evidence for the mechanism of signal peptide binding. *J Mol Biol.* **292**, 697-705

Cohen SH, Chang AC, Hsu L (1972). Nonchromosomal antibiotic resistance in bacteria: genetic transformation of Escherichia coli by R-factor DNA. *Proc. Natl. Acad. Sci. U.S.A.* **69**, 2110-2114

Collinson I, Breyton C, Duong F, Tziatzios C, Schubert D, Or E, Rapoport T, Kuhlbrandt W (2001). Projection structure and oligomeric properties of a bacterial core protein translocase. *EMBO J.* **20**, 2462-71.

Connolly T, Gilmore R (1986). Formation of a functional ribosome-membrane junction during translocation requires the participation of a GTP-binding protein. *J Cell Biol.* **103**, 2253-61

Connolly T, Rapiejko PJ, Gilmore R (1991). Requirement of GTP hydrolysis for dissociation of the signal recognition particle from its receptor. *Science* **252**, 1171-1173

Crowley KS, Liao S, Worrell VE, Reinhart GD, Johnson AE (1994). Secretory proteins move through the endoplasmic reticulum membrane via an aqueous, gated pore. *Cell* **78**, 461-71

De Keyzer J, Van Der Does C, Driessen AJ (2002). Kinetic analysis of the translocation of fluorescent precursor proteins into Escherichia coli membrane vesicles. *J Biol Chem.* **277**, 46059-65

Deshaies RJ, Sanders SL, Feldheim DA, Schekman R (1991). Assembly of yeast Sec proteins involved in translocation into the endoplasmic reticulum into a membrane-bound multisubunit complex. *Nature* **349**, 806-8

Deshaies RJ, Schekman R (1987). A yeast mutant defective at an early stage in import of secretory protein precursors into the endoplasmic reticulum. *J Cell Biol.* **105**, 633-45

Driessen AJ, Manting EH, van der Does C (2001). The structural basis of protein targeting and translocation in bacteria. *Nat Struct Biol.* **8**, 492-8

Dubochet J, Adrian M, Chang JJ, Homo JC, Lepault J, McDowall AW, Schultz P (1988). Cryo-electron microscopy of vitrified specimens. *Q Rev Biophys.* **21**, 129-228

Economou A, Wickner W (1994). SecA promotes preprotein translocation by undergoing ATP-driven cycles of membrane insertion and deinsertion. *Cell* **78**, 835-43

Egea PF, Shan SO, Napetschnig J, Savage DF, Walter P, Stroud RM (2004). Substrate twinning activates the signal recognition particle and its receptor. *Nature* **427**, 215-21

Egea PF, Stroud RM, Walter P (2005). Targeting proteins to membranes: structure of the signal recognition particle. *Curr Opin Struct Biol.* **15**, 213-20.

Erickson AH, Blobel G (1983). Cell-free translation of messenger RNA in a wheat germ system. *Methods Enzymol.* **96**, 38-50

Evans MS, Ugrinov KG, Frese MA, Clark PL (2005). Homogeneous stalled ribosome nascent chain complexes produced in vivo or in vitro. *Nat Methods.* **2**, 757-62.

Finke K, Plath K, Panzner S, Prehn S, Rapoport TA, Hartmann E, Sommer T (1996). A second trimeric complex containing homologs of the Sec61p complex functions in protein transport across the ER membrane of S. cerevisiae. *EMBO J.* **15**, 1482-94

Flanagan JJ, Chen JC, Miao Y, Shao Y, Lin J, Bock PE, Johnson AE (2003). Signal recognition particle binds to ribosome-bound signal sequences with fluorescence-detected subnanomolar affinity that does not diminish as the nascent chain lengthens. *J. Biol. Chem* **278**,18628-18637

Focia PJ, Shepotinovskaya IV, Seidler JA, Freymann DM (2004). Heterodimeric GTPase core of the SRP targeting complex. *Science* **303**, 373-7

Frank J (2002). Single-particle imaging of macromolecules by cryo-electron microscopy. *Annu Rev Biophys Biomol Struct.* **31**, 303-19

Frank J, Radermacher M, Penczek P, Zhu J, Li Y, Ladjadj M, Leith A (1996). SPIDER and WEB: Processing and visualization of images in 3D electron microscopy and related fields. *J. Struct. Biol.* **116**, 190-199

Fresno M, Carrasco M, Vazquez M (1976). Initiation of the Polypeptide Chain by Reticulocyte-Free Systems. Survey of Different Inhibitors of Translation. *Eur. J. Biochem.* **68**, 355-364

Fulga TA, Sinning I, Dobberstein B, Pool MR (2001). SRbeta coordinates signal sequence release from SRP with ribosome binding to the translocon. *EMBO J.* **20**, 2338-47

Gilmore R, Collins P, Johnson J, Kellaris K, Rapiejko P (1991).Transcription of full-length and truncated mRNA transcripts to study protein translocation across the endoplasmic reticulum. *Methods Cell Biol.* **34**, 223-39

Gilmore R, Walter P, Blobel G (1982). Protein translocation across the endoplasmic reticulum. II. Isolation and characterization of the signal recognition particle receptor. *J Cell Biol.* **95**, 470-7

Gonzalez RG, Haxo RS, Schleich T (1980). Mechanism of action of polymeric aurintricarboxylic acid, a potent inhibitor of protein-nucleic acid interactions. *Biochemistry* **19**, 4299-303

Gorlich D, Prehn S, Hartmann E, Kalies KU, Rapoport TA (1992). A mammalian homolog of SEC61p and SECYp is associated with ribosomes and nascent polypeptides during translocation. *Cell* **71**, 489-503

Gorlich D, Rapoport TA (1993). Protein translocation into proteoliposomes reconstituted from purified components of the endoplasmic reticulum membrane. *Cell* **75**, 615-30

Gumbart J, Schulten K (2006). Molecular dynamics studies of the archaeal translocon. *Biophys J.* **90**, 2356-67

Halic M, Becker T, Pool MR, Spahn CM, Grassucci RA, Frank J, Beckmann R (2004). Structure of the signal recognition particle interacting with the elongation-arrested ribosome. *Nature* **427**, 808-14

Halic M, Gartmann M, Schlenker O, Mielke T, Pool MR, Sinning I, Beckmann R (2006). Signal recognition particle receptor exposes the ribosomal translocon binding site. *Science* **312**, 745-747

Hamman BD, Chen JC, Johnson EE, Johnson AE (1997). The aqueous pore through the translocon has a diameter of 40-60Å during cotranslational translocation at the ER membrane. *Cell* **89**, 535-544

Hanein D, Matlack KE, Jungnickel B, Plath K, Kalies KU, Miller KR, Rapoport TA, Akey CW (1996). Oligomeric rings of the Sec61p complex induced by ligands required for protein translocation. *Cell* **87**, 721-32

Hanes J, Pluckthun A (1997). In vitro selection and evolution of functional proteins by using ribosome display. *Proc Natl Acad Sci U S A*. **94**, 4937-42

Hann BC, Walter P (1991). The signal recognition particle in S. cerevisiae. *Cell* **67**, 131-144

Harris CR, Silhavy TJ (1999). Mapping an interface of SecY (PrlA) and SecE (PrlG) by using synthetic phenotypes and in vivo cross-linking. *J Bacteriol.* **181**, 3438-44

Heinrich SU, Rapoport TA (2003). Cooperation of transmembrane segments during the integration of a double-spanning protein into the ER membrane. *EMBO J.* **22**, 3654-63

Helmers J, Schmidt D, Glavy JS, Blobel G, Schwartz T (2003). The beta-subunit of the protein-conducting channel of the endoplasmic reticulum functions as the guanine nucleotide

exchange factor for the beta-subunit of the signal recognition particle receptor. *J Biol Chem.* **278**, 23686-90

Herskovits AA, Bochkareve ES, Bibi E (2000). New prospects in studying the bacterial signal recognition particle pathway. *Mol. Microbiol.* **38**, 927-939

Herskovits AA, Seluanov A, Rajsbaum R, Hagen-Jongman CM, Henrichs T, Bochkareva ES, Phillips GJ, Probst FJ, Nakae T, Ehrmann M, Luirink J, Bibi E (2001). Evidence for coupling of membrane targeting and function of the signal recognition particle (SRP) receptor FtsY. *EMBO rep.* **2**, 1040-1046

Herskovits AA, Shimoni E, Minsky A, Bibi E (2002). Accumulation of endoplasmic membranes and novel membrane-bound ribosome-signal recognition particle receptor complexes in Escherichia coli. *J. Cell Biol.* **159**, 403-410

High S, Flint N, Dobberstein B (1991). Requirements for the membrane insertion of signal-anchor type proteins. *J Cell Biol.* **113**, 25-34

Higy M, Junne T, Spiess M (2004). Topogenesis of membrane proteins at the endoplasmic reticulum. Biochemistry **43**, 12716-22

Hubbard R (1954). The molecular weight of rhodopsin and the nature of the rhodopsin-digitonin complex. *Journal of General Physiology* **37**, 381-399

Ionasescu V, Braga S, Kaeding L, Rubenstein P, Kalnitsky G, Chatterjee R (1981). Muscle ribosome detachment factor. Does it have a role in the pathogenesis of Duchenne muscular dystrophy? *Acta Neurol Scand.* **64**, 108-21

Jagath JR, Rodnina MV, Lentzen G, Wintermeyer W (1998). Interaction of guanine nucleotides with the signal recognition particle from Escherichia coli. *Biochemistry* **37,** 15408-13

Jagath JR, Rodnina MV, Wintermeyer W (2000). Conformational changes in the bacterial SRP receptor FtsY upon binding of guanine nucleotides and SRP. *J Mol Biol.* **295**, 745-53

Jungnickel B, Rapoport TA (1995). A posttargeting signal sequence recognition event in the endoplasmic reticulum membrane. *Cell* **82**, 261-270

Kalies KU, Allan S, Sergeyenko T, Kroger H, Romisch K (2005).The protein translocation channel binds proteasomes to the endoplasmic reticulum membrane. *EMBO J.* **24**, 2284-93

Kalies KU, Görlich D, Rapoport TA (1994). Binding of ribosomes to the rough endoplasmic reticulum mediated by the Sec61p-complex. *J. Cell Biol.* **126**, 925-934

Kalies KU, Rapoport TA, Hartmann E (1998). The beta subunit of the Sec61 complex facilitates cotranslational protein transport and interacts with the signal peptidase during translocation. *J Cell Biol.* **141**, 887-94

Keenan RJ, Freymann DM, Stroud RM, Walter P (2001). The signal recognition particle. *Annu Rev Biochem.* **70**, 755-75

Kleizen B, Braakman I (2004). Protein folding and quality control in the endoplasmic reticulum. *Curr Opin Cell Biol.* **16**, 343-9

Knop M, Schiebel E (1998). Receptors determine the cellular localization of a gamma-tubulin complex and thereby the site of microtubule formation. *EMBO J.* **17**, 3952-67

Kuglstatter A, Oubridge C, Nagai K (2002). Induced structural changes of 7SL RNA during the assembly of human signal recognition particle. *Nat Struct Biol.* **9**, 740-4

Kurzchalia TV, Wiedmann M, Breter H, Zimmermann W, Bauschke E, Rapoport TA (1988). tRNA-mediated labelling of proteins with biotin. A nonradioactive method for the detection of cell-free translation products. *Eur J Biochem.* **172**, 663-8

Legate KR, Falcone D, Andrews DW (2000). Nucleotide-dependent binding of the GTPase domain of the signal recognition particle receptor beta-subunit to the alpha-subunit. *J Biol Chem.* **275**, 27439-46

Levy R, Wiedmann M, Kreibich G (2001). In vitro binding of ribosomes to the β-subunit of the Sec61p protein translocation complex. *J. Biol. Chem.* 276, 2340-2346

Ludtke SJ, Baldwin PR, Chiu W (1999). EMAN: semiautomated software for high-resolution single-particle reconstructions. *J Struct Biol.* **128**, 82-97

Luirink J, Sinning I (2004). SRP-mediated protein targeting: structure and function revisited. - *Biochim Biophys Acta.* **1694**,17-35

Malkin LI, Rich A (1967). Partial Resistance of Nascent Polypeptide Chains to Proteolytic Digestion due to Ribosomal Shielding. *J. Mol. Biol.* **26**, 329-346

Mandon E, Jiang Y, Gilmore R (2003). Dual recognition of the ribosome and the signal recognition particle by the SRP receptor during protein targeting to the endoplasmic reticulum. *J. Cell Biol.* **162**, 575-585

Mason N, Ciufo LF, Brown JD (2000). Elongation arrest is a physiologically important function of signal recognition particle. *EMBO J* **19**, 4164-4174

Matlack KE, Misselwitz B, Plath K, Rapoport TA (1999). BiP acts as a molecular ratchet during posttranslational transport of prepro-alpha factor across the ER membrane. *Cell* **97**, 553-64

Matlack KE, Walter P (1995). The 70 carboxyl-terminal amino acids of nascent secretory proteins are protected from proteolysis by the ribosome and the protein translocation apparatus of the endoplasmic reticulum membrane. *J Biol Chem.* **270**, 6170-80.

Menetret JF, Hegde RS, Heinrich SU, Chandramouli P, Ludtke SJ, Rapoport TA, Akey CW (2005). Architecture of the ribosome-channel complex derived from native membranes. *J Mol Biol.* **348**, 445-57

Menetret JF, Neuhof A, Morgan DG, Plath K, Radermacher M, Rapoport TA, Akey CW (2000). The structure of ribosome-channel complexes engaged in protein translocation. *Mol Cell.* **6**, 1219-32.

Meusser B, Hirsch C, Jarosch E, Sommer T (2005). ERAD: the long road to destruction. *Nat Cell Biol.* **7**, 766-72

Meyer DI, Krause E, Dobberstein B (1982). Secretory protein translocation across membranes- the role of the docking protein. *Nature* **297**, 647-650

Miller JD, Tajima S, Lauffer L, Walter P (1995). The beta subunit of the signal recognition particle receptor is a transmembrane GTPase that anchors the alpha subunit, a peripheral membrane GTPase, to the endoplasmic reticulum membrane. *J Cell Biol.* **128**, 273-82

Miller JD, Wilhelm H, Gierasch L, Gilmore R, Walter P (1993). GTP binding and hydrolysis by the signal recognition particle during initiation of protein translocation. *Nature* **366**, 351-4

Mitra K, Schaffitzel C, Shaikh T, Tama F, Jenni S, Brooks CL 3rd, Ban N, Frank J (2005). Structure of the E. coli protein-conducting channel bound to a translating ribosome. *Nature* **438**, 318-24.

Mitra K, Ubarretxena-Belandia I, Taguchi T, Warren G, Engelman DM (2004). Modulation of the bilayer thickness of exocytic pathway membranes by membrane proteins rather than cholesterol. *Proc Natl Acad Sci U S A.* **101**, 4083-8

Montoya G, Kaat K, Moll R, Schafer G, Sinning I (2000). The crystal structure of the conserved GTPase of SRP54 from the archaeon Acidianus ambivalens and its comparison with related structures suggests a model for the SRP-SRP receptor complex. *Struct. Fold. Des.* **8**, 515-525

Morgan DG, Menetret JF, Neuhof A, Rapoport TA, Akey CW (2002). Structure of the mammalian ribosome-channel complex at 17A resolution. *J Mol Biol.* **324**, 871-86

Mori H, Ito K (2001).The Sec protein-translocation pathway. *Trends Microbiol.* **9**, 494-500

Mori H, Tsukazaki T, Masui R, Kuramitsu S, Yokoyama S, Johnson AE, Kimura Y, Akiyama Y, Ito K (2003). Fluorescence resonance energy transfer analysis of protein translocase. *J Biol Chem.* **278**, 14257-14264

Mothes W, Jungnickel B, Brunner J, Rapoport TA (1998). Signal sequence recognition in cotranslational translocation by protein components of the endoplasmic reticulum membrane. *J Cell Biol.* **142**, 355-64

Mothes W, Prehn S, Rapoport TA (1994).Systematic probing of the environment of a translocating secretory protein during translocation through the ER membrane. *EMBO J.* **13**, 3973-82

Murphy EC, Zheng T, Nicchitta CT (1997). Identification of a Novel Stage of Ribosome/Nascent Chain Association with the Endoplasmic Reticulum Membrane. *J. Cell Biol.* **136**, 1213-1226

Nagai K, Oubridge C, Kuglstatter A, Menichelli E, Isel C, Jovine L (2003). Structure, function and evolution of the signal recognition particle. *EMBO J.* **22**, 3479-85

Nakatogawa H, Murakami A, Ito K (2004). Control of SecA and SecM translation by protein secretion. *Curr Opin Microbiol.* **7**, 145-50

Neuhof A, Rolls MM, Jungnickel B, Kalies KU, Rapoport TA (1998). Binding of signal recognition particle gives ribosome/nascent chain complexes a competitive advantage in endoplasmic reticulum membrane interaction. *Mol Biol Cell.* **9**, 103-15

Ng DT, Brown JD, Walter P (1996). Signal sequences specify the targeting route to the endoplasmic reticulum membrane. *J Cell Biol.* **134**, 269-78

Nikonov AV, Snapp E, Lippincott-Schwartz J, Kreibich G (2002). Active translocon complexes labeled with GFP-Dad1 diffuse slowly as large polysome arrays in the endoplasmic reticulum. *J. Cell Biol.* **158**, 497-506

Ogg SC, Barz WP, Walter P (1998). A functional GTPase domain, but not its transmembrane domain, is required for function of the SRP receptor beta-subunit. *J Cell Biol.* **142**, 341-54

Osborne AR, Rapoport TA, van den Berg B (2005). Protein translocation by the Sec61/SecY channel. *Annu Rev Cell Dev Biol.* **21**, 529-50

Palade GE (1955). A small particulate component of the cytoplasm. *J Biophys Biochem Cytol.* **1**, 59-68

Palade GE, Porter KR (1954). Studies on the endoplasmic reticulum. I. Its identification in cells in situ. *J Exp Med.* **100**, 641-56

Panzner S, Dreier L, Hartmann E, Kostka S, Rapoport TA (1995). Posttranslational protein transport in yeast reconstituted with a purified complex of Sec proteins and Kar2p. *Cell* **81**, 561-70

Partis MD, Griffiths DG, Roberts GC, Beechey RB (1983). Cross-linking of protein by maleimido alkanoyl N-hydroxysuccinimidoesters. *J. Protein Chem.* **2**, 263-277

Phillips GJ, Silhavy TJ (1992). The E. coli ffh gene is necessary for viability and efficient protein export. *Nature* **359**, 744-6

Ulbrandt ND, Newitt JA, Bernstein HD (1997). The E. coli signal recognition particle is required for the insertion of a subset of inner membrane proteins. *Cell* **88**, 187-96

Phillips GJ, Silhavy TJ (1992). The E. coli ffh gene is necessary for viability and efficient protein export. *Nature* **359,** 744-6

Plath K, Mothes W, Wilkinson BM, Stirling CJ, Rapoport TA (1998). Signal sequence recognition in posttranslational protein transport across the yeast ER membrane. *Cell* **94**, 795-807

Pool MR, Stumm J, Fulga TA, Sinning I, Dobberstein B (2002). Distinct modes of signal recognition particle interaction with the ribosome. *Science* **297**, 1345-8.

Potter MD, Nicchitta CV (2000).Regulation of ribosome detachment from the mammalian endoplasmic reticulum membrane. *J Biol Chem.* **275**, 33828-35

Potter MD, Nicchitta CV (2002). Endoplasmic reticulum-bound ribosomes reside in stable association with the translocon following termination of protein synthesis. *J Biol Chem.* **277**, 23314-20.

Potter MD, Seiser RM, Nicchitta CV (2001).Ribosome exchange revisited: a mechanism for translation-coupled ribosome detachment from the ER membrane. *Trends Cell Biol.* **11**, 112-5

Powers T, Walter P (1995). Reciprocal stimulation of GTP hydrolysis by two directly interacting GTPases. *Science* **269**, 1422-24

Prehn S, Wiedmann M, Rapoport T, Zwieb C (1987). Protein translocation across wheat germ microsomal membranes requires an SRP-like component. EMBO J. **6**, 2093–2097

Prinz A, Behrens C, Rapoport TA, Hartmann E, Kalies KU (2000). Evolutionarily conserved binding of ribosomes to the translocation channel via the large ribosomal RNA. *EMBO J.* **19**, 1900-1906

Raden D, Gilmore R (1998). Signal recognition particle-dependent targeting of ribosomes to the rough endoplasmic reticulum in the absence and presence of the nascent polypeptide-associated complex. *Mol Biol Cell.* **9**, 117-30

Raden D, Song W, Gilmore R (2000). Role of the cytoplasmic segments of Sec61alpha in the ribosome-binding and translocation-promoting activities of the Sec61 complex. *J Cell Biol.* **150**, 53-64

Ramsey JC, Steele WJ (1976). A procedure for the quantitative recovery of homogeneous populations of undegraded free and bound polysomes from rat liver. *Biochemistry* **15**, 1704-12

Rapiejko PJ, Gilmore R (1997). Empty site forms of the SRP54 and SRa GTPases mediate targeting of ribosome-nascent chain complexes to the endoplasmic reticulum. *Cell* **89**, 703-713

Rapiejko PJ, Gilmore R (1994). Signal sequence recognition and targeting of ribosomes to the endoplasmic reticulum by the signal recognition particle do not require GTP. M*ol Biol Cell* **5**, 887-97

Riggs PD, Derman AI, Beckwith J (1988). A mutation affecting the regulation of a secA-lacZ fusion defines a new sec gene. *Genetics* **118**, 571-9

Sabatini DD, Blobel G (1970). Controlled Proteolysis of nascent polypeptides in rat liver cell fractions. II. Location of the polypeptides in rough microsomes. *J. Cell Biol.* **45**, 146-157

Sabatini DD, Tashiro Y, Palade GE (1966). On the attachment of ribosomes to microsomal membranes. *J Mol Biol.* **19**, 503-24

Sauer-Eriksson AE, Hainzl T (2003). S-domain assembly of the signal recognition particle. *Curr Opin Struct Biol.* 13, 64-70

Scheuring J, Braun N, Nothdurft L, Stumpf M, Veenendaal AK, Kol S, van der Does C, Driessen AJ, Weinkauf S (2005). The oligomeric distribution of SecYEG is altered by SecA and translocation ligands. *J Mol Biol.* **354**, 258-7

Schuwirth BS, Borovinskaya MA, Hau CW, Zhang W, Vila-Sanjurjo A, Holton JM, Cate JH (2005). Structures of the bacterial ribosome at 3.5 A resolution. *Science* **310**, 827-34

Seiser RM, Nicchitta CV (2000). The fate of membrane-bound ribosomes following the termination of protein synthesis. *J Biol Chem.* **275**, 33820-7

Shepotinovskaya IV, Freymann DM (2002). Conformational change of the N-domain on formation of the complex between the GTPase domains of Thermus aquaticus Ffh and FtsY. *Biochim Biophys Acta* **1597**, 107-14

Shires TK, Ekren T, Hinderaker P, Pitot HC (1974). Effect of Ribosome Removal on Rough Microsomal Composition and Polysome Attachment in vitro. *Biochim. Biophys. Acta* **374**, 59-74

Shires TK, Narurkar LM, Pitot HC (1971). Polysome interaction in vitro with microsomal membranes from rat liver. *Biochem Biophys Res Commun.* **45**, 1212-8

Simon SF, Blobel G, Zimmerberg J (1989). Large aqueous channels in membrane vesicles derived from the rough endoplasmic reticulum of canine pancreas or the plasma membrane of Escherichia coli. *Proc. Natl. Acad. Sci. USA* **86**, 6176-6180

Simon SM, Blobel G (1991). A protein-conducting channel in the endoplasmic reticulum. *Cell* **65**, 371-80

Smith WP, Tai PC, Davis BD (1978). Nascent peptide as sole attachment of polysomes to membranes in bacteria. *Proc. Natl. Acad. Sci. USA*, **75**, 814-817

Smith WP, Tai PC, Thompson RC, Davis BD (1977). Extracellular labeling of nascent polypeptides traversing the membrane of Escherichia coli. *Proc. Natl. Acad. Sci. USA* **74**, 2830-34

Snapp EL, Reinhart GA, Bogert BA, Lippincott-Schwartz J, Hegde RS (2004). The organization of engaged and quiescent translocons in the endoplasmic reticulum of mammalian cells. *J Cell Biol.* **164**, 997-1007

Song W, Raden D, Mandon EC, Gilmore R (2000). Role of Sec61alpha in the Regulated Transfer of the Ribosome-Nascent Chain Complex from the Signal Recognition Particle to the Translocation Channel. *Cell* **100**, 333-343

Stirling CJ, Rothblatt J, Hosobuchi M, Deshaies R, Schekman R (1992). Protein translocation mutants defective in the insertion of integral membrane proteins into the endoplasmic reticulum. *Mol Biol Cell* **3**, 129-42

Tajima S, Lauffer L, Rath VL, Walter P (1986). The signal recognition particle receptor is a complex that contains two distinct polypeptide chains. *J Cell Biol.* **103**, 1167-78

Tam PCK, Maillard AP, Chan KKY, Duong F (2005). Investigating the SecY plug movement at the SecYEG translocation channel. *EMBO J.* **24**, 3380-8

Tani K, Tokuda H, Mizushima S (1990). Translocation of ProOmpA possessing an intramolecular disulfide bridge into membrane vesicles of Escherichia coli. Effect of membrane energization. *J Biol Chem.* **265**, 17341-7

Terzi L, Pool MR, Dobberstein B, Strub K (2004). Signal recognition particle Alu domain occupies a defined site at the ribosomal subunit interface upon signal sequence recognition. *Biochemistry* **43**, 107-17

Tian P, Andricioaei I (2006). Size, motion and function of the SecY translocon revealed by molecular dynamics with virtual probes. *Biophys. J.* **90**, 2718-30

Urbanus ML, Scotti PA, Froderberg L, Saaf A, de Gier JW, Brunner J, Samuelson JC, Dalbey RE, Oudega B, Luirink J (2001). Sec-dependent membrane protein insertion: sequential interaction of nascent FtsQ with SecY and YidC. *EMBO Rep.* **2**, 524-9

Van den Berg B, Clemons WM Jr, Collinson I, Modis Y, Hartmann E, Harrison SC, Rapoport TA (2004). X-ray structure of a protein-conducting channel. *Nature* **427**, 36-44

van der Laan M, Houben EN, Nouwen N, Luirink J, Driessen AJ (2001). Reconstitution of Sec-dependent membrane protein insertion: nascent FtsQ interacts with YidC in a SecYEG-dependent manner. *EMBO Rep.* **2**, 519-23

Walter P, Blobel G (1983a). Preparation of Microsomal Membranes for Cotranslational Protein Translocation. *Methods in Enzymology* **96**, 84-93

Walter P, Blobel G (1983b). Signal Recognition Particle: A Ribonucleoprotein Required for Cotranslational Translocation of Proteins, Isolation and Properties. *Methods Enzymol.* **96**, 682-691

Walter P, Ibrahimi I, Blobel G (1981). Translocation of proteins across the endoplasmic reticulum. I. Signal recognition protein (SRP) binds to in-vitro-assembled polysomes synthesizing secretory protein. *J Cell Biol.* **91**, 545-550

Wessel D, Flugge UI (1984). A method for the quantitative recovery of protein in dilute solution in the presence of detergents and lipids. *Anal Biochem.* **138**, 141-3

Wickner W, Schekman R (2005). Protein translocation across biological membranes. *Science* **310**, 1452-6

Wild K, Sinning I, Cusack S (2001). Crystal structure of an early protein-RNA assembly complex of the signal recognition particle. *Science* **294**, 598-601

Wirth A, Jung M, Bies C, Frien M, Tyedmers J, Zimmerman R, Wagner R (2003). The Sec61p complex is a dynamic precursor activated channel. *Mol. Cell* **12**, 261-268

Young JC, Ursini J, Legate KR, Miller JD, Walter P, Andrews DW (1995). An amino-terminal domain containing hydrophobic and hydrophilic sequences binds the signal recognition particle receptor alpha subunit to the beta subunit on the endoplasmic reticulum membrane. *J Biol Chem.* **270**, 15650-7

Zelazny A, Seluanov A, Cooper A, Bibi E (1997). The NG domain of the prokaryotic signal recogntion particle receptor, FtsY, is fully functional when fused to an unrelated integral membrane polypeptide. *Proc. Natl. Acad. Sci. USA* 94, 6025-6029

Zito CR, Oliver D (2003). Two-stage binding of SecA to the bacterial translocon regulates ribosome-translocon interaction. *J. Biol. Chem.* **278**, 40640-40646

8 ABBREVIATIONS

3D:	three-dimensional
A_{260}:	Absorbance at a wavelength of 260nm
A_{280}:	Absorbance at a wavelength of 280nm
ATA:	Aurintricarboxylic Acid
B.t.:	Bos taurus (cattle)
B_{max}:	Maximum number of binding sites
BMH:	Bismaleimidohexane
C.f.:	Canis familiaris (dog)
CT:	Chymotrypsin
CTF:	Contrast transfer function
Cryo-EM:	Cryo electron-microscopy
DBC:	DeoxyBigCHAP
DDM:	Dodecylmaltopyranoside
DMSO:	Dimethylsulfoxid
DTT:	Dithiothreitol
E.c.:	Escherichia coli
EDTA:	Ethylendiamide-tetraacetate
eq:	equivalent ($50A_{280}$=1eq/µl; Walter and Blobel, 1983a)
ER:	endoplasmic reticulum
Ffh:	Fifty-four-homolog; Bacterial SRP54-homolog
GDP:	Guanosinediphosphate
GEF:	Guanine exchange factor
GMPPNP:	5-guanosyl-imido-triphosphate
GTP:	Guanosinetriphosphate
HEPES:	N2-hydroxyethylpiperazine-N'2-ethanesulfonic acid
HRP:	Horseradish peroxidase
HU-Buffer:	Urea-containing sample buffer (Knop and Schiebel., 1998)
IVT:	In vitro translation
K_D:	Concentration of ligand at which 50% of binding sites are occupied

kD:	kilo-Dalton
KOAc:	Potassium acetate
k_{off}:	Dissociation rate
L1:	Large ribosomal protein
L7/L12:	Large ribosomal proteins
luc120:	N-terminal 120 amino acids of firefly luciferase (P. pyralis)
$Mg(OAc)_2$:	Magnesium diacetate
mRNA:	messenger RNA
OD_{600}:	Optical density at a wavelength of 600nm
PBS:	Phosphate buffered saline
PCR:	Polymerase chain reaction
PK:	Proteinase K
PKRMs:	Puromycin/high salt-treated RMs, i.e. endogenous ribosomes have been removed
PMSF:	Phenylmethylsulfonylfluouride
ppl86:	N-terminal 86 amino acids of B.t. preprolactin
PTC:	Peptidyl-transferase-center in the ribosome
rER:	rough endoplasmic reticulum
RBB:	Ribosome binding buffer
RMs:	rough microsomes
RNA:	ribonucleic acid
RNC:	Ribosome-nascent chain-complex
rpm:	revolutions per minute
RT:	room temperature
SDS:	sodium dodecyl sulfate
SDS-PAGE:	SDS polyacrylamide gelelectrophoresis
SecA:	Eubacterial ATPase that translocates substrates across the plasma membrane
Sec61:	Eukaryotic protein-conducting channel; consists of subunits α (10 TM-domains), β (1 TM domain) and γ (1 TM domain)
SecYEG:	Eubacterial protein-conducting channel; consists of Y, E, and G subunit

SecYEβ:	Archaebacterial protein-conducting channel; consists of Y, E, and β-subunit
SR:	SRP-receptor; consists of subunits α and β
SRP:	Signal Recognition Particle (ribonucleoprotein)
SRP54:	54kD-subunit of SRP, mediates signal sequence recognition and ribosome binding
TCA:	Trichloroacetic acid
TM:	Transmembrane helix
TRAP:	Translocon associated protein
U:	enzymatic Unit
v/v:	volume per volume
wt:	wildtype
w/v:	weight per volume

9 CURRICULUM VITAE

Name: Julia Schaletzky

Address: 115 St. Botolph Street #4

                 Boston, MA 02115

                 USA

Date of Birth: 30.01.1978 in Munich, Germany

Nationality: German

School education:

1984-86:   Grundschule Dasing

1986-88:   Grundschule St. Anna, Augsburg

1988-97:   Maria-Theresia-Gymnasium Augsburg,

                 finished with Abitur 1997

Academic education and experience:

1997-2002:   Study of Biochemistry, Universitaet Bayreuth

2002:   Diploma thesis, MPI of Biochemistry, Martinsried

                 Advisors: Dr. Francis Barr, Dr. Christian Lehner

                 Project: "Characterization of the Myotubularin-related protein

MTMR6"

2002:   Diploma in Biochemistry, Universitaet Bayreuth

2003-2006:   PhD candiate, LMU Muenchen

                 Research performed in Harvard Medical School, Dept. of Cell Biology

                 Advisors: Prof. Tom Rapoport, Prof. J. Soll

Publications:

Short B, Preisinger C, Schaletzky J, Kopajtich R, Barr FA. The Rab6 GTPase
regulates recruitment of the dynactin complex to Golgi membranes. Curr Biol.
12:1792-5 (2002)

Schaletzky J, Dove SK, Short B, Lorenzo O, Clague MJ, Barr FA.
Phosphatidylinositol-5-phosphate activation and conserved substrate specificity of the
myotubularin phosphatidylinositol 3-phosphatases. Curr Biol. 13:504-9 (2003)